THE ANISOTROPIC ANTIFERROMAGNET-THEORY AND EXPERIMENT

Thesis for the Degree of Ph. D. MICHIGAN STATE UNIVERSITY CHRISTOPHER WARREN FAIRALL.



10 3 X X

This is to certify that the

thesis entitled

THE ANISOTROPIC ANTIFERROMAGNET-

THEORY AND EXPERIMENT

presented by

Christopher Warren Fairall

has been accepted towards fulfillment of the requirements for

Ph.D. degree in Physics

Sa Cower

Major professor

Date 10/23/70

O-7639

THERE

ABSTRACT

THE ANISOTROPIC ANTIFERROMAGNET-THEORY AND EXPERIMENT

Ву

Christopher Warren Fairall

The phase transitions of the two sublattice antiferromagnet with general second order anisotropy have been studied in the molecular field approximation. The interactions included were the isotropic and anisotropic exchange, uniaxial crystal field anisotropy and Dzyaloshinski-Moriya antisymmetric exchange anisotropy of the form $\vec{D} \cdot \vec{S}_1 X \vec{S}_2$. The \vec{D} vector was chosen perpendicular to the antiferromagnetic axis and the phase transitions induced by applied magnetic field were calculated numerically from the equations of equilibrium and stability. The antiferromagnetic to spin flop transition remains first order while the second order paramagnetic transition is destroyed by the D-M interaction unless the field is applied parallel to \vec{D} .

The principal axis susceptibilities were calculated, revealing an inflection point corresponding to a quasiparamagnetic transition and an infinite anamoly at the spin flop critical field. Included is a calculation of the angle

dependence of the susceptibility of the uniaxial antiferromagnet in applied field.

Magnetic susceptibility measurements were made on $\text{Cs}_2\text{MnCl}_4 \cdot 2\text{H}_20$, $\text{Rb}_2\text{MnCl}_4 \cdot 2\text{H}_20$ and $\text{CuCl}_2 \cdot 2\text{H}_20$. The susceptibility was measured as a function of temperature and magnitude and orientation of applied field in liquid He^4 . The magnetic H-T phase diagrams of $\text{Cs}_2\text{MnCl}_4 \cdot 2\text{H}_20$ and $\text{Rb}_2\text{MnCl}_4 \cdot 2\text{H}_20$ were measured and no spin flop boundaries were found to exist above 1.2 Kelvins.

The molecular field theory developed in the text was used to interpret the data including data taken from the literature on MnCl₂·4H₂O. The results are as following:

- 1. $\text{Cs}_2\text{MnCl}_4 \cdot 2\text{H}_2\text{O}$ and $\text{Rb}_2\text{MnCl}_4 \cdot 2\text{H}_2\text{O}$ exhibit an unusually large anisotropy that is significantly larger in the ordered state than in the paramagnetic state. Molecular field calculations indicate $\text{Cs}_2\text{MnCl}_4 \cdot 2\text{H}_2\text{O}$ will spin flop below $\text{T}_{\text{tp}} = 0.55$ K at a critical field $\text{H}_{\text{tp}} = 17$ kOe and $\text{Rb}_2\text{MnCl}_4 \cdot 2\text{H}_2\text{O}$ will spin flop below $\text{T}_{\text{tp}} = 0.83$ K at a critical field $\text{H}_{\text{tp}} = 17$ kOe.
- 2. Excellent agreement between theory and experiment was found for the susceptibility as a function of magnitude and orientation of applied field for CuCl₂·2H₂0.
- 3. Molecular field theory gave consistent results for phase diagram and susceptibility data on MnCl₂·4H₂0.

THE ANISOTROPIC ANTIFERROMAGNETTHEORY AND EXPERIMENT

By

Christopher Warren Fairall

A THESIS

Submitted to

Michigan State University
in partial fulfillment of the requirements
for the degree of

DOCTOR OF PHILOSOPHY

Department of Physics

:37206

ACKNOWLEDGMENTS

The author wishes to express thanks to his mentor Dr. J. A. Cowen and to Drs. R. D. Spence and E. H. Carlson for many helpful discussions and assistance; to Dr. G. L. Pollack for much appreciated encouragement; to John Ricks and Edward Grabowski for help in the laboratory; and to the machine shop for construction of apparatus. The author is especially grateful for financial assistance from the National Science Foundation and an N.D.E.A. Title IV Fellowship.

TABLE OF CONTENTS

LIST OF TABLES LIST OF FIGURES LIST OF APPENDICES INTRODUCTION I. THE HEISENBERG HAMILTONIAN A. Exchange 1. The two electron system	v viii 1 3 3 3 5 6
LIST OF APPENDICES INTRODUCTION I. THE HEISENBERG HAMILTONIAN A. Exchange	viii 1 3 3 3 5
INTRODUCTION I. THE HEISENBERG HAMILTONIAN A. Exchange	1 3 3 3 5
I. THE HEISENBERG HAMILTONIAN A. Exchange	3 3 5
A. Exchange	3 3 5
	3 5
1. The two electron system	5
2. Many electron exchange 3. Superexchange	
B. Anisotropy	9
 Dipolar anisotropy Crystal field anisotropy Spin orbit anisotropic effects 	9 10 11
C. The General Second Order Interaction	13
D. The Question of Generality	15
II. MAGNETIC ORDERING	16
A. The Simple Paramagnet	16
B. The Ordered State	17
 Molecular field theory Green function theory Other methods 	18 21 23
III. MAGNETIC PHASE DIAGRAM	26
A. The Classical Energy	27
B. The Zero Temperature Phases	31
 The zero field equilibrium configuration The parallel configuration The perpendicular configuration The D configuration Discussion of the effects of h_D on the zero temperature phases 	31 32 41 42

Cha	pter	1	Page
	c.	The Temperature Dependence of the Critical Fields and the H-T Phase Diagram	43
		 The paramagnetic boundaries The spin flop boundary 	44 45
IV.		THEORETICAL DEPENDENCE OF THE SUSCEPTIBILITY ON LIED FIELD AND TEMPERATURE - THE ANTIFERROMAGNET	47
	A.	The Zero Field Susceptibility	47
		1. The susceptibility as a function of temp- erature for H=0	47
		 The susceptibility as a function of angle for H=0 	53
	в.	The Susceptibility in Applied Field	53
		1. The susceptibility as a function of H for the canted antiferromagnet at T=0 2. The susceptibility as a function of angle	54
		 The susceptibility as a function of angle in applied field for the uniaxial anti- ferromagnet at T=0 	64
v.		ERIMENTAL APPARATUS - THE MEASUREMENT OF SOTROPIC SUSCEPTIBILITY	68
	A.	The Great Unit Debate	68
	В.	The Measurement of Susceptibility	70
	c.	The Parametric Apparatus	71
		 Susceptibility vs. temperature Susceptibility vs. orientation Susceptibility in applied field 	72 72 77
	D.	Low Susceptibility Materials	81
VI.	EXP	ERIMENTAL RESULTS AND DISCUSSION	88
	A.	Cs2MnCl4.2H2O and Rb2MnCl4.2H2O	88
	в.	CuCl ₂ ·2H ₂ O	108
	c.	MnCl ₂ ·4H ₂ O	121
	D.	Conclusions	127
REF	EREN	CES	130
ADD	FNDT	CES	134

LIST OF TABLES

Table		Page
I.	Physical parameters of the susceptibility coils	76
II.	Experimental data and molecular field calculations for $\text{Cs}_2^{\text{MnCl}_4 \cdot 2\text{H}_2\text{O}}$ and $\text{Rb}_2^{\text{MnCl}_4 \cdot 2\text{H}_2\text{O}}$	109
III.	The zero temperature phase boundaries and molecular fields for MnCl ₂ ·4H ₂ O	126

LIST OF FIGURES

Figure		Page
1.	Definition of the angles describing the spin array	30
2.	The superheated critical angle $\alpha_{\rm sh}(h_{\rm D})$ vs. $h_{\rm D}$ with $h_{\rm K}^{=0}$ and $h_{\rm L}^{=0.1}$	35
3.	The spin flop critical fields vs. h_D with $h_K^{=0}$ and $h_L^{=0.1}$	37
4.	A comparison of numerically calculated h_{sc} with the approximation of equation 3.27	40
5.	Susceptibility vs. temperature in the molecular field approximation	52
6.	Susceptibility vs. applied field with $h_D^{=0}$, $h_K^{=0}$ and $h_L^{=0.1}$	58
7.	Susceptibility vs. applied field with $h_D^{=0.05}$, $h_K^{=0}$ and $h_L^{=0.1}$	60
8.	Numerical calculation of $d\chi/dh$ vs. h with $h_D^{=0.05}$, $h_K^{=0}$ and $h_L^{=0.1}$	62
9.	Numerical calculation of susceptibility vs. angle in applied field	67
10.	The crystal rotation device	74
11.	Coil #5 with rotator	79
12.	Calibration of resistance vs. H for the magnetoresistor	83
13.	A cross section of the apparatus for measuring susceptibility in applied field	85
14.	Susceptibility vs. angle for Rb2MnCl ₄ ·2H ₂ O in the paramagnetic and antiferromagnetic states with zero applied field	91
15.	Zero field susceptibility vs. temperature for Cs2MnCl4·2H2O in the parallel and perpendicular orientations	93
16.	Zero field susceptibility vs. temperature for Rb2MnCl4·2H2O in the parallel and perpendicular orientations	95

Figure		Page
17.	Magnetic phase diagram of Cs ₂ MnCl ₄ ·2H ₂ O. The predicted spin flop boundary is represented by a dotted line.	98
18.	Magnetic phase diagram of Rb2MnCl4.2H2O. The predicted spin flop boundary is represented by a dotted line	100
19.	Susceptibility vs. temperature in applied field for Cs ₂ MnCl ₄ ·2H ₂ O, typical data used for obtaining phase boundaries	103
20.	Extrapolation of the phase boundaries to T=0 for Cs ₂ MnCl ₄ ·2H ₂ O	105
21.	Extrapolation of the phase boundaries to T=0 for Rb ₂ MnCl ₄ ·2H ₂ O	107
22.	Susceptibility vs. temperature in applied field for CuCl ₂ ·2H ₂ O	111
23.	Extrapolation of the amplitude of the spin flop transition vs. temperature for CuCl ₂ ·2H ₂ O	113
24.	Magnetic phase diagram of CuCl ₂ ·2H ₂ O (Ref. 58)	115
25.	Susceptibility vs. angle for various applied fields for CuCl ₂ ·2H ₂ O; experimental and theoretical results normalized to the zero field parallel and perpendicular values	118
26.	Susceptibility vs. applied field at constant temperature for CuCl ₂ ·2H ₂ O	120
27.	Magnetic phase diagram of MnCl ₂ ·4H ₂ O (Refs. 66 and 67)	123
28.	Susceptibility vs. applied field at constant temperature for MnCl. 4H.O (Ref. 66)	125

LIST OF APPENDICES

Appendix		Page
A.	Newton's Method	134
в.	Crystallography	136
c.	Computer Programs	138

± -
39
::
Ą
ž
÷
4.
ŧ
4
:
;
:
di d
4

INTRODUCTION

Magnetic ordering, though known at least experimentally for centuries, was first understood with the development of quantum mechanics in the 1920's. It is now known that the magnetic moments associated with magnetic ions in crystals can take on many possible arrangements including ferromagnetic, antiferromagnetic, canted antiferromagnetic, ferrimagnetic and spiral configurations. The arrangement a given lattice of spins will acquire depends upon the interactions of the system. The interaction that has been most successful in describing the arrangement and properties of magnetic insulators is the general Heisenberg interaction, second order in the spin operators.

Magnetic materials can be studied by a number of experiments including resonance, specific heat, neutron diffraction and susceptibility. Antiferromagnets are particularly interesting because in applied magnetic fields they can undergo various phase transitions corresponding to realignment or saturation of the spin system. The basis of these transitions is the interplay between the isotropic and anisotropic parts of the interaction.

The first successful theory describing these magnetic systems was the molecular or effective field approximation where one considers the interaction of a given spin with its neighbors to be an average effect that can be replaced by an effective magnetic field. Although more sophisticated theories now exist, our primary concern in this work is to explore the ability of molecular field theory to explain the properties of the

	<u>:</u> ;;
	2
	.:.
	11.
	:
	:
	•
	•
	::
	3
	ţ

anisotropic magnetic insulator. Specifically, we wish to accomplish the following:

- 1. Unify the existing theoretical base of the Heisenberg interaction and the magnetic ordering it produces.
- 2. Extend the theory of the magnetic phase diagram to a general second order interaction for the canted antiferromagnet.
- 3. Write a theoretical description of the magnetic susceptibility as a function of orientation, applied field and temperature. Particular emphasis is placed on the anisotropic properties of canted or uniaxial antiferromagnets in applied fields and the behavior of the susceptibility near critical points.
- 4. Describe the construction and use of apparatus capable of measuring suceptibility as a function of orientation, applied field and temperature.
- 5. Present the results of susceptibility measurements made with this apparatus and their theoretical interpretation. We also apply the theory to previously existing data on a material that is well understood. The purpose is to evaluate the consistency and accuracy of the theory.

I. THE HEISENBERG HAMILTONIAN

The interactions that govern the behavior of a system of electron spins in an insulating solid are multitudinous, but one can describe many of the magnetic properties by considering two separate but not wholly orthogonal interactions: exchange and anisotropy.

A. Exchange

1. The two electron system.

Exchange is a purely quantum mechanical effect and, having no classical analogue, it is difficult to employ physical intuition when discussing it. However, the next best thing to physical intuition is history, so I will describe a simple example demonstrated by Heisenberg¹ in 1926.

Suppose we have two electrons in similar potentials. The Hamiltonian for the pair is

$$H = -\frac{\hbar^2}{2m} \nabla_1^2 - \frac{\hbar^2}{2m} \nabla_2^2 + V(1) + V(2) + e^2/r_{12}$$
 (1.1)

where 1 and 2 refer to coordinates of the respective electrons and $\mathbf{r}_{12} = |\vec{\mathbf{r}}_1 - \vec{\mathbf{r}}_2|$.

Let

$$H = H_0 + e^2/r_{12}$$
 (1.2)

and assume e^2/r_{12} is a perturbation on H_0 ,

$$H_{O}Y_{ij}^{O} = E_{ij}^{O}Y_{ij}^{O} \tag{1.3}$$

where

$$\Psi_{ij}^{O} = \Psi_{i}^{O}(1)\Psi_{j}^{O}(2)$$

$$E_{ij}^{O} = E_{i}^{O} + E_{j}^{O}$$
(1.4)

We can make this separation because H_{O} contains no interaction between 1 and 2.

First order perturbation theory gives a correction to the energy

$$E_{ij} = E_{ij}^{o} + B_{ij}$$

$$B_{ij} = \int_{i}^{\phi_{o}}(1) \, \dot{\psi}_{j}^{o}(2) e^{2} / r_{12} \, \dot{\psi}_{i}^{o}(1) \, \dot{\psi}_{j}^{o}(2) d\tau$$
(1.5)

where B_{ij} is the average repulsive coulomb interaction of the electrons in states i and j.

The Pauli exclusion principle requires the total wave function to be antisymmetric under "exchange" of particles 1 and 2. The appropriate wave functions including spin are given by the Slater determinant

$$\Psi_{ij}^{1}(1,2) = \frac{1}{\sqrt{2}} \begin{vmatrix} \Psi_{i}^{O}(1)\alpha(1) & \Psi_{i}^{O}(2)\alpha(2) \\ & & & \\ \Psi_{j}^{O}(1)\alpha(1) & \Psi_{j}^{O}(2)\alpha(2) \end{vmatrix}$$
(1.6)

where alpha is the "spin up" wave function. There are three more possible wave functions Ψ^2 , Ψ^3 , Ψ^4 corresponding to different spin configurations. Diagonalization of the matrix elements of H with these wave functions results in a singlet of energy

$$E_s = E_{ij}^O + B_{ij} + J_{ij}$$
 (1.7)

;
::
.:
ć
.i.
·
: -
\$ ¹
\$
(২)

and a triplet of energy

$$E_t = E_{ij}^0 + B_{ij} - J_{ij}$$
 (1.8)

where

$$J_{ij} = \int \tilde{\Psi}_{i}^{O}(1) \tilde{\Psi}_{j}^{O}(2) e^{2} / r_{12} \Psi_{j}^{O}(1) \Psi_{i}^{O}(2) d\tau \qquad (1.9)$$

is called the direct exchange integral.

2. Many electron exchange

Unfortunately, one cannot describe the behavior of a crystal in terms of two electron wave functions. If we consider N electrons (designated \vec{r}_i) on N reasonably localized lattice sites (\vec{R}_{alpha}) , the Hamiltonian is

$$H = \sum_{i}^{\Sigma} \frac{P_{i}^{2}}{2m} - \sum_{i,\alpha}^{\Sigma} \frac{Ze^{2}}{|\vec{r}_{i} - \vec{R}_{\alpha}|} + \sum_{i,j}^{\Sigma} \frac{1}{2} \frac{e^{2}}{r_{i,j}}$$
(1.10)

and a convenient set of wave functions are Wannier functions 2 $\phi_{n\lambda}$ $(\vec{r}-\vec{R}_{\alpha})$ which resemble the n^{th} atomic orbital with spin λ on lattice site α but drop off through the lattice in such a way as to be orthogonal. If one rewrites the Hamiltonian in 2^{nd} quantized field operator form 3,4 , one can show that the exchange term can be expressed

$$H_{ex} = -\frac{\Sigma}{\alpha \alpha}, J_{nn}, (\vec{R}_{\alpha}, \vec{R}_{\alpha}') \left\{ \frac{1}{4} + S(\vec{R}_{\alpha}) \cdot \vec{S}(\vec{R}_{\alpha}') \right\}$$
(1.11)

where

$$J_{nn'}(\vec{R}_{\alpha}, \vec{R}_{\alpha}') = (\alpha n; \alpha'n' | V | \alpha'n'; \alpha n)$$

$$V = H - T$$
(1.12)

Equation 1.11 is referred to as the Heisenberg exchange

		<i>:</i> .
		•5
		:
		-
		3
		ii:
		u:
		· <u>:</u>
		ě
		¥
		ং
		*

Hamiltonian, originally derived for two electrons by Dirac⁵.

3. Superexchange

In most insulating crystals the magnetic ions are separated by large distances with intervening ligands; it follows that the direct exchange of equation 1.12 is very small and cannot account for the much larger interactions that are usually observed.

Let us consider a system of two Mn⁺⁺ ions joined by an

0 ion. The ground state is illustrated by

$$Mn^{++}$$
 O^{--} Mn^{++} (A) d_1 pp' d_2

where p and d refer to atomic orbital states. The excited state corresponds to promotion of one 0 p electron into the d shell of Mn⁺⁺.

$$Mn^{+}$$
 0^{-} Mn^{++} (B) $d_{1}d_{1}^{+}$ p d_{2}

The wave functions for the configurations are written 6,7

$$\Psi_{A} = \Psi_{d_{1}}(1)\Psi_{p}(2)\Psi_{p}(3)\Psi_{d_{2}}(4)$$

$$\Psi_{B} = \Psi_{d_{1}}(1)\Psi_{d_{1}}(2)\Psi_{p}(3)\Psi_{d_{2}}(4)$$
(1.13)

The perturbing Hamiltonian is assumed to consist of a spin independent part, V_t , connecting states A and B, and a spin dependent part, V_e , diagonal with respect to orbital states. Spin dependence shows up first in the 3^{rd} order energy correction as

$$E_{3} = \sum_{t,\mu} \frac{(A^{t}|V_{t}|B^{t'})(B^{t'}|V_{e}|B^{u'})(B^{u'}|V_{t}|A^{\mu})}{(E_{B}^{t'} - E_{A}^{t})(E_{B}^{u'} - E_{A}^{u})}$$
(1.14)

		;
		:
		*
		;
		3
		•

t, u denoting spin configurations.

One rewrites the wave functions in states of definite parity in terms of the spin coupling of the Mn to one 0 electron. For example $\Psi_{A}[(pd_{1})^{3}(p'd_{2})^{1}]$ is a ground state wave function with the d_{1} electron of Mn₁ and the p electron of 0^{--} in a triplet state and the d_{2} electron of Mn₂ and the p' electron of 0^{--} in a singlet state. The energy of this system can be written

$$E = \left[\frac{1}{\Delta E(t)^2} - \frac{1}{\Delta E(S)^2}\right] 2b^2 J_{pd}(\vec{s}_1 \cdot \vec{s}_2)$$

$$- \frac{1}{4} \left[\frac{3}{\Delta E(t)^2} + \frac{1}{\Delta E(S)^2}\right] 2b^2 J_{pd}$$
(1.15)

where the transfer integral is

$$b = \int \Psi_{d_1}(1) \Psi_{p}(1) V_{t} d\tau$$
 (1.16)

and

$$J_{pd} = \int {^{*}\!\!\!/}_{p}(1) {^{*}\!\!\!/}_{d}(2) V_{e} Y_{p}(2) Y_{d}(1) d\tau \qquad (1.17)$$

is the exchange of the Mn^{++} 0⁻⁻ system. The energy of the Mn^{+} in the singlet and triplet states is given by $\Delta E(s)$ and $\Delta E(t)$ respectively.

Let us suppose that Mn_1 has spin up. Now assume that $\mathrm{J}_{\mathrm{pd}}>0$, therefore, the p electron associated with Mn_1 will have spin up. The p' electron will have spin down and therefore Mn_2 will have spin down - the interaction is antiferromagnetic. Another way of describing this process is to assume $\mathrm{J}_{\mathrm{pd}}>0$ implies $\Delta\mathrm{E}(s)\to\infty$ and $\Delta\mathrm{E}(t)\to U$, the average coulomb interaction of an electron with another electron on the same ion

... 7.7 :: -: ... 1,147

$$E_{\text{spin}} = \left[\frac{2b^2}{U^2} J_{\text{pd}}\right] (\vec{s}_1 \cdot \vec{s}_2) \qquad (1.18a)$$

Since $J_{pd}^{>0}$, the coupling is antiferromagnetic.

Now we assume $J_{pd}^{<0}$, the p electron associated with Mn_1 will have spin down, p' will have spin up and Mn_2 will have spin down - the interaction is antiferromagnetic if $J_{pd}^{<0}$, let $\Delta E(t) \rightarrow \infty$ and $\Delta E(s) \rightarrow U$. Consequently

$$E_{\text{spin}} = -\frac{2b^2}{U^2} (J_{\text{pd}}) (\vec{s}_1 \cdot \vec{s}_2)$$
 (1.18b)

but now J_{pd}<0 so

$$E_{\text{spin}} = +\frac{2b^2}{U^2} |J_{pd}| (\vec{s}_1 \cdot \vec{s}_2)$$
 (1.18c)

which is an antiferromagnetic coupling. We therefore express the superexchange in the form of equation 1.18 and note that it is always antiferromagnetic.

It is customary 8 to define direct exchange and superexchange as

$$J_{ij}^{O} = \int_{1}^{4} (1)^{\frac{1}{4}} (2) e^{2} / r_{12} V_{j} (1) V_{i} (2) d\tau \qquad (1.19a)$$

 $J_{ij}^{O} > 0$, always ferromagnetic and

$$J_{ij}^{s} = -\frac{2b^{2}}{U^{2}} |J_{pd}|$$
 (1.19b)

 J_{ij}^{s} <0 always antiferromagnetic.

The Hamiltonian is written

$$H_{ij} = (|J_{ij}^{S}| - J_{ij}^{O}) \dot{S}_{i} \cdot \dot{S}_{j}$$
 (1.20)

Of course there exist many other exchange interactions⁸, of either sign, but these rarely dominate the magnetic properties. Theoretical calculations of J are very difficult so one usually

151
Li
45.
73
ii
.
Ę
Ę
€:
² 4
i i i i i i i i i i i i i i i i i i i
<u> </u>
Ş

considers J to be an experimentally determined quantity.

B. Anisotropy

It is a fact of life that magnetically ordered single crystals are anisotropic. Although many of their properties can be described purely on the basis of exchange, we are particularily interested in their anisotropy. I will consider three sources of anisotropy: dipolar, crystal field, and spin-orbit interactions.

1. Dipolar anisotropy

The interaction between two magnetic dipoles a distance r apart is

$$H_{ij} = 1/r_{ij}^{3} [\vec{u}_{i} \cdot \vec{u}_{j} - 3(\vec{u}_{i} \cdot \hat{r}_{ij})(\vec{u}_{j} \cdot \hat{r}_{ij})]$$
 (1.21)

The magnetic moment of an electron is

$$u_{i}^{\mu} = u_{R}g_{i}^{\mu\nu}S_{i}^{\nu}$$
 (1.22)

Let us assume an isotropic g tensor and define

$$C_{ij}^{\mu\nu} = g^{2} u_{B}^{2} r_{ij}^{-3} [\delta^{\mu\nu} - 3\gamma_{ij}^{\mu} \gamma_{ij}^{\nu}] (1 - \delta_{ij})$$
 (1.23)

where γ_{ij}^{u} is the direction cosine of \dot{r}_{ij} with the u axis. The total Hamiltonian can now be written^{9,10} to lowest order

$$H_{\text{dipolar}} = \sum_{ij}^{\Sigma} \sum_{\mu,\nu} C_{ij}^{\mu\nu} S_{i}^{\mu} S_{j}^{\nu}$$
 (1.24)

If one knows the structure of a crystal with magnetic ions, one assumes a magnetic arrangement and performs the sums of equation 1.24 on the ubiquitous computer. A typical calculation might be over 10,000 neighbors with 75 per cent of the interaction

:
:
:
`
ž
*
:
į

being due to nearest neighbors.

2. Crystal field anisotropy

Crystal field anisotropy is intimately connected with the spin-orbit interaction, but I feel it warrants individual discussion. The coulomb interaction between each unpaired electron and the charge distribution of the crystal can be described by an electrostatic potential $V(\vec{r})$. The charge distributions surrounding the magnetic ion may overlap the electron and analysis of this rather hairy problem is called ligand field theory 11. It is much easier, and still very educational, to consider the neighbors as point charges, a consideration I shall designate as crystal field theory. This has the advantage that $V(\vec{r})$ can be expanded in spherical harmonics $Y_{\ell,m}(\theta,\phi)$.

$$V(r,\theta,\phi) = \frac{\sum \sum_{\ell,m} A_{\ell,m} r^{\ell} Y_{\ell,m}(\theta,\phi) \qquad (1.25)$$

The symmetry of the crystal field resides in the $A_{\ell m}$. Because the electrons will be in nearly atomic orbital ℓ ' states, the $\ell > \ell'$ terms in the expansion will be negligible. The spherical harmonic $y_{\ell m}(\theta,\phi)$ is a spherical tensor of rank ℓ , order $\ell > \ell'$. The spin operator S_i^u is a spherical tensor operator of rank one and order three, the elements being S_i^z , S_i^t , and S_i^t . The Wigner-Eckart theorem justifies an expansion of $Y_{\ell m}(\theta,\phi)$ in a linear combination of the products of ℓ spin operators. In the absence of applied magnetic field, time reversal invariance allows us to eliminate odd product terms in our expansion. The crystal field can be written as a bilinear expansion of spin operators, the second order part can be written

$$H_{i} = \vec{S}_{i} \cdot \vec{K}_{ij} \cdot \vec{S}_{i} \qquad (1.26)$$

. 3 Ξ. 12 -٠. 1 • ۲,

3. Spin-orbit anisotropic effects

Suppose we express the interaction of an electron spin with the field produced by its orbital motion in a potential V(r) as 12

$$H_{S} = \dot{n}^{2}/2m^{2}c^{2}\vec{S} \cdot (\vec{\nabla}V(r) \times \vec{P}) = \lambda \vec{l} \cdot \vec{S}$$
 (1.27a)

In a magnetic field we add a Zeeman term and the total Hamiltonian is

$$H_{i} = \lambda \vec{l}_{i} \cdot \vec{s}_{i} + U_{B}(\vec{l}_{i} + 2\vec{s}_{i}) \cdot \vec{H}$$
 (1.27b)

Assuming that the states of the unperturbed system can be reasonably described by orbitally nondegenerate wave functions, a second order perturbation calculation gives

$$H_{i}^{\text{effective}} = \sum_{\mu,\nu} \mu_{B} g^{\mu\nu} H^{\mu} s^{\nu} - \lambda^{2} \Lambda^{\mu\nu} s^{\mu} s^{\nu}$$
$$- u_{B}^{2} \Lambda^{\mu\nu} H^{\mu} H^{\nu} \qquad (1.28)$$

where

$$g^{\mu\nu} = 2 (\delta^{\mu\nu} - \lambda \Lambda^{\mu\nu})$$

represents the admixture of orbital angular momentum into a spin only ground state.

$$\Lambda^{\mu\nu} = \sum_{n \neq 0} \frac{(0 | \ell^{\mu} | n) (n | \ell^{\nu} | 0)}{E_n - E_0}$$
 (1.29)

n represents excited states and $2\lambda\Lambda^{\mu\nu}$ is called the g-shift, Δg .

The second term of equation 1.28 is the single ion anisotropy. Note that, as mentioned in section 2, the $\Lambda^{\mu\nu}$ reflects the crystal field symmetry. The wave functions we used can be written 13

$$|n\rangle = |\Gamma, \gamma\rangle |S, M_S\rangle$$

		T.
		.÷
		, e e
		: -
		900 1000 1
		<u></u>
		î:
		<u>:</u>
		:
		•
		:
		13,
		٠.
		**
		ζ;

where Γ is the irreducible point group symmetry representation and is orbitally nondegenerate.

The most interesting effect of spin orbit interactions is their ability to couple with superexchange to produce anisotropic exchange effects. Moriya has done a rather general calculation of this effect but I prefer to examine a simplification employed by Nagamiya et al has been a simplification of two magnetic ions are crystal field split orbitally nondegenerate states. Let our perturbation be

$$V = \lambda (\vec{k}_{i} \cdot \vec{s}_{i}) + \lambda (\vec{k}_{j} \cdot \vec{s}_{j}) - J(\vec{s}_{i} \cdot \vec{s}_{j})$$
 (1.30)

The second and third order energy corrections are, respectively,

$$H_{ij} = \vec{D}_{ij} \cdot (\vec{S}_{i} \times \vec{S}_{j}) + \vec{S}_{i} \cdot \vec{K}_{ij} \cdot \vec{S}_{j}$$
 (1.31)

where

$$\vec{D}_{ij} = i\lambda \left\{ \sum_{m_i} \frac{Jm_i (0|\vec{\ell}_i|m_i)}{EO_i - Em_i} - \sum_{m_j} \frac{Jm_j (0|\vec{\ell}_j|m_j)}{EO_j - Em_j} \right\}$$
(1.32)

$$\kappa_{\mathbf{i}\mathbf{j}}^{\mu\nu} = \frac{\lambda^{2}}{2} \left\{ \frac{1}{3} \delta^{\mu\nu\Sigma}_{} (\Gamma_{\mathbf{i}}^{\eta\eta} + \Gamma_{\mathbf{j}}^{\eta\eta}) - (\Gamma_{\mathbf{i}}^{\mu\nu} + \Gamma_{\mathbf{j}}^{\mu\nu}) \right\}$$
 (1.33)

$$\Gamma_{i}^{\mu\nu} = \sum_{m_{i}}^{\Sigma} \frac{Jm_{i} (0 | \ell_{i}^{\mu} | m_{i}) (m_{i} | \ell_{i}^{\nu} | 0)}{(Eo_{i} - Em_{i})^{2}}$$
(1.34)

and $J_{m_{1}}$ is the superexchange between the i th ion in its m th excited state and the j th ion. Comparing equations 1.34, 1.32 and 1.29 we may roughly estimate D and K as

$$D \simeq \frac{\Delta g}{g} J$$
 $K \simeq (\frac{\Delta g}{g})^2 J$ (1.35)

The $\vec{D}_{ij} \cdot (\vec{S}_i \vec{X} \vec{S}_j)$ anisotropy is called Dzyaloshinsky-Moriya antisymmetric exchange anisotropy because it is antisymmetric

		3.
		•
		i
		.3
		Ţ.
		.:
		:
		:

under exchange of coordinates. The K_{ij} term is called anisotropic exchange and is symmetric.

The D-M interaction is particularly interesting because it exists only when the crystal symmetry is low. Moriya 14 has devised criteria for determining the direction of \vec{D} based on crystal symmetry. Consider atoms 1 and 2 located at lattice sites A and B, the line connecting them is AB.

(i) When a center of inversion is located at the point halfway between A and B,

$$\vec{D} = 0$$

- (ii) When a mirror plane perpendicular to AB bisects AB,
 D is parallel to the mirror plane
- (iii) When there is a mirror plane including A and B

 D is perpendicular to the mirror plane
- (iv) When a two-fold rotation axis perpendicular to AB passes through the midpoint of AB

D is perpendicular to the two-fold axis

(v) When there is an n-fold axis along AB \overrightarrow{D} is parallel to AB

The total Hamiltonian for our system is written

$$H = H_{ex} + H_{dd} + H_{DM} + H_{CF} + H_{AK} + H_{Z}$$
 (1.36)

The terms are respectively isotropic exchange, dipolar, D-M antisymmetric exchange, crystal field anisotropy, anisotropic exchange and Zeeman interactions.

C. The general second order interaction

The general second order interaction between a spin on a lattice site i with a spin on lattice site j is given by 6,9,10

. . ż ; • .

$$H_{ij} = -\frac{\Sigma}{\mu,\nu} \mathbf{A}_{ij}^{\mu\nu} \mathbf{S}_{i}^{\mu} \mathbf{S}_{j}^{\nu} \tag{1.37}$$

Let us decompose the tensor $A_{ij}^{\mu\nu}$ into symmetric and antisymmetric parts 15,16

$$A_{ij}^{\mu\nu}(s) = \frac{1}{2}(A_{ij}^{\mu\nu} + A_{ij}^{\nu\mu})$$
 (1.38a)

$$A_{ij}^{\mu\nu}(a) = \frac{1}{2}(A_{ij}^{\mu\nu} - A_{ij}^{\nu\mu})$$
 (1.38b)

where

$$A_{ij}^{\mu\nu} = A_{ij}^{\mu\nu}(s) + A_{ij}^{\mu\nu}(a)$$

We define the isotropic exchange by the trace of $A_{ij}^{\mu\nu}(s)$

$$J_{ij} = 1/3 \operatorname{tr}(A_{ij}^{\mu\nu}(s))$$
 (1.39)

The anisotropic part of the symmetric exchange is

$$K_{ij}^{\mu\nu} = J_{ij} - A_{ij}^{\mu\nu}(s)$$
 (1.40)

The antisymmetric coefficient is defined by

$$D_{ij}^{\lambda} = A_{ij}^{\mu\nu}(a) \varepsilon_{\mu\nu\lambda}$$
 (1.41)

where $\epsilon_{\mu\nu\lambda}$ is the completely antisymmetric tensor of rank 3. The Hamiltonian is written

$$H_{ij} = -J_{ij}\vec{s}_{i}\cdot\vec{s}_{j} + \vec{D}_{ij}\cdot(\vec{s}_{i}\vec{x}_{j}) + \vec{s}_{i}\cdot\vec{k}_{ij}\cdot\vec{s}_{j} \qquad (1.42)$$

which represents the decomposition of a second order Heisenberg Hamiltonian. Note that when i = j

$$H_{i} = \vec{S}_{i} \cdot \vec{K}_{ii} \cdot \vec{S}_{i} \tag{1.43}$$

which is a general second order crystal field interaction. Finally,

$$H = \frac{1}{2} \sum_{ij} \left\{ -J_{ij} \dot{\vec{s}}_{i} \cdot \dot{\vec{s}}_{j} + \vec{D}_{ij} \cdot (\dot{\vec{s}}_{i} \times \dot{\vec{s}}_{j}) + \dot{\vec{s}}_{i} \cdot \dot{\vec{k}}_{ij} \cdot \dot{\vec{s}}_{j} \right\}$$

$$(1.44)$$

D. The question of generality

The Heisenberg Hamiltonian has been successful to the point of exceeding one's best expectations in describing, at least qualitatively, a host of different magnetic effects. There exists only a handful of materials that require more than second order terms to explain their gross features. The crystals

MnF₂,FeF₂ and CoF₂ which have orthorhombic coordination and d orbitals permitting fourth order anisotropy are very well understood on a basis of second order terms only⁶.

The most important failure of the spin Hamiltonian occurs when the crystal field interaction is too weak to raise the excited states significantly above the ground state, a situation common in rare-earths. Even more disastrous is the non-Kramers, or even number of electrons, case in which the ground state may be orbitally degenerate and all bets are off.

		5]
		٠.
		7.
		3
		•.

II. MAGNETIC ORDERING

The theory of magnetic ordering is fraught with difficulty, in fact the most complicated problem yet to be solved exactly is the two dimensional Ising lattice 17. The fact that one's beginning Hamiltonian is an approximation makes one reluctant to worry about exact solutions. However, before discussing the various magnetic ordering theories, I wish to examine a very simple magnetic system.

A. The simple paramagnet

Consider a system of N identical noninteracting spins with total angular momentum S and magnetic moment \mathbf{u}_{S} . The Hamiltonian for one spin in an applied magnetic field is

$$H = -\overrightarrow{\mu}_{S} \cdot \overrightarrow{H} = -u_{SZ}H \qquad (2.1)$$

If we let $u_S^z = gu_B^m$, then

$$H_{\rm m} = -g u_{\rm B} m H \tag{2.2}$$

The partition function is

$$z_{s} = \sum_{m=-s}^{s} exp \left\{ gu_{B}^{mH}/k_{B}^{T} \right\}$$
 (2.3)

which we can write

$$Z_s(s) = sinh\left(\frac{2S+1}{2S}x\right)/sinh\left(\frac{x}{2S}\right)$$
 (2.4)

where

$$x = gu_{R}SH/kT$$
 (2.5)

The magnetization is

$$M = Ngu_{R} < m >$$
 (2.6)

which can be written 18

$$M = Ngu_BSB_S(x)$$
 (2.7)

 $B_{S}(x)$ is called the Brillouin function.

$$B_S(x) = \frac{(2S+1)}{2S} \coth(x(2S+1)/2S) - \frac{1}{2S} \coth(x/2S)$$
 (2.8)

The susceptibility of this system is

$$\chi = \frac{dM}{dH} = \frac{N(gU_B)^2 S^2 B_S'(x)}{kT}$$
 (2.9)

The zero field susceptibility we obtain by letting $H \rightarrow 0$ and expanding $B_S(x)$ for x << 1.

$$B_{S}(x) \simeq (S+1)x/3S \qquad (2.10)$$

$$B_{S}'(x) \simeq (S+1)/3S$$
 (2.11)

Consequently

$$\chi_{o} = Ng^{2}U_{B}^{2}S(S+1)/3k_{B}^{T}$$
 (2.12)

Written in the form

$$\chi_{O} = C/T \tag{2.13}$$

it is known as Curie's law for paramagnetic susceptibility. Since $\langle m \rangle = \langle S^2 \rangle$

$$< S^{2}> = SB_{S}(x)$$
or $< S^{2}> = 0$ for H=0

B. The Ordered State

A more realistic appraisal of N spins in a crystal will suggest that one must include interactions between spins. In

chapter I we discussed the Heisenberg Hamiltonian as a general second order spin-spin interaction. For simplicity, the present consideration of magnetic ordering may use only the isotropic exchange part of the Hamiltonian. Given a system of magnetic ions we ask the obvious questions: at what temperature does the system order and what is the nature of the ordered state?

1. Molecular field theory

The MFT was employed in the earliest solutions to magnetic ordering problems. The interactions of all the ions in the crystal with a given spin are replaced by an effective field. This is equivalent to letting $\langle \vec{s}_i \cdot \vec{s}_j \rangle = \langle \vec{s}_i \rangle \cdot \langle \vec{s}_j \rangle$ and ignores all correlation effects.

Consider the interaction of the i th spin

$$H_{i} = -\vec{S}_{i} \cdot \stackrel{\Sigma_{j}^{\ddagger}}{j}_{ij} \cdot \vec{S}_{j}$$
 (2.15)

or

$$H_{i} = -gu_{B} \dot{\vec{S}}_{i} \cdot \dot{\vec{H}}_{i}$$
 (2.16)

$$\vec{H}_{i} = \frac{1}{gu_{B}} \vec{j}_{ij} \cdot \vec{s}_{j}$$
 (2.17)

where H_i is the molecular field. The average of \vec{S} is

$$\vec{\sigma}_{1} = \vec{\Sigma} \vec{S}_{i} \exp{\{\vec{S}_{i} \cdot \vec{H}_{i} g u_{B} / k_{B} T\}} / \vec{\Sigma} \exp{\{\vec{S}_{i} \cdot \vec{H}_{i} \frac{g u_{B}}{k_{B} T}\}}$$
(2.18)

The molecular field approximation is made by letting

$$\vec{H}_{i} = \frac{1}{gu_{B}} \sum_{j} \vec{J}_{ij} \cdot \vec{\sigma}_{j}$$
 (2.19)

Equation 2.18 is written

$$\vec{\sigma}_{i} = \vec{S}_{i} B_{S} (g u_{R} \vec{H}_{i} \vec{\sigma}_{i} / k_{R} T)$$
 (2.20)

:
zi
+ -
j.
2
i.
े -
4
:
·
. :
2
8
;

The disordered state is represented by $\vec{\sigma}=0$. If we are in the ordered state, near the ordering temperature T_{c} , σ will be small so we expand the exponentials and keep the first order terms 19 .

$$\sum_{j} \vec{J}_{ij} \cdot \vec{\sigma}_{j} = 3k_{B} T_{c} / S(S+1) \vec{\sigma}_{i}$$
 (2.21)

This coupled set of equations is solved by letting $\vec{\sigma}_i(\vec{R})$ represent the i th sublattice ion in the primitive cell at \vec{R} . We now must sum over primitive cells

$$\sum_{j,\vec{R}'} \vec{J}_{ij}(\vec{R},\vec{R}') \cdot \vec{\sigma}_{j}(\vec{R}') = \lambda \vec{\sigma}_{i}(\vec{R})$$
 (2.22)

where

$$\lambda = 3k_B T_C / S(S+1)$$
 (2.23)

Suppose we let the μ th component of the spin be written

$$\sigma_{\mathbf{i}}^{\mu}(\mathbf{R}) = \sigma_{\mathbf{i}}^{\mu}(\mathbf{0})e^{\mathbf{i}\mathbf{k}\cdot\mathbf{R}}$$
 (2.24)

where the k's are appropriate propagation vectors consistent with periodic boundary conditions. Equation 2.23 is now written in component form

$$\sum_{j,\vec{R}',\mu} J_{ij}^{\mu\nu}(0,\vec{R}') \sigma_{j}^{\mu}(0) e^{i\vec{K}\cdot\vec{R}'} = \lambda \sigma_{i}^{\nu}(0)$$
(2.25)

let

$$\xi_{ij}^{\mu\nu}(\vec{k}) = \vec{R}, J_{ij}^{\mu\nu}(0, \vec{R}') e^{i\vec{k}\cdot\vec{R}'}$$
(2.26)

$$\sum_{j,\mu} \xi_{ij}^{\mu\nu}(\vec{k}) \sigma_{j}^{\mu}(0) = \lambda \sigma_{i}^{\nu}(0)$$
 (2.27)

$$\sum_{j,\mu} \left\{ \xi_{ij}^{\mu\nu}(\vec{k}) - \delta^{\mu\nu} \delta_{ij} \lambda(\vec{k}) \right\} \sigma_{j}^{\mu}(0) = 0 \qquad (2.28)$$

Solutions to 2.27 exist if the determinant is zero

$$\det \left| \xi_{ij}^{\mu\nu}(\vec{k}) - \delta^{\mu\nu} \delta_{ij} \lambda(\vec{k}) \right| = 0 \qquad (2.29)$$

		•
		-
		•
		ä
		;
		:

The transition temperatures are proportional to the eigenvalues of the Fourier transform of the exchange operator.

$$\lambda(\vec{k}) = 3k_B T_C / S(S+1) \qquad (2.23)$$

Let us consider the following example, suppose we have a simple cubic lattice with lattice parameter a. Let J be isotropic and nearest neighbor only. Considering two sublattices

$$\xi(\vec{k}) = \begin{pmatrix} 0 & J[\cos(k^{x}a) + \cos(k^{y}a) + \cos(k^{z}a)] \\ \\ J[\cos(k^{x}a) + \cos(k^{y}a) + \cos(k^{z}a)] & 0 \end{pmatrix}$$

The eigenvalues of this matrix are

$$\lambda(k) = \pm J[\cos(k^{X}a) + \cos(k^{Y}a) + \cos(k^{Z}a)] \qquad (2.30)$$

Consequently, the ordering temperatures are given by

$$T_{c} = S(S+1)J[\cos(k^{x}a) + \cos(k^{y}a) + \cos(k^{z}a)]/3k_{B}$$
 (2.31)

Since the system will order in the mode with the highest transition temperature, we maximize the eigenvalues with respect to \vec{k} . If J>0 then \vec{k} =0, corresponding to ferromagnetism. If J<0 then \vec{k} = $(1,1,1)\pi/a$, corresponding to antiferromagnetism. The ordering temperature is

$$T_{C} = S(S+1) |J|/3k_{B}$$
 (2.32)

The general molecular field theory that we have discussed here is particularly poor for large crystal field anisotropy because it assumes $\langle S^Z S^Z \rangle = \langle S^Z \rangle \langle S^Z \rangle$. If one suspects crystal field terms to be large, a better approximation should be used²⁰.

2. Green function theory

The main fault of molecular field theory is that it neglects correlation and short range order effects. Green functions are statistical mechanical generalizations of the concept of correlation. For a general review of Green functions I recommend a paper by Zubarev²¹ or books by Kadanoff and Baym²² and Abrikosov et al²³.

The double-time temperature dependent retarded Green function involving two Heisenberg operators 21 A(t) and B(t') is

$$<> = -i\theta(t-t')<[A(t),B(t')]>$$
 (2.33)

where θ (t-t') is the step function, <> denotes the thermal average and [] denotes a commutator. We can Fourier transform this quantity into a function of E = $\hbar\omega$, whose equation of motion is

$$E << A; B>>_{E} = \frac{1}{2\pi} <[A,B]> + << [A,H]; B>>_{E}$$
 (2.34)

The correlation function of A and B is

$$\langle B(t')A(t) \rangle = \lim_{\varepsilon \to 0} \int_{-\infty}^{\infty} \frac{\langle \langle A;B \rangle \rangle_{\omega + i\varepsilon} - \langle \langle A;B \rangle \rangle_{\omega - i\varepsilon}}{\frac{\omega}{k_B T}}$$

$$e^{-i\omega(t - t')}d\omega$$
(2.35)

For simplicity we choose the isotropic Heisenberg Hamiltonian

$$H = -\frac{1}{2} \sum_{ij} J_{ij} \vec{s}_{i} \cdot \vec{s}_{j}$$
 (2.36)

Choosing A and B as spin operators, equation 2.34 becomes

$$E << s_{g}^{+}; s_{h}^{-}> = \frac{2\bar{s}}{2\pi} \delta g h - \int_{f}^{\Sigma} J_{fg} \{$$

$$<< s_{f}^{+} s_{g}^{z}; s_{h}^{-}> _{E} - << s_{f}^{z} s_{g}^{+}; s_{h}^{-}> _{E} \}$$
(2.37)

where g, h denote lattice sites and \bar{S} is the average value of $S^{\mathbf{Z}}$. The equation will be solved in the Tyablikov or random phase decoupling approximation where

$$<>_{E} = <>_{E}$$
 (2.38)

Using this decoupling scheme the equation of motion is 24

$$E << s_{g}^{+}; s_{h}^{-}>_{E} = \frac{2\bar{s}}{2\pi} \delta g h - \int_{f}^{\Sigma} J_{fg} < s_{g}^{z} >< s_{f}^{+}; s_{h}^{-}>_{E}$$

$$+ \int_{f}^{\Sigma} J_{fg} < s_{f}^{z} >< < s_{g}^{+}; s_{h}^{-}>_{E}$$
(2.39)

We now assume we have n sublattices and define Fourier transforms of the Green functions

$$G_1(\vec{k},E) = \sum_{q,h} << S_q^+; S_h^->>_E e^{i\vec{k}\cdot(\vec{R}_g-\vec{R}_h)}$$
 (2.40)

for \vec{R}_{g} and \vec{R}_{h} on sublattice 1 and

$$G_{i}(\vec{k},E) = \sum_{g,h} << S_{g}^{+}; S_{h}^{-}> e^{i\vec{k}\cdot(\vec{R}g^{-\vec{R}}h)}$$
 (2.41)

for $\vec{R}_{_{\bf G}}$ on sublattice i and $\vec{R}_{_{\bf h}}$ on sublattice 1.

We define the Fourier transform of the exchange operator as

$$\xi_{ij}(\vec{k}) = \vec{R}_{q} - \vec{R}_{h} \quad J_{gh} e^{i\vec{k} \cdot (\vec{R}_{g} - \vec{R}_{h})}$$
 (2.42)

for \vec{R}_g on the i sublattice and \vec{R}_h on the j sublattice. We define the parameter $\theta_i = \langle S_g^z \rangle / S$ for \vec{R}_g on sublattice i, and

$$\bar{\xi} = \sum_{j=1}^{\Sigma} \xi_{jj}(0) \theta_{j} \theta_{j}$$
 (2.43)

Equation 2.39 can be written in matrix form 25

$$\sum_{j} \{ \xi_{ij}(\vec{k}) - (\bar{\xi} - \theta_{j}E/2\pi) \delta_{ij} \} G_{j}(\vec{k},E) = + \delta_{ij/2\pi} \quad (2.44)$$

	• ::
	1.
	H.
	::
	:
	:
	.*
	•
	;
	•
	•
	;

In order to find the ordering temperature we need only $G_1(\vec{k},E)$ evaluated at E=0. If $\lambda_i(\vec{k})$ is the i th eigenvalue of $\xi_{ij}(\vec{k})$, then

$$G_1(\vec{k},0) = \frac{-1}{2\pi} \frac{1}{n} \sum_{i=1}^{n} \frac{1}{\lambda_i(\vec{k}) - \bar{\xi}}$$
 (2.45)

and

$$T_C = \frac{S(S+1)}{3k_B} \frac{1}{\langle G_1(\vec{k},0) \rangle_k}$$
 (2.46)

There are two points worthy of comment. The average exchange interaction of equation 2.43 is defined assuming that all magnetic sublattices are crystalographically equivalent (called a Bravais system). The molecular field result for this system can be obtained by setting λ_i (\vec{k})=0.

3. Other methods

Molecular field theory gives a good qualitative description of many magnetic systems but has two serious shortcomings: quantitatively, MFT is only an order of magnitude theory and it contains no discussion of effects based on correlation between spins. The MFT takes no account of short range order and fails to predict the correct behavior of the magnetization near T=0 and T=T_C²⁶. GFT is much better quantitatively but suffers from a complexity requiring elaborate approximation schemes such as Callen decoupling²⁷ and moment conserving²⁸. These are essentially all temperature theories, Green function theory becoming equivalent to spin wave theory²⁹ at low temperatures. Some other methods are:

(a) The Lyons-Kaplan 30 or generalized method of Luttinger and Tisza 31,15 is a method for finding the classical ground

state configuration by minimizing the Hamiltonian subject to a "weak constraint"

$$\sum_{\mathbf{n},\mathbf{v}} (\vec{\mathbf{s}}_{\mathbf{n}\mathbf{v}} \cdot \vec{\mathbf{s}}_{\mathbf{n}\mathbf{v}}) = N_{\mathbf{v}}^{\Sigma} S_{\mathbf{n}\mathbf{v}}^{2}$$
 (2.47)

or

$$\sum_{n,\nu}^{\Sigma} \alpha_{n\nu}^2 \vec{S}_{n\nu} \cdot \vec{S}_{n\nu} = \sum_{n,\nu}^{\Sigma} \alpha_{n\nu}^2 S_{n\nu}^2$$
 (2.48)

The ground state spin configuration is found by solving the eigenvalue problem for the Fourier transform of the exchange operator subject to conditions on the α_{nv} .

(b) Probably the best available method for calculation transition temperatures involves high temperature expansions 32 . At temperatures above the ordering temperature the thermodynamical quantities are expanded in powers of J/k_BT . Given the Heisenberg Hamiltonian with Zeeman interaction

$$Z = tr[exp(-H/k_BT)]$$
 (2.49)

$$\chi = \frac{\partial^2}{\partial H^2} \left[k_B^{TlnZ} \right]$$
 (2.50)

Defining reduced susceptibility and temperature we find

$$\bar{\chi} = 1/3 \text{ S(S+1)} \sum_{n=0}^{\infty} a_n / \theta^n$$
 (2.51)

where

$$\bar{\chi} = \frac{1}{Ng^2 u_R^2} \chi \qquad (2.52)$$

$$\theta = k_{R}T/J \tag{2.53}$$

The real work is involved in finding the a_n 's. For a simple cubic ferromagnet with nearest neighbor interactions only, Rushbrooke and Wood³² quote the relation

$$k_{B}^{T}C/J = (5/96)(z-1)(11S(S+1) -1)$$
 (2.54)

for z nearest neighbors.

The high temperature expansion is exact in the limit of including enough coefficients (for the interaction assumed). Ordering temperatures by HTE are 30 per cent to 50 per cent lower than the MFT values.

. . .

...

:

III. THE MAGNETIC PHASE DIAGRAM

Antiferromagnets have very interesting behavior in applied magnetic fields. Suppose we have an antiferromagnet with isotropic exchange and uniaxial anisotropy L. The energy of the system with applied field H in the easy, or parallel, direction is, using MFT³³

$$\varepsilon'' = -\frac{1}{2}\chi''(H'')^2 - NLS^2$$
 (3.1)

where N is the total number of spins. The energy for H perpendicular to the antiferromagnetic axis is

$$\varepsilon^{\perp} = -\frac{1}{2}\chi^{\perp}(H^{\perp})^{2} \tag{3.2}$$

Since antiferromagnets in the ordered state are characterized by $\chi^{\perp}>\chi$ ", when H = H" becomes large enough, the perpendicular configuration will be energetically favorable and the spins will flop perpendicular to the field - called spin-flop. The critical field is found by equating the energies

$$\varepsilon^{\perp} = \varepsilon^{\parallel}$$
 (3.3)

which yields

$$H_{SF} = \sqrt{2NLS^2/(\chi^{\perp} - \chi^{*})}$$
 (3.4)

If one continues to increase the field, the spins will saturate and the system is said to be in a paramagnetic state. We are interested in investigating in detail the behavior of antiferromagnets with a more general anisotropic interaction.

		·
		ŧ.,
		 57
		 .
		4.
		•
		(
		,

A. The Classical Energy

Let us consider the properties of an antiferromagnet at T=0. We will rewrite the Hamiltonian, in the molecular field approximation, as a free energy and solve the problem classically. We assume a simple Hamiltonian but one which includes each type of second order anisotropy.

$$H = H_{ex} + H_{aL} + H_{aK} + H_{D} + H_{Z}$$
 (3.5)

where

$$H_{\text{ex}} = -\frac{1}{2} \sum_{ij} J_{ij} \dot{S}_{i} \cdot \dot{S}_{j} \qquad \text{isotropic} \qquad (3.6a)$$
exchange

$$Ha_{L} = -\frac{1}{2}L' \stackrel{\Sigma}{i} S_{i}^{z}S_{i}^{z} \qquad \text{uniaxial}$$
anisotropy (3.6b)

$$Ha_{K} = \frac{1}{2} \sum_{ij}^{\Sigma} K_{ij} S_{ij}^{z}$$
 anisotropic exchange (3.6c)

$$H_{D} = \frac{1}{2} \sum_{ij}^{\Sigma} D_{ij} (S_{i}^{z} S_{j}^{x} - S_{i}^{x} S_{j}^{z})$$

$$Moriya anti-$$
symmetric exchange

$$H_{z} = -gu_{B} \vec{H} \cdot \vec{i} \vec{S}_{i}$$
 Zeeman (3.6e) interaction

where $K_{ii} = J_{ii} = 0$ and $D_{ij} = -D_{ji}$. We now express the Hamiltonian as a free energy, considering the spins to be classical vectors interacting with molecular fields³⁴.

$$\varepsilon' = E/N_s = S^2 \{ J \cos(\alpha_1 - \alpha_2)$$

$$-\frac{1}{2}L(\cos^2\alpha_1 + \cos^2\alpha_2) + K \cos\alpha_1 \cos\alpha_2$$

$$+ D \cos\theta \sin(\alpha_1 - \alpha_2) \} -gu_B S \{ (3.7) \}$$

 $H^{x}(\sin \alpha_{1} + \sin \alpha_{2})\cos \theta + H^{y}(\sin \alpha_{1} + \sin \alpha_{2})\sin \theta + H^{z}(\cos \alpha_{1} + \cos \alpha_{2})$

where N_S is the number of spins per sublattice, α_1 denotes sublattice A, a ϵ A, and α_2 denotes sublattice B, b ϵ B (Fig. 1).

$$J = -\frac{\Sigma}{a \in A} Jab = -\frac{\Sigma}{b \in B} Jab$$
 (3.8a)

$$L = L'(1-1/2S)$$
 (3.8b)

$$K = \sum_{a \in A} Kab = \sum_{b \in B} Kab$$
 (3.8c)

$$D = \frac{\Sigma}{a \varepsilon A} Dab = \frac{\Sigma}{b \varepsilon B} Dab$$
 (3.8c)

We define the molecular fields as

$$H_{E} = JS/gu_{B}$$

$$H_{L} = LS/gu_{B}$$

$$H_{K} = KS/gu_{B}$$

$$H_{D} = DS/gu_{B}$$
(3.9)

The angles are expressed in a more convenient set by the transformation

$$\alpha_{1} = \alpha + \phi$$

$$\alpha_{2} = \pi + \alpha - \phi$$
(3.10)

The energy is expressed as a dimensionless quantity by dividing out the exchange field

$$\varepsilon = E/NJS^{2} = -\cos(2\phi) - h_{L}[\cos(2\phi)\cos^{2}\alpha + \sin^{2}\phi] - h_{K}[\cos^{2}\alpha - \sin^{2}\phi]$$

$$- h_{D}\sin(2\phi)\cos\theta - 2h^{X}\sin\phi\cos\alpha\cos\theta$$

$$- 2h^{Y}\sin\phi\cos\alpha\sin\theta + 2h^{Z}\sin\phi\sin\alpha$$
(3.11)

Figure 1. Definition of the angles describing the spin array

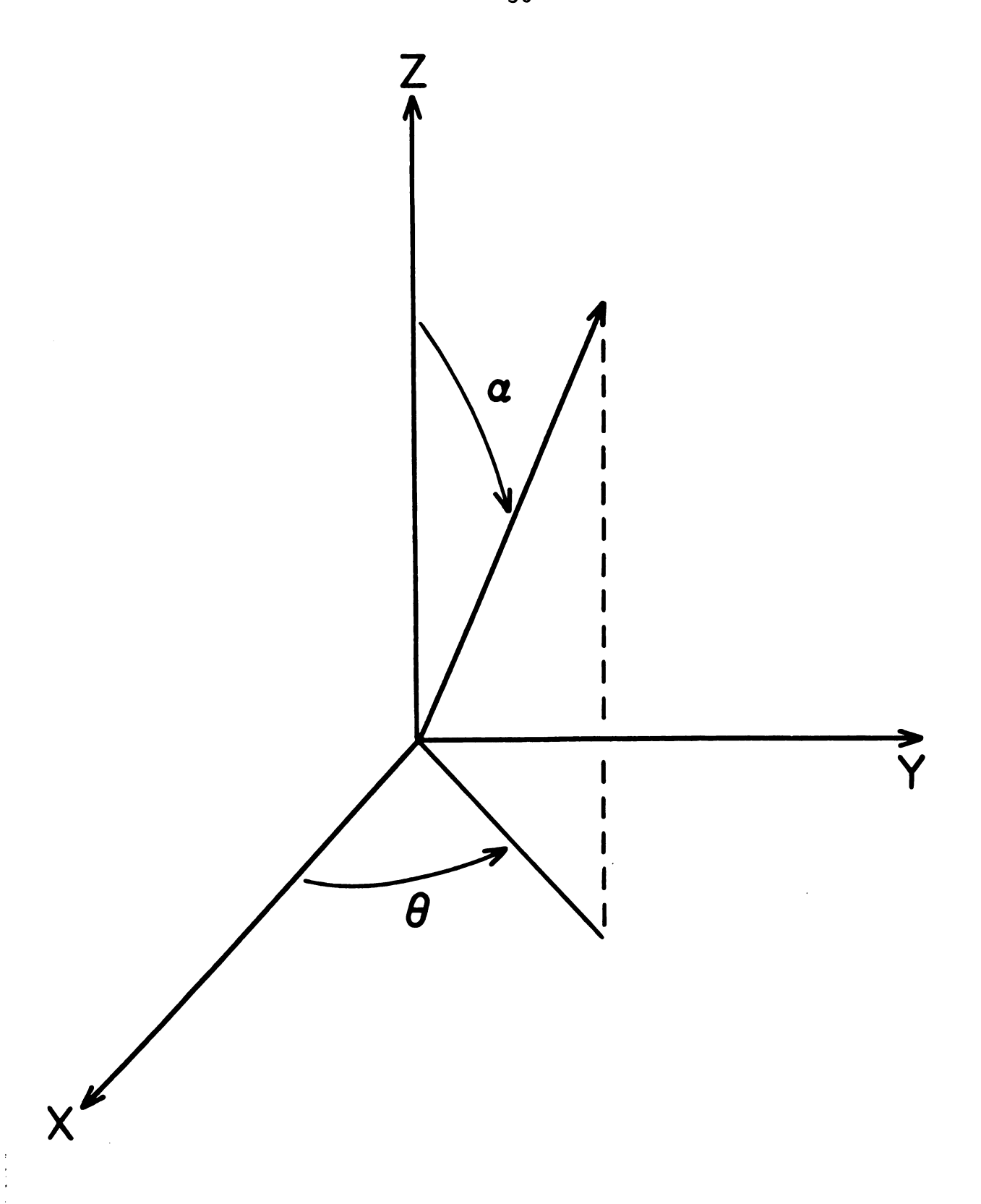


Figure 1

where $h_L = H_L/H_E$, etc.

Our problem is now thermodynamical - we must solve the equations of equilibrium and stability. The equilibrium equations are

$$\frac{\partial \varepsilon}{\partial \eta_i} = 0 \tag{3.12}$$

The stability equations are

$$\frac{\partial^{2} \varepsilon}{\partial \eta_{i}^{2}} \frac{\partial^{2} \varepsilon}{\partial \eta_{i}^{2}} - \left| \frac{\partial^{2} \varepsilon}{\partial \eta_{i}^{3} \eta_{j}} \right|^{2} = s(\eta_{i}, \eta_{j}) > 0$$
 (3.13)

where

$$\dot{n} = (\phi, \alpha, \theta)$$

B. The Zero Temperature Phases

The zero temperature phases of the uniaxial antiferromagnet $(h_D=0)$ have been studied in the molecular field approximation 6,34 , in the spin wave approximation 35 , and in the RPA and Callen decoupled Green function approximations. 36 More recently 37,38,39 , the solutions to equation 3.11 have been considered in the limit of $h_D<<1$. However, three subjects need to be investigated in detail: the nature of the spin flop discontinuity, the effects of large h_D and the paramagnetic boundaries.

1. The zero field equilibrium configuration

If we let h=0 and evaluate equation 3.12 for α , θ and ϕ we find the equilibrium conditions are

$$\theta_0 = \alpha_0 = 0 \tag{3.14a}$$

and

$$\phi_{O} = \frac{1}{2} \tan^{-1} \{ 2h_{D} / (2 + h_{K} + h_{L}) \}$$
 (3.14b)

The spins lie in the xz plane, perpendicular to the D vector, "antiferromagnetically" aligned on the Z axis but tipped an angle ϕ_{0} toward the X axis. This produces a net moment

$$M_{O}^{X} = \sin \phi_{O}$$

in the X direction

2. The parallel configuration

If we let $\vec{h} = (0,0,h)$ the applied field is parallel to the easy axis, from symmetry we see $\theta=0$. The spin flop transition described in the beginning of Chapter III is actually a first order transition. The first order phase transition is characterized 36 by discontinuities in the energy or magnetization and a magnetic hysteresis. There is no unique spin flop field but a region in which both the AF state and the SF state are stable. The upper boundary of this region is h and the lower is h sc. If one increases the applied field from zero, the AF state remains stable up to h_{sh}, analogous to the superheated liquid-gas transition. If one then reverses the process, reducing the field, the SF state remains stable down to h_{sc}, analogous to the supercooled gas-liquid transition. The energies of the AF and SF states are equal at the thermodynamical transition h, implying that if $h_{th} < h < h_{sh}$, the AF state is metastable, and if $h_{sc} < h < h_{th}$, the SF state is metastable. Let us examine the equations of the parallel configuration. The equilibrium equations are

$$\partial \varepsilon / \partial \phi = [2 + h_K + h_L \cos(2\alpha)] \sin(2\phi) - 2h_D \cos(2\phi) + 2h \cos\phi \sin\alpha = 0$$
 (3.15)

$$\partial \varepsilon / \partial \alpha = [h_{K} + h_{L} \cos(2\phi)] \sin(2\alpha) + 2h \sin\phi \cos\alpha = 0$$
 (3.16)

The stability function is

$$S(\phi,\alpha) = \{[2 + h_K + h_L\cos(2\alpha)]\cos(2\phi) + 2h_D\sin(2\phi)$$

$$-h \sin \phi \sin \alpha\}\{[h_K + h_L\cos(2\phi)]\cos(2\alpha)$$

$$-h \sin \phi \sin \alpha\}-\{h_L\sin(2\phi)\sin(2\alpha)$$

$$-h \cos \phi \cos \alpha\}^2 = 0$$
(3.17)

If $\cos (\alpha) \neq 0$, ϕ and α are related by equation 3.16

$$\sin \alpha = -h \sin \phi/(h_{\kappa} + h_{\tau} \cos(2\phi))$$
 (3.18)

The transition from AF to SF states, called the superheated transition, is defined by $S(\alpha,\phi)=0$. The solution for $h_D=0$ is well known and is given by

$$h_{sh}(0) = \sqrt{(2+h_K+h_L)(h_K+h_L)}$$
 (3.19)

The $h_D^{=0}$ case is characterized by $\alpha=\phi=0$ for $h< h_{sh}(0)$ and $\alpha=-\frac{\pi}{2}$ for $h>h_{sh}(0)$. When $h_D\neq 0$, the net moment is pulled from the x axis, increasing in magnitude as it approaches the z axis. Therefore, when $h_D\neq 0$, $h< h_{sh}(h_D)$, α and ϕ are not zero. As h approaches h_{sh} , $|\alpha|$ becomes larger and approaches a critical angle $\alpha_{sh}(h_D)$ (Fig. 2). When h exceeds h_{sh} , then $\alpha=-\frac{\pi}{2}$ with an accompanying discontinuity. The $h_D\neq 0$ equations were solved by computer (Fig. 3) using Newton's method for three unknowns (Appendix A).

The spin flop state is defined by letting $\alpha=-\frac{\pi}{2}$. The boundaries of this phase occur at $S(-\frac{\pi}{2},\phi)=0$. When $h_D=0$, there are two phase boundaries, a first order spin flop to antiferromagnetic, called the supercooled boundary, and a second order spin flop to

Figure 2. The superheated critical angle $\alpha_{\mbox{sh}}\,(h_{\mbox{D}})$ vs. $h_{\mbox{D}}$ with $h_{\mbox{K}}{=}0$ and $h_{\mbox{L}}{=}0.1$

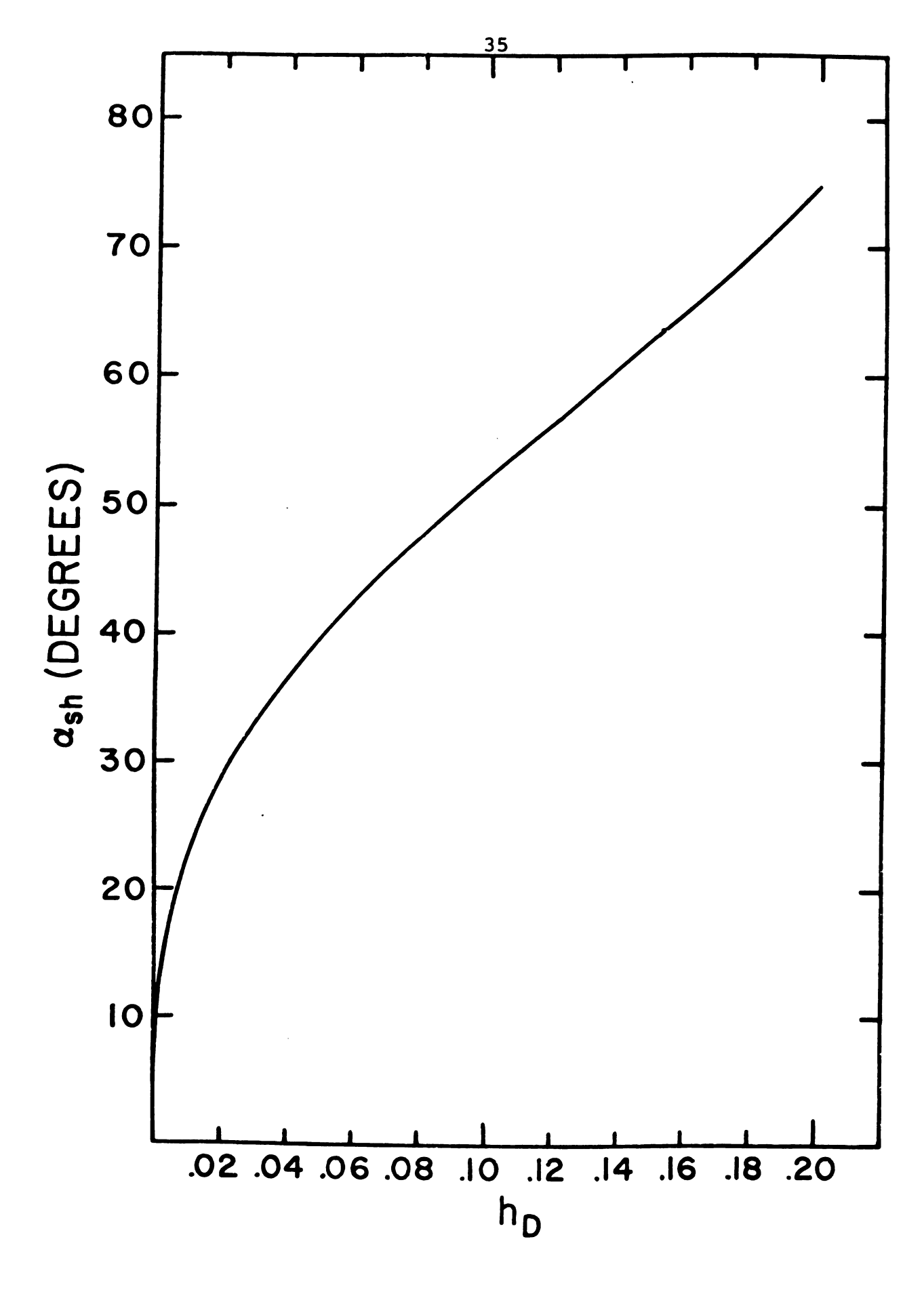


Figure 2

Figure 3. The spin flop critical fields vs. \mathbf{h}_{D} with $\mathbf{h}_{K}\text{=0}$ and $\mathbf{h}_{L}\text{=0.1}$

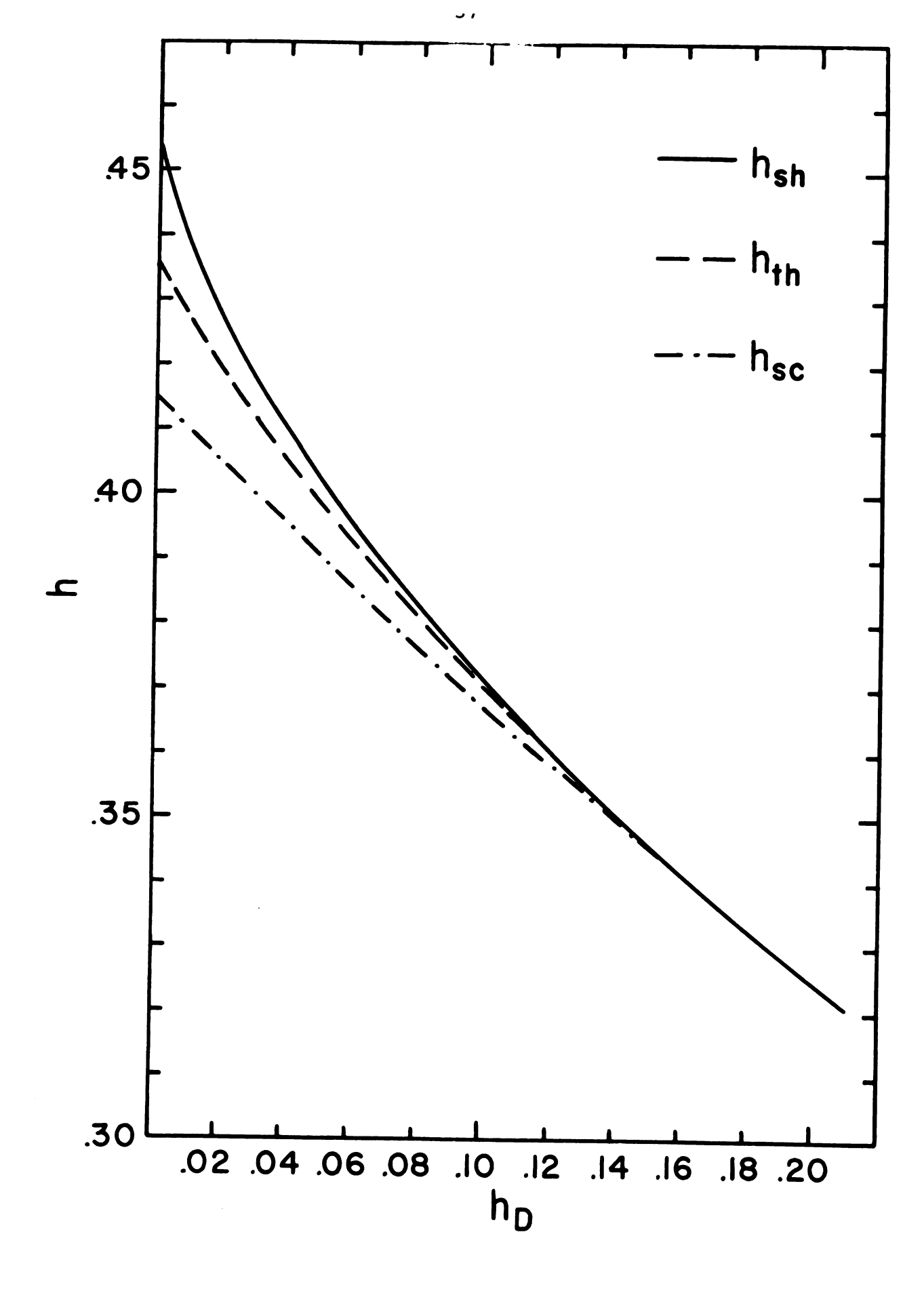


Figure 3

paramagnetic boundary at higher field. The h_D^{-2} solutions are

$$h_{sc}(0) = (2+h_K-h_L) \sqrt{(h_K+h_L)/(2+h_K+h_L)}$$
 (3.20)

$$h_{p}^{"}(0) = 2 + h_{K} - h_{L}$$
 (3.21)

Consequently, the spin flop state is stable for h_{sc}<h<h_p.

The $h_D \neq 0$ solutions were found numerically (Fig. 3). The paramagnetic transition, which corresponds to $\phi = \frac{\pi}{2}$, does not occur at finite fields, since the D-M interaction will lower the energy of the spins if they cant slightly. To see this, examine the energy when h is large, but finite, and $\phi = \frac{\pi}{2} - \delta$. From equation 3.15 we see that $\delta \approx \frac{h_D}{h}$ so the energy, to order h_D^2/h , is

$$\varepsilon \simeq 1 + h_{K} - h_{T} - 2h - h_{D}\delta$$

No matter how large h is, $\delta \neq 0$ will give a lower energy.

Experimentally, one almost always observes the thermodynamic transition defined by $\varepsilon_{AF} = \varepsilon_{SF}$. This is because for fields in the metastable regions, a slight disturbance foments the transition. One usually argues that nucleation centers in the crystal prevent metastable states from being long lived 40 . The procedure for finding the thermodynamic critical field h_{th} is to define

$$\Delta = \epsilon_{AF} - \epsilon_{SF}$$

and solve for $\Delta=0$. When $h_D=0$, the solution is

$$h_{th}(0) = \sqrt{(2+h_K-h_L)(h_K+h_L)}$$
 (3.22)

which is equivalent to equation 3.4. The $h_D \neq 0$ equations were solved numerically (Fig. 3) and as one would expect $\alpha_{th} < \alpha_{sh}$.

Figure 4. A comparison of numerically calculated $h_{\mbox{sc}}$ with the approximation of equation 3.27

The critical fields obey h sch th h but

$$h_{th} = \sqrt{h_{sc}h_{sh}}$$

only when $h_D=0$.

Suppose we let $\theta=0$ and $\alpha=-\frac{\pi}{2}$, then if $h_D^{<<1}$ and $h_L^{<<1}$, we can solve equations 3.15 and 3.17 to obtain an approximation for $h_{SC}(h_D)$.

$$(2+h_K-h_L)\sin(2\phi) - 2h_D\cos(2\phi) - 2h\cos\phi = 0$$
 (3.23)

$$h_{K} + h_{T} \cos(2\phi) - h \sin \phi = 0$$
 (3.24)

Assuming ϕ is small, equation 3.23 gives

$$\sin(\phi) = (h+h_D)/(2+h_K-h_L)$$
 (3.25)

It is important to notice that the term $(h)\sin(\phi)$ is second order in ϕ , so we write equation 3.24

$$h_{K} + h_{L} - 2h_{L}\sin^{2}\phi - h \sin \phi = 0$$
 (3.26)

Substituting $\sin(\phi)$ and neglecting h_D^2 terms we get, assuming $h_D^{<}h_{T,'}$

$$h_{sc}(h_D) = (-h_D + \sqrt{h_D^2 + 4h_{sc}^2(0)})/2$$
 (3.27)

In Figure 4 we have a comparison of the numerically calculated solutions and the approximate solution of equation 3.27.

3. The perpendicular configuration

The magnetic field applied perpendicular to both D and the easy axis, h=(h,0,0), results in $\theta=\alpha=0$. When $h_D=0$, a second order paramagnetic transition occurs at

$$h_{p}(0) = 2 + h_{K} + h_{L}$$
 (3.28)

As in the previous case, $h_{D}\neq 0$ destroys the second order paramagnetic transition

4. The D configuration

When $\vec{h}=(0,h,0)$ is parallel to \vec{D} and perpendicular to the plane of the spins (for zero field), we can solve the equations exactly. For $h_D=0$ the problem is equivalent to the perpendicular configuration (section 3). For $h_D\neq 0$, the equilibrium equations are, for $\alpha=0$

$$\frac{\partial \varepsilon}{\partial \phi} = (2 + h_K + h_L) \sin(2\phi) - 2h_D \cos(2\phi) \cos\theta$$

$$-2h \cos \phi \cos \theta = 0$$
(3.29)

and

$$\partial \varepsilon / \partial \theta = 2h_{D} \sin \phi \cos \phi \sin \theta - 2h \sin \phi \cos \theta = 0$$
 (3.30)

The stability function is

$$S(\phi,\theta) = \{(2+h_K+h_L)\cos(2\phi) + 2h_D\sin(2\phi)\cos\theta + h\sin\phi\sin\theta\} \{h\sin\phi\sin\theta + h_D\cos\phi\sin\phi\cos\theta$$
 (3.31)
$$-\{h_D\sin\theta\cos(2\phi) - h\cos\phi\cos\theta\} ^2 \ge 0$$

Equation 3.30 yields the immediate result

$$\cos\theta = (h_D/h) \cos\phi \sin\theta$$
 (3.32)

We see that the magnetic field pulls the net moment an angle θ from the x axis. The solution to equations 3.29 and 3.31 is $\theta = \phi = \frac{\pi}{2}$ at a critical field

$$h_p^{\perp} = (h_p^{\perp}(0) + \sqrt{[h_p^{\perp}(0)]^2 + 4h_p^2})/2$$
 (3.33)

5. Discussion of the effect of $h_{\overline{D}}$ on the zero temperature phases

The antisymmetric canting interaction has had an interesting effect on our system. The net moment produced by the canting is rotated toward a magnetic field. For h applied parallel to the easy axis, the spin flop transition is still first order, but as h_D increases the transition occurs at greater angles and the hysteresis is reduced until the metastable region becomes extremely narrow. The effect of h_D is to reduce the spin flop fields; we can see this by examining equation 3.25

$$\sin \phi \simeq (h+h_D)/(2+h_K - h_L) \qquad (3.25)$$

Imagine that $h_D^{=0}$, $h_L^{<<1}$ and $h=h_{SC}^{}(0)+\delta h$, where $\delta h<<1$, so that the spins are in the spin flop state. We can simultaneously decrease h and increase $h_D^{}$ without changing ϕ , consequently, for small $h_D^{}$

$$h_{sc}(h_D) - h_{sc}(0) \sim h_D$$

The paramagnetic transition occurs at h= ∞ unless \vec{h} is parallel to \vec{D} . If \vec{h} is parallel to \vec{D} the D-M interaction is weakened as $\theta + \frac{\pi}{2}$ and the h_D term in the energy of equation 3.22 becomes second order in (h_D/h) and is overpowered by lower order terms in h.

C. The Temperature Dependence of the Critical Fields
and the H-T Magnetic Phase Diagram

One can calculate with little difficulty the temperature dependence of the critical fields for a uniaxial antiferromagnet in the molecular field approximation. The quantitative results

will be inaccurate but we can get a good picture of the qualitative behavior.

We assume a Hamiltonian of the form

$$H = \frac{1}{2} |\mathbf{J}|_{\mathbf{i}\mathbf{j}}^{\Sigma} \dot{\mathbf{s}}_{\mathbf{i}} \cdot \dot{\mathbf{s}}_{\mathbf{j}} - \frac{1}{2} \mathbf{L}_{\mathbf{i}}^{\Sigma} (\mathbf{S}_{\mathbf{i}}^{\mathbf{z}})^{2} - g \mathbf{u}_{\mathbf{B}} \dot{\mathbf{H}} \cdot \dot{\mathbf{s}}_{\mathbf{i}}^{\Sigma} \dot{\mathbf{s}}_{\mathbf{i}}$$
(3.34)

1. The paramagnetic boundaries

Consider an antiferromagnet in the ordered state in an applied field \vec{H} . The effective fields acting on the respective sublattices are, where $M_O=N_Sgu_BS$

The equilibrium condition for \overrightarrow{H} perpendicular to the easy axis gives 41

$$\hat{H}_{1}^{\text{effective}} = \hat{H}_{2}^{\text{effective}} = (H_{E} + H_{L})\hat{M}_{1}/M_{O}$$
 (3.36)

where $\vec{M}_1 = -\vec{M}_2$. The AF to paramagnetic transition occurs at 41

$$H_D^{\perp}(H) = (2H_E + H_L)M_1(0,T)/M_0$$
 (3.37)

If $T \simeq T_N(0)$, then⁴¹

$$M_{1}(0,T) = M_{0} \left\{ \frac{10(S+1)^{2}}{3(2S^{2}+2S+1)} \right\}^{\frac{1}{2}} (1-T/T_{N})^{\frac{1}{2}}$$
(3.38)

We can express the field dependence of the critical temperature as

$$\frac{T_N(0) - T_N(H)}{T_N(0)} = \beta \left[H / H_p^{\perp}(0) \right]^2$$
 (3.39)

where

$$\beta = (3/10)(2s^2 + 2s + 1)/(s + 1)^2 \tag{3.40}$$

A similar treatment for H parallel to the easy axis gives

$$\frac{T_{N}(0)-T_{N}''(H)}{T_{N}(0)} = 3\beta [H/H_{p}^{L}(0)]^{2}$$
 (3.41)

for H<H_{SF} and

$$\frac{T_{N}(0)-T_{N}^{"}(H)}{T_{N}(0)} = 3\beta [H/H_{p}^{"}(0)]^{2}$$
 (3.42)

for H>H_SF. We can also express this as a temperature dependence of the critical field, for ${\tt T\simeq T}_N$

$$H_{p}^{-}(T) = H_{p}^{-}(0) [(1-T/T_{N})/\beta]^{\frac{1}{2}}$$
 (3.43)

$$H_{p}^{"}(T) = H_{p}^{-}(0) [(1-T/T_{N})/3\beta]^{\frac{1}{2}}$$
 (3.44)

For $T \simeq 0$, we write, assuming $H > H_{SF}$

$$H_D''$$
 (T) = H_D'' (0) M_1 (0,T)/ M_O (3.45)

2. The spin flop boundaries

If we neglect the hysteresis effects, we can write the spin flop critical field

$$H_{SF} = [2N_{S}LS^{2}/(\chi^{3}-\chi^{"})^{\frac{1}{2}}$$
 (3.46)

If we examine the equations we used to derive this result, we see that the anisotropy term is actually the difference of the $L'<(S^Z)^2>$ term in the Hamiltonian for the spin flop and antiferromagnetic states.

$$LS^{2} = L'[\langle (S^{2})^{2} \rangle_{AF} - \langle (S^{2})^{2} \rangle_{SF}]$$
 (3.47)

Since the spin flop corresponds to a spin axis reorientation, let

$$\langle (S^z)^2 \rangle_{SF} \simeq \langle (S^y)^2 \rangle_{AF} = \frac{1}{2} [S(S+1) - \langle (S^z)^2 \rangle_{AF}]$$
 (3.48)

Therefore

$$LS^{2} = (L'/2) [3 < (S^{2})^{2} >_{AF} -S (S+1)] = L'S (S-\frac{1}{2}) F (T)$$
 (3.49)

Yosida 42 has shown that F(T) can be written

$$F(T) = (S/(S-\frac{1}{2}))[(S+1)/S-3B_{S}(x) \coth(x/2S)/2S]$$

$$x = JS/k_{R}T$$
(3.50)

and $\langle S^z \rangle = SB_S(x)$. The susceptibility in the AF state in the molecular field approximation is given by (see section IV)⁴¹

$$\chi^{\perp} - \chi^{\prime\prime} \simeq \chi^{\perp}(0) (1-T/T_N)$$
 (3.51)

so we can express the temperature dependence of the spin flop field as

$$H_{SF}(T) = H_{SF}(0) [F(T)/(1-T/T_N)]^{\frac{1}{2}}$$
 (3.52)

Where F(0)=1 and $F(T_N)=0$. At T=0, equations 3.8b and 3.49 are equivalent.

The temperature dependence of F(T) is such that, in the present approximation, H_{SF} increases slightly with temperature, increasing by 12 per cent at the Néel point. In practice, H_{SF} can increase or decrease with increasing temperature.

IV. THE THEORETICAL DEPENDENCE OF SUSCEPTIBILITY ON APPLIED FIELD AND TEMPERATURE -

THE ANTIFERROMAGNET

There are a number of techniques for studying magnetic insulators: nuclear and electron spin resonance 43, specific heat 44, neutron diffraction 45, and susceptibility to name a few. The primary advantage of susceptibility measurements is their sheer simplicity and minimal equipment requirements.

Our goal is to theoretically describe the behavior of susceptibility as a function of H and T so that we can determine the interactions dominating a given crystal by interpreting susceptibility data. The three parameters of interest are T, H, and the orientation of H with respect to the magnetic axes.

We will limit our treatment to the two sublattice antiferromagnet with second order anisotropy. In order to lay the groundwork, we will first consider the zero field susceptibility and
then the field dependence.

A. Zero Field Susceptibility

Susceptibility as a function of temperature for H=0
 We will be considering only the antiferromagnet, so we
 write the exchange as a positive quantity in the Hamiltonian

$$H = \frac{1}{2} \sum_{ij} J_{ij} \vec{S}_{i} \cdot \vec{S}_{j} - L' \frac{1}{2} \sum_{i} \{ (S_{i}^{z})^{2} \} - g\mu_{\beta} \vec{H} \cdot \sum_{i} \vec{S}_{i}$$
 (4.1)

The partition function Z is defined as

$$Z = tr[exp(-H/k_RT)]$$
 (4.2)

The susceptibility for small H is

$$\chi = (kT/H) (\partial Z/\partial H)/Z \tag{4.3}$$

a. The paramagnetic susceptibility is found by expanding Z in terms of $H/k_BT<<1$, which is the condition that $T_N<<T$. In order to make this expansion converge more rapidly, we write the Hamiltonian as a traceless quantity.

$$H_{i} = J \vec{S}_{i} \cdot \vec{S}_{j} - (L'/2) [(S_{i}^{z})^{2} - S(S+1)/3] - gu_{B} \vec{H} \cdot \vec{S}_{i}$$
 (4.4)

The partition function is expanded

$$Z = tr(I) - (1/k_BT)tr(H) + (1/k_BT)^2tr(H^2/2)$$
 . . . (4.5)

where tr(I) = S(S+1) and tr(H) = 0. Neglecting terms in $(1/k_BT)^3$ and H^2 , we find 42

$$\chi_{\rm p} = \frac{{\rm Ng}^2 {\rm u_B S \, (S+1)/3k_B}}{{\rm T + J \, S \, (S+1)/3k_B + (1-3\cos^2\theta) L' \, (2S+3) \, (2S-1)/60k_B}}$$
(4.6)

which we write

$$x_{p} = \frac{C}{T + \Theta + \gamma(1 - 3\cos^{2}\theta)}$$
 (4.7)

where $\cos(\theta)=1$ for χ_p^- and $\cos(\theta)=0$ for χ_p^- . The two constants are given by

$$\theta = JS(S+1)/3k_B = gu_B^H_E(S+1)/3k_B$$
 (4.8)

$$\gamma = (2S+3)(2S-1)L'/60k_B = gu_BH_L(2S+3)/30k_B$$
 (4.9)

Using equation 4.5, we can show that

$$1/\chi_{D} - 1/\chi_{D}^{"} = (2S+3)gu_{B}H_{L}/10k_{B}C$$
 (4.10)

Moriya has calculated the paramagnetic susceptibility for a canted antiferromagnet with Dzyaloshinsky-Moriya interaction included in H. Although his calculation is for D parallel to the easy axis, whereas our previous work assumed D perpendicular to the easy axis, one expects the existence of a weak moment to be the most important factor. The paramagnetic susceptibility is given by

$$\chi_{p}^{"} = C^{"}/(T+T_{o})$$
 (4.11)

$$\chi_{p} = C \left[1 + (T_{N}^{-T}_{O})/(T-T_{N}^{-T})\right]/(T+T_{N}^{-T})$$
 (4.12)

$$\chi_{p}^{N} = C T_{a}/[(T+T_{N})(T-T_{N})]$$
 (4.13)

where " denotes parallel to the easy axis, N denotes parallel to the net moment and \perp denotes the perpendicular to these directions. The temperatures are given by

$$T_{O} = JS(S+1)/3k_{R}$$
 (4.14)

$$T_a = DS(S+1)/3k_B$$
 (4.15)

$$T_{N} = (T_{O}^{2} + T_{a}^{2})^{\frac{1}{2}}$$
 (4.16)

Note that in the canted antiferromagnet the paramagnetic susceptibility measured perpendicular to D increases much faster than 1/T as one approaches the critical temperature.

b. The susceptibility in the antiferromagnetic state is calculated by writing the effective field acting on the i th spin and expanding the Brillouin function about a small applied field. The effective field acting on the i th spin is

$$\vec{H}_{i}^{\text{effective}} = \vec{H} - H_{E} < \vec{S}_{j} > /S + H_{L} < S_{i}^{z} > /S \hat{z}$$
(4.17)

If we let $\vec{H} = \vec{H}\hat{z}$, S_i and S_j will remain parallel to the z axis, with thermal average values

$$\langle S_i \rangle = SB_S \{ [gu_B S/k_B T] [H-H_E \langle S_i \rangle/S + H_L \langle S_i \rangle/S] \}$$
 (4.18)

We now expand the Brillouin function⁶ about H=0, letting $\delta S_i = \delta S_j$ and $\langle S_i \rangle_0 = -\langle S_j \rangle_0$,

$$\langle S_i \rangle = SB_S(x_0) + S\delta x B_S(x_0)$$
 (4.19)

Combining equations 4.18 and 4.19 we can write

$$\delta S = (gu_B S^2 / k_B T) [H + (-H_E + H_L) \delta S / S] B_S' (x_O)$$
 (4.20)

Therefore, if we define

$$\hat{c}M = Ngu_{R}\delta S \tag{4.21}$$

and

$$\chi = \delta M/\delta H \tag{4.22}$$

then the parallel susceptibility is

$$\chi'' = [Ng^2 u_B^2 S^2 B_S'(x_0)] / [k_B^T + g u_B^S (H_E - H_L) B_S'(x_0)]$$
 (4.23)

where $x_0 = gu_B(H_E + H_L) < S >_O/k_BT$. A similar treatment shows the perpendicular susceptibility to be approximately temperature independent

$$\chi' = Ngu_B S/(2H_E + H_L)$$
 (4.24)

Since the derivative of the Brillouin function goes to zero exponentially as T goes to zero, the parallel susceptibility is zero at T=0. The results for the zero field susceptibility are summed up in Figure 5 for the antiferromagnet with negligible paramagnetic anisotropy.

Figure 5. Susceptibility vs. temperature in the molecular field approximation

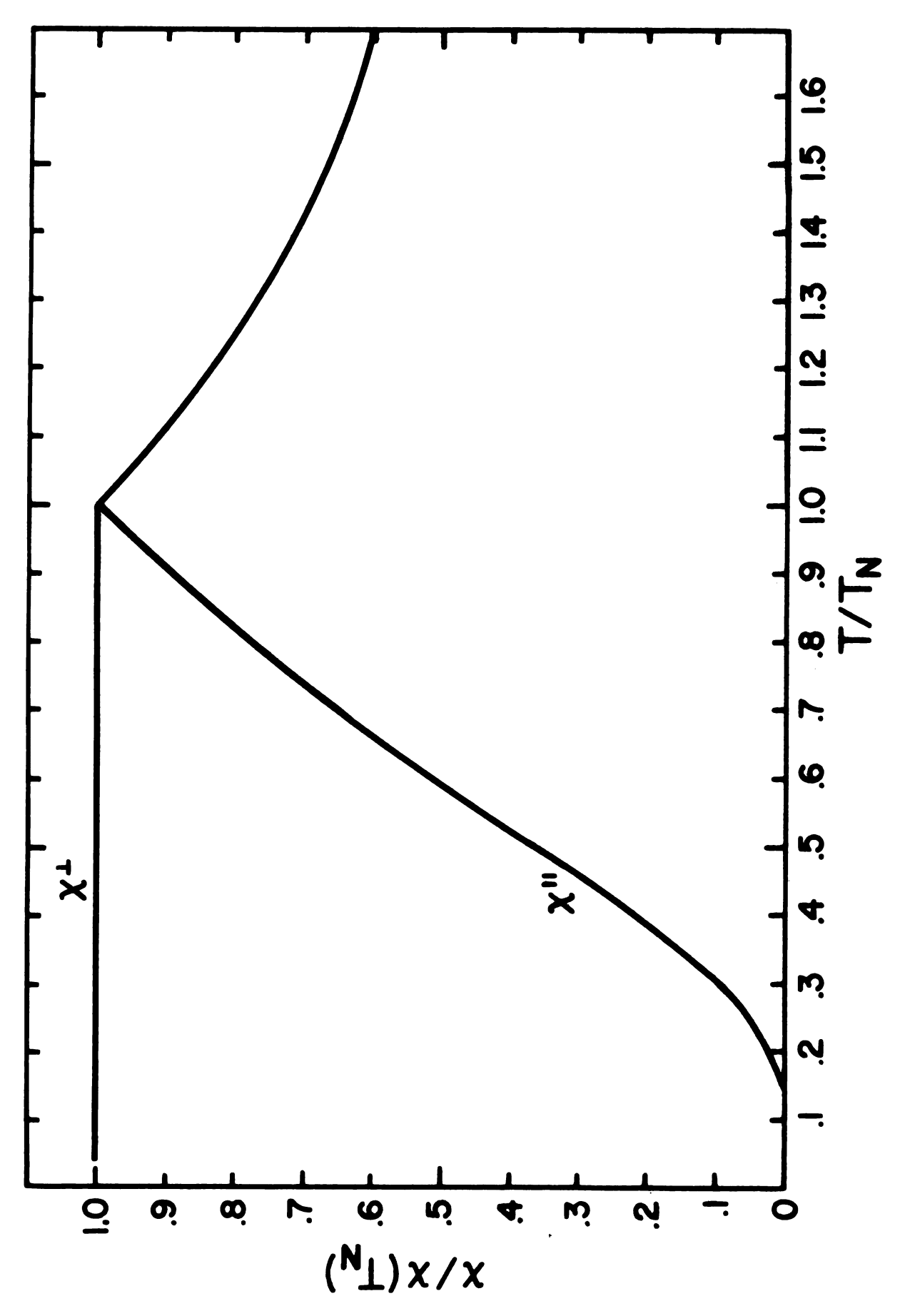


Figure 5

2. Susceptibility as a function of angle for H=0.

Consider a system whose susceptibility is uniaxial. If a magnetic field is applied at an angle θ with respect to the easy axis, then the magnetizations produced will be, assuming H is very small,

$$M'' = \chi''H\cos(\theta) \tag{4.25}$$

$$M^{\perp} = \chi^{\perp} H \sin(\theta) \tag{4.26}$$

The magnetization in the direction of the applied field is the sum of the components of M'' and M^{\perp} in this direction.

$$M^{H} = M^{"}\cos(\theta) + M^{\perp}\sin(\theta)$$
 (4.27)

or

$$M^{H} = \chi'' H \cos^{2}(\theta) + \chi^{\perp} H \sin^{2}(\theta)$$
 (4.28)

The susceptibility measured in the direction given by θ is

$$\chi(\theta) = dM^{H}/dH = \chi''\cos^{2}(\theta) + \chi^{\pm}\sin^{2}(\theta)$$
 (4.29)

B. The Susceptibility in Applied Field

We will first consider the susceptibility in applied field along the principal axes for the canted antiferromagnet. We are particularly interested in the directions perpendicular to \vec{D} in which we discovered that no second order paramagnetic critical field exists at T=0. Since the behavior for T>T_N is that of a simple paramagnet, that is a gradual saturation with increasing H, we will limit our discussion to the ordered state at T=0. The behavior of the susceptibility with the applied field off the principal axes is more difficult so we will consider it only for the uniaxial antiferromagnet.

1. Susceptibility vs. H for the canted antiferromagnet at T=0.

The canted antiferromagnet has easy, medium and hard axes. The components of the magnetization written in reduced form are

$$\mathbf{m}^{\mathbf{X}} = \sin(\phi)\cos(\alpha)\cos(\theta) \tag{4.30}$$

$$m^{Y} = \sin(\phi)\cos(\alpha)\sin(\theta)$$
 (4.31)

$$m^{Z} = -\sin(\phi)\sin(\alpha) \tag{4.32}$$

where θ designates the location of the spin plane in the xy plane, α designates the orientation of the antiferromagnetic axis relative to the z axis and ϕ is the angle of cant (Fig. 1). The zero field equilibrium of this system is

$$\alpha_0 = 0$$
 $\theta_0 = 0$
 $\tan (2\phi_0) = 2h_D/(2+h_K+h_L)$

(4.33)

The zero field reduced susceptibilities are found by evaluating

$$dm^{i}/dh^{i} = \chi^{i}$$
 (4.34)

in the limit that $h \rightarrow 0$.

$$\chi_0^{x} = \cos^2 \phi_0 / [h_p^{\lambda}(0)\cos(2\phi_0) + 2h_D \sin(2\phi_0)]$$
 (4.35)

$$\chi_0^{\mathbf{Y}} = 2/[h_{\mathbf{p}}^{\perp}(0) + h_{\mathbf{p}}^{\perp}(h_{\mathbf{p}})]$$
 (4.36)

$$\chi_0^z = \sin^2 \phi_0 / [h_K + h_L \cos(2\phi_0)]$$
 (4.37)

The most interesting point is that the parallel susceptibility $\chi^{\mathbf{z}}_{n}$ is not zero at T=0.

The parallel susceptibility χ^2 is written from equations 4.32 and 4.34 as

$$\chi'' = -\sin\phi\cos\alpha \, d\alpha/dh - \cos\phi\sin\alpha \, d\phi/dh$$
 (4.38)

If we let $h_D^{=0}$, we can find the exact solutions for three possible states

i) Antiferromagnetic state

$$\alpha=0$$
 $\phi=0$ and (4.39) $\chi_{AF}^{m}=0$

ii) Spin flop state

$$\alpha = -\pi/2$$
 $\sin \phi = h/(2+h_K-h_L)$ (4.40) $\chi_{SF}^{"} = 1/(2+h_K-h_L)$

iii) Paramagnetic state

$$\alpha = -\pi/2$$
 $\phi = \pi/2$ (4.41) $\chi_D^n = 0$

The susceptibility is zero until the field reaches h_{SF} , it is a delta function at h_{SF} , then it is a step function out to $h_{S}^{*}(0)$ (Fig.6).

The $h_D\neq 0$ solutions were calculated numerically by computer. We see that the step function has become rounded (Fig.7) and χ " remains finite until $h\rightarrow \infty$, indicative of the fact that the paramagnetic transition has been destroyed by the D-M term. However, we note that a quasi-paramagnetic transition can be defined as an inflection point in the susceptibility. We have calculated $d\chi$ "/dh numerically and we see broad maximum (Fig.8) that becomes narrower as we decrease h_D .

The perpendicular susceptibility $\chi^{\mathbf{X}}$ is calculated from equations 4.30 and 4.34 as

$$\chi^{\perp} = \cos(\phi) \cos(\alpha) d\phi/dh - \sin\phi \sin(\alpha) d\alpha/dh$$
 (4.42)

i de

r.e

If we let $h_D^{=0}$, the exact solutions for the two possible states are

i) Antiferromagnetic state

$$\alpha = 0$$
 $\sin \phi = h/(2+h_K+h_L)$
 $\chi_{AF}^{\perp} = 1/(2+h_K+h_L)$ (4.43)

ii) Paramagnetic state

$$\alpha = 0 \qquad \qquad \phi = \pi/2$$

$$\chi_{AF}^{\perp} = 0 \qquad \qquad (4.44)$$

The $h_D^{=0}$ perpendicular susceptibility is a step function out to $h_D^{=0}$ (0) (Fig.6). The $h_D^{\neq 0}$ solutions were calculated numerically by computer. The perpendicular susceptibility is also rounded (Fig.7) and we can calculate $d\chi^{-1}/dh$ (Fig.8) for the inflection point.

The susceptibility χ^Y for $h_D^{=0}$ is the same as the perpendicular susceptibility. Since the system undergoes a phase transition even when $h_D^{\neq 0}$, the susceptibility in the y direction goes to zero at $h_D^{\downarrow}(h_D)$ of equation 3.33.

The quasiparamagnetic transition which manifests itself as an inflection point in the susceptibility can be defined by the criteria

$$d^{2}\chi/dh^{2} \mid_{h_{qp}} = 0 (4.45)$$

The equilibrium equation for $h>h_{sh}$ can be written from equations 3.15 and 3.29 as

$$h_{p}(0) \sin(2\phi) - 2h_{p}\cos(2\phi) - 2h \cos\phi = 0$$
 (4.46)

where $h_p(0) = h_p^w(0) = 2+h_K-h_L$ for h in the z direction $h_p(0) = h_p^{-1}(0) = 2+h_K+h_L$ for h in the x direction

Figure 6. Susceptibility vs. applied field with $h_{\rm D}^{\rm =0}$, $h_{\rm K}^{\rm =0}$ and $h_{\rm L}^{\rm =0.1}$

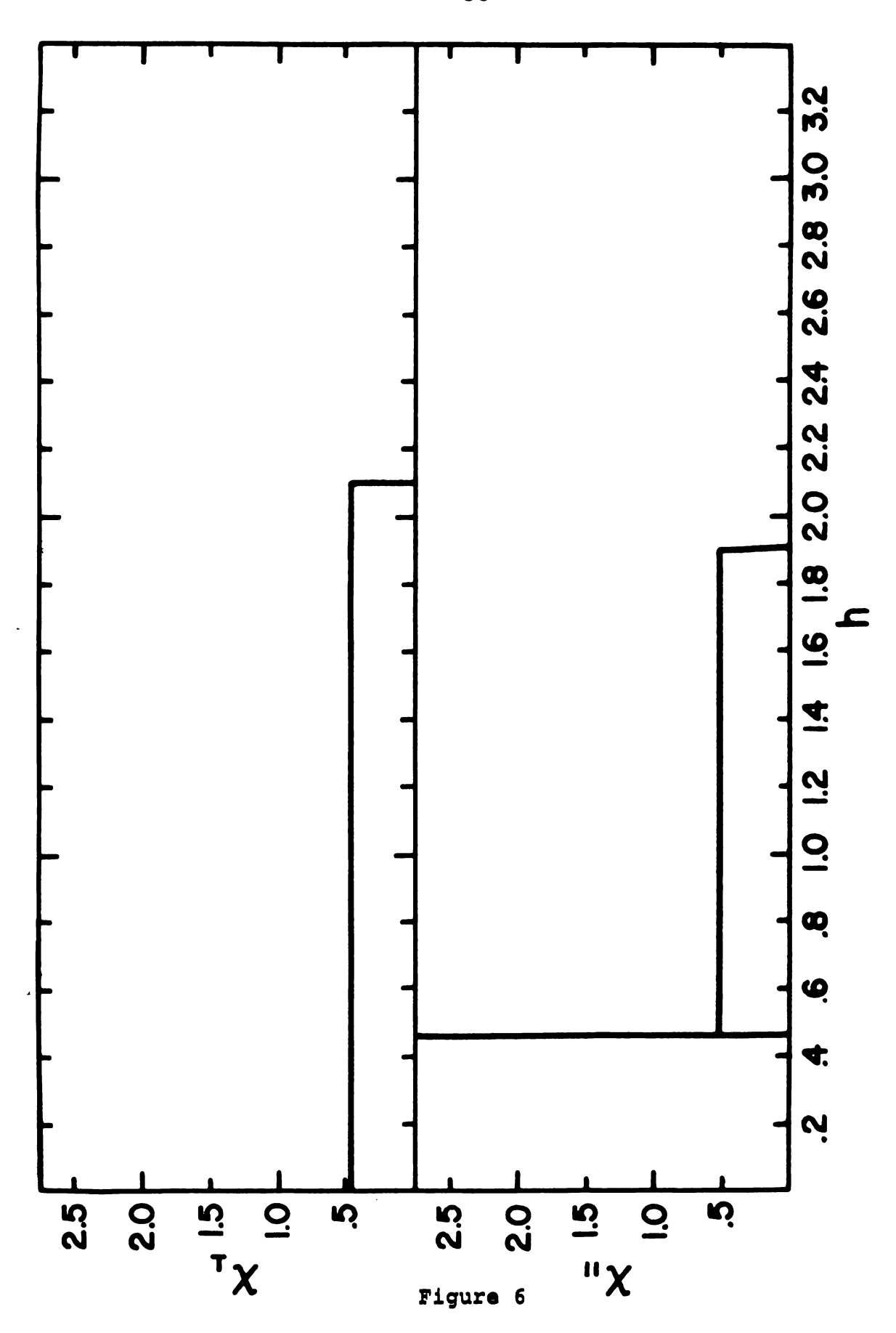


Figure 7. Susceptibility vs. applied field with $h_D^{=0.05}$, $h_K^{=0}$ and $h_L^{=0.1}$

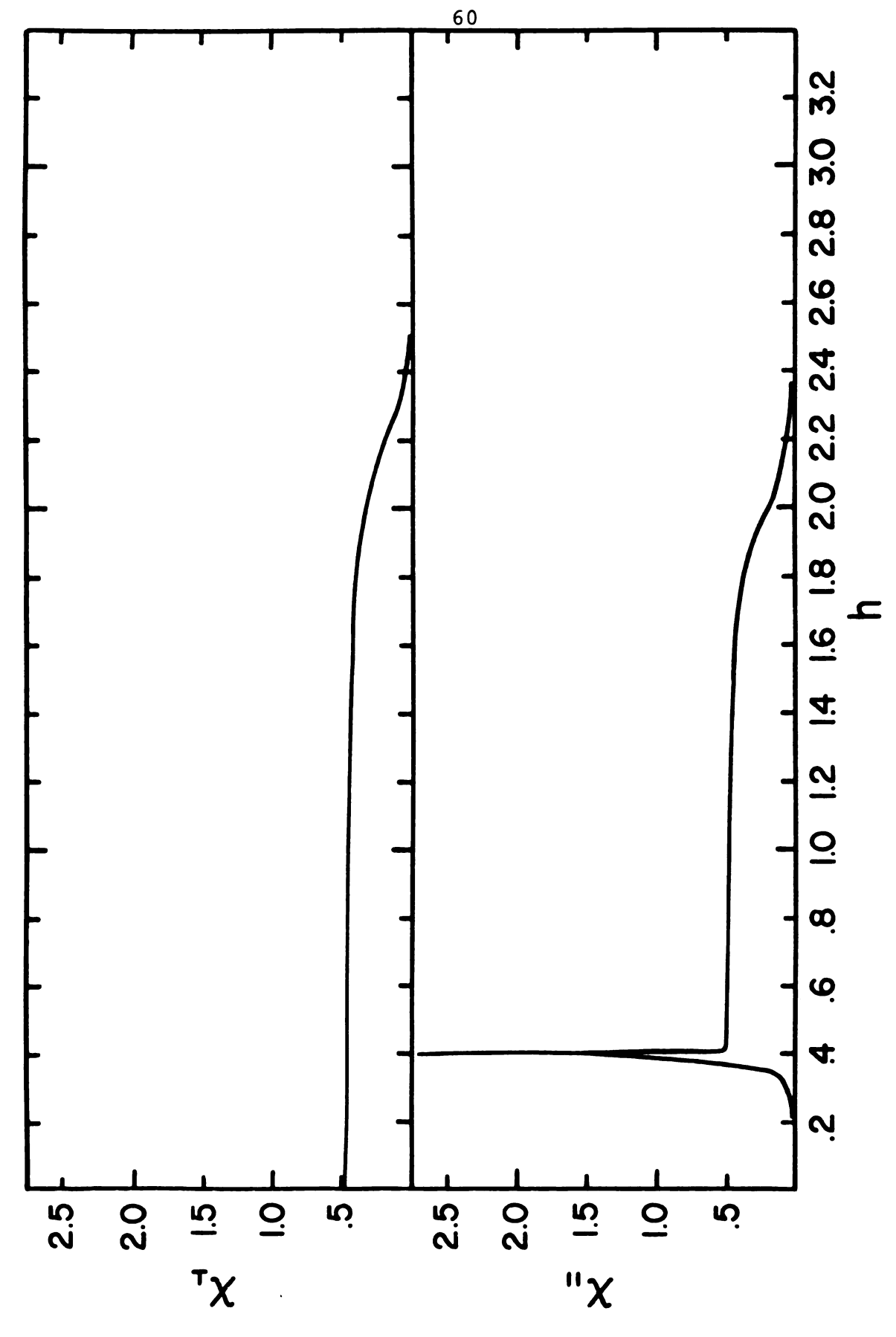
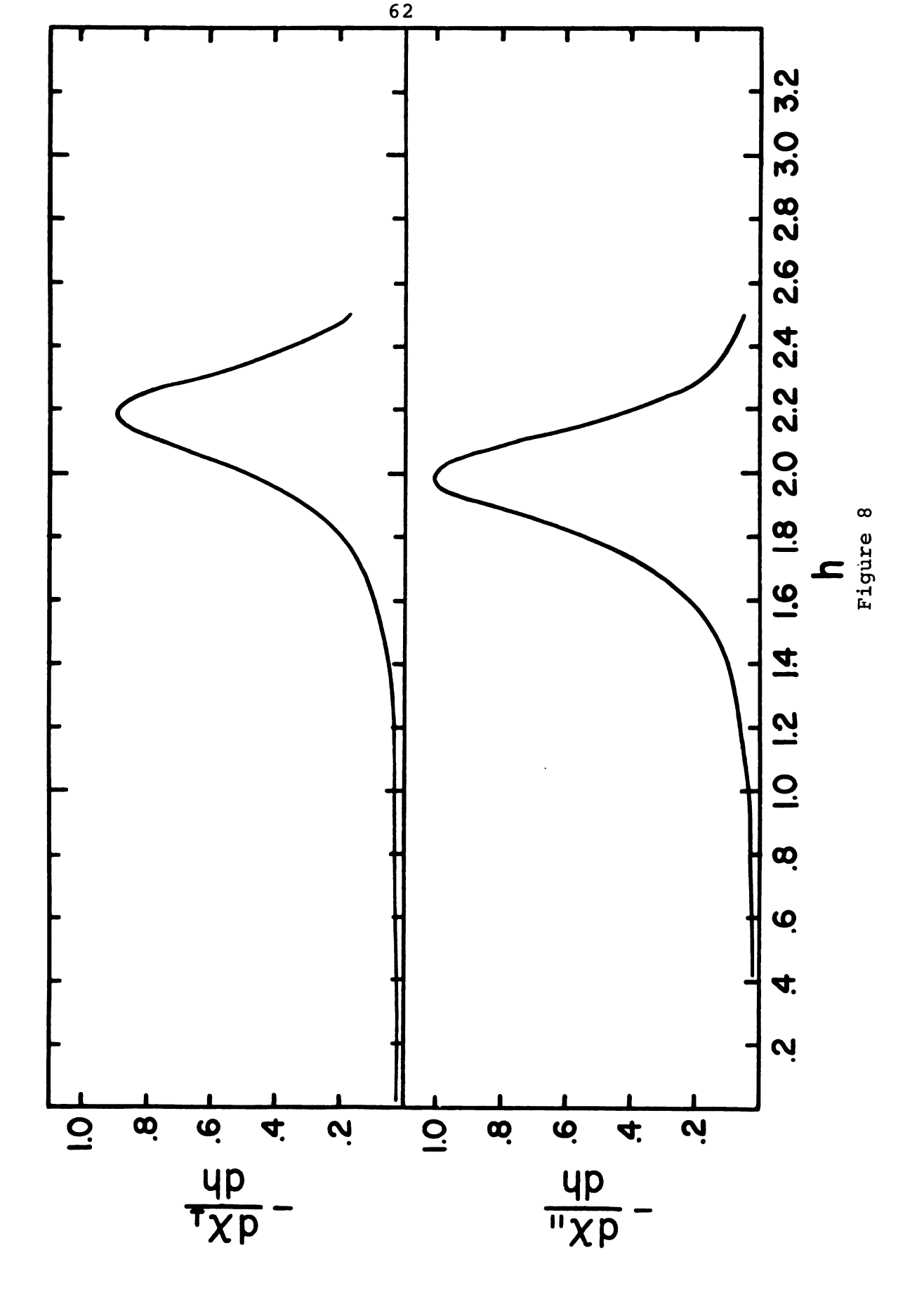


Figure 7

Figure 8. Numerical calculation of d\chi/dh vs. h with $h_{\mbox{\scriptsize D}} = 0.05$, $$h_{\mbox{\scriptsize K}} = 0$$ and $$h_{\mbox{\scriptsize L}} = 0.1$$



We divide the equilibrium equation by $cos(\phi)$

$$h_{D}(0) \sin \phi - h - h_{D}\cos(2\phi)/\cos(\phi) = 0$$
 (4.47)

and write the magnetization as

$$m = \sin(\phi) \tag{4.48}$$

The susceptibility is then written

$$\chi = \cos\phi \, d\phi/dh \tag{4.49}$$

Differentiating the equilibrium equation (4.47) we obtain an expression for $d\phi/dh$

$$-1 + \{h_p(0) - h_p \sin\phi [4-\cos(2\phi)/\cos^3\phi)\} \cos\phi d\phi/dh=0$$
 (4.50)

From equation 4.49 we express the susceptibility as

$$\chi = 1/[h_{D}(0) + h_{D}\sin\phi(4 - \cos(2\phi)/\cos^{3}\phi)]$$
 (4.51)

If we consider $h_D^{<<1}$, we can solve equations 4.51 and 4.45 to calculate the quasiparamagnetic critical field. This transition occurs at a field h_{QD} and an angle of cant ϕ_{QD} given by

$$\cos^{3}(\phi_{qp}) = (4/5)h_{p}/h_{p}(0)$$
 (4.52)

$$h_{qp} = h_{p}(0) + (3/5)h_{p}/\cos(\phi_{qp})$$
 (4.53)

For the case $h_D^{=0.05}$, $h_K^{=0}$, and $h_L^{=0.1}$ the numerically calculated quasiparamagnetic points are

$$h_{qp}^{z} = 1.990$$
 $\phi_{qp}^{z} = 74.44^{\circ}$

$$h_{qp}^{X} = 2.195$$
 $\phi_{qp}^{X} = 74.97^{\circ}$

The approximate equations (4.52 and 4.53) give

$$h_{qp}^{z} = 2.009$$
 $\phi_{qp}^{z} = 74.0^{\circ}$

$$h_{qp}^{x} = 2.212$$
 $\phi_{qp}^{x} = 74.5^{\circ}$

2. The susceptibility vs. angle in applied field for the uniaxial antiferromagnet at T=0.

The angle dependence of susceptibility in applied fields is more difficult to treat than the zero field case of part A, primarily because the field is strongly affecting the system. Fortunately, a simple calculation for the uniaxial antiferromagnet will shed considerable light on the subject. Let us consider an antiferromagnet with uniaxial crystal field anisotropy, with a magnetic field applied at an angle θ with respect to the z (easy) axis. The energy at T=0 can be written from equation 3.11 as

$$\varepsilon = -\cos(2\phi) - h_L(\cos(2\phi)\cos^2\alpha + \sin^2\phi) - 2h \sin\phi\cos\alpha\sin\theta + 2h \sin\phi\sin\alpha\cos\theta$$
 (4.54)

The equilibrium equations are

$$[2+h_{L}\cos(2\alpha)]\sin(2\phi) + 2h \cos\phi[\sin\alpha\cos\theta-\cos\alpha\sin\theta] = 0$$

$$(4.55)$$

 $h_L \cos(2\phi) \sin(2\alpha) + 2h \sin\phi[\cos\alpha\cos\theta + \sin\alpha\sin\theta] = 0$

The susceptibility is written

$$\chi^{i} = dm^{i}/dh^{i}$$
 (4.56)

The components of the magnetization are

$$m^{X} = \cos \alpha \sin \phi$$
 (4.57)

$$m^2 = -\sin\alpha\sin\phi \tag{4.58}$$

The magnetization in the direction of the applied field is

$$m = m^{X} \sin(\theta) + m^{Z} \cos(\theta)$$
 (4.59)

The reduced susceptibility is

$$\chi(\theta, H) = d/dh \left[\sin\phi \sin(\theta - \alpha) \right]$$
 (4.60)

The susceptibility was calculated for various applied fields using Newton's method on the computer 47. The behavior of the susceptibility can be described in four regions (Fig.9).

Region I	$0 < h < h_{sh}(0)$	AF
Region II	$h_{sh}(0) < h < h_{p}''(0)$	AF-SF
Region III	$h_{p}^{"}(0) < h < h_{p}^{-}(0)$	SF-P
Region IV	$\bar{h_p}(0) < h$	P

The points in the figure are identified by equations 4.39 through 4.44 with $h_{\kappa}=0$

$$\chi_{\mathbf{A}} = \chi_{\mathbf{AF}}^{"} = 0 \tag{4.61}$$

$$\chi_{\rm B} = \chi_{\rm AF}^2 = 1/(2+h_{\rm L}^2)$$
 (4.62)

$$\chi_{\rm C} = \chi_{\rm SF}^{\rm n} = 1/(2-h_{\rm L})$$
 (4.63)

The reduced susceptibility we have been using can be converted to cgs units by multiplying by the total saturation magnetization

$$\chi_{cgs} = Ngu_{B}S\chi_{reduced}/H_{E}$$

where N is the total number of spins.

Figure 9. Numerical calcualtion of susceptibility vs. angle in applied field

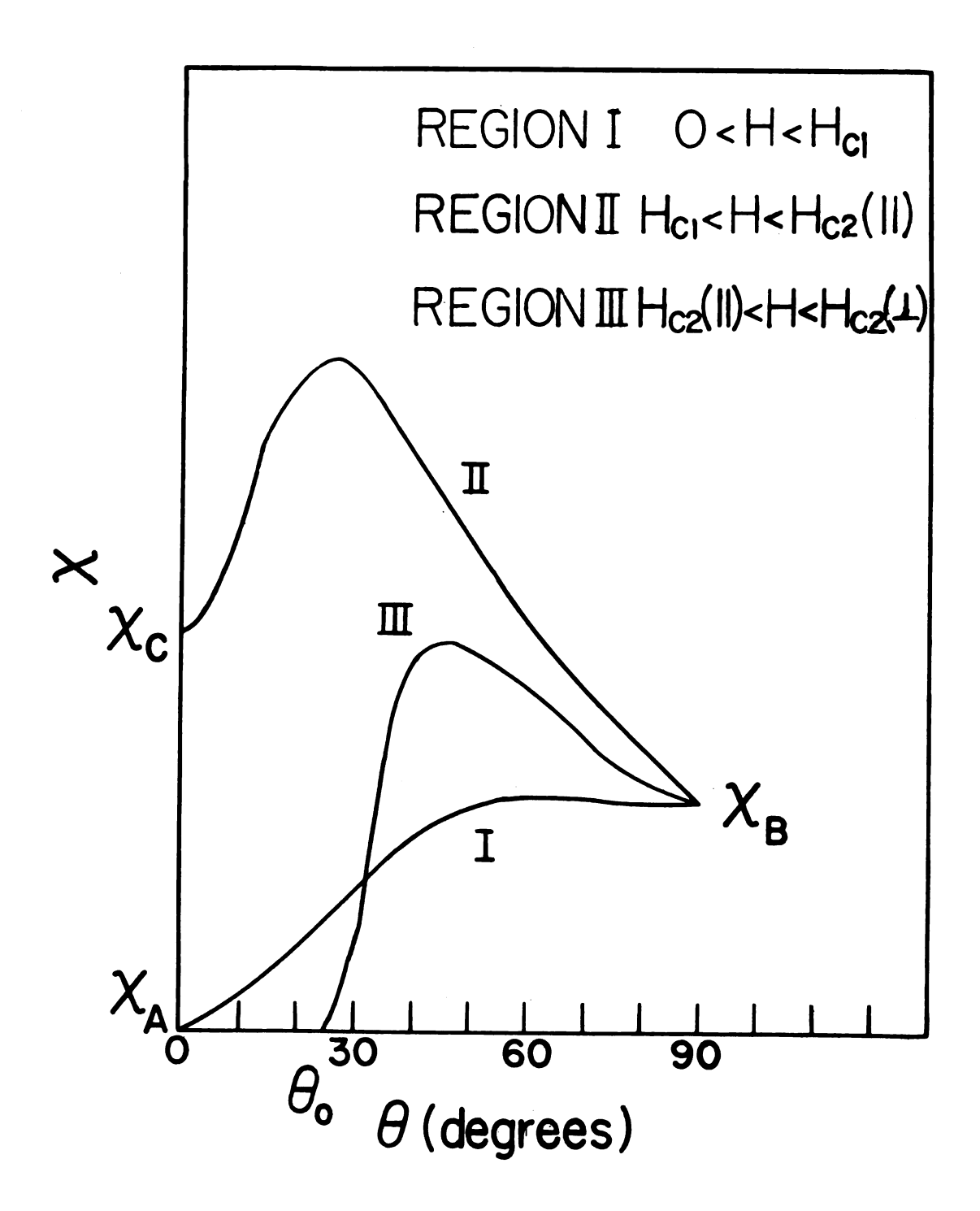


Figure 9

2
ś
ä
:
:
-
· :
:

V. EXPERIMENTAL APPARATUS - THE MEASUREMENT OF ANISOTROPIC SUSCEPTIBILITY

Susceptibility measurements are well suited to observing magnetic anisotropy because they are inherently directional, as opposed to, for instance, specific heat measurements. In this section, our primary aim is to discuss the apparatus required to measure susceptibility and vary the three parameters mentioned in chapter IV: temperature, applied field and orientation. First, we will attempt to clear up one of the great mysteries of physics - what are the units of susceptibility?

A. The Great Unit Debate

If one considers the magnetic permeability of a substance and wishes to express it in terms of the susceptibility, then (using c.g.s. units throughout)

$$u = 1 + \gamma \tag{5.1}$$

where χ is a dimensionless quantity measured in "electromagnetic units per cubic centimeter" or e.m.u./cm³. In the literature one can find susceptibility expressed in the following units: cm³/mole, cm³/gm, c.g.s. units/mole, c.g.s. units/gm, e.m.u./mole, e.m.u./gm, dimensionless, and arbitrary units. One can obtain a consistent relation among these systems with the following three definitions. The total magnetic energy of a system is

$$E = \frac{1}{2} \int \vec{B} \cdot \vec{H} dV$$
 or erg = gauss-Oersted cm³ (5.2)
The magnetization is written

$$M = Ngu_{R} < S >$$
 (5.3)

.:

and the Bohr magneton is defined as

$$u_B = 0.927 \times 10^{-20} \text{ erg/gauss}$$
 (5.4)

Since g and S are dimensionless and

$$\chi = dM/dH \frac{N(erg/gauss)}{Oersted}$$

we see that the units of susceptibility are N(erg)/(gaussOersted) which can be converted using equation 5.2 to the equivalent unit: N(cm³) where the units of N have yet to be chosen. Since we have previously stated that e.m.u./cm³ is a dimensionless unit, we let

$$1 \text{ e.m.u.} = 1 \text{ c.g.s. unit} = 1 \text{ cm}^3$$
 (5.5)

The susceptibility as expressed in equation 5.1 is dimensionless so we must choose N as the number of spins per unit volume. The following table shows possible other choices for N and the resulting susceptibility units, assuming one spin S per molecule.

Choice of	No	No/Mw	Nop/Mw
N			
Units of	#/mole	#/gm	#/cm ³
Units of	cm ³ /mole	cm ³ /gm	1
X	e.m.u./mole	e.m.u./gm	e.m.u./cm ³

Where N is Avagadro's number, M is the gram molecular weight, and ρ is the density in gm/cm $^3.$

B. The Measurement of Susceptibility

There are at least four methods of measuring magnetic susceptibility: Faraday or Gouy balance 48, vibrating magnetometer 49, nuclear magnetic resonance 4 and ac mutual inductance 50. Since we have used only the mutual inductance technique for the measurements to be discussed, the description will be limited to this method.

The ac mutual inductance method utilizes the fact that the mutual inductance of two concentric solenoids is proportional to the magnetic susceptibility of a material within the solenoids. If we let ΔM be the change in mutual inductance of the coils upon introduction of a sample of mass m, then

$$\Delta M = \frac{1}{W} m \chi \tag{5.6}$$

where W is a constant that is a characteristic of the coil.

The susceptibility coils used consist of a primary and two oppositely wound secondaries. The number of turns on the opposing secondaries is adjusted to make the mutual inductance approximately zero. The change of mutual inductance produced by the introduction of a sample into one secondary is measured with a Cryotronics⁵¹ Model 17B electronic mutual inductance bridge, operating at 17 Hertz. With the range switch (R) on 0.1, the coarse dial (c) and the fine dial (f) balanced, the mutual inductance is given by

$$M = Rcf(50x10^{-5})$$
 microHenries (5.7)

The susceptibility of a sample is given by combining equations 5.6 and 5.7

$$\chi = \text{RcWf/m}(50 \times 10^{-5}) \text{cm}^3/\text{gm}$$
 (5.8)

			1.7
			j a sed
			ε
			: :
			÷
			ja∎ ™k
			3
			.: ••
			.
			:
		•	

which we write

$$\chi = \text{Rcf K/m cm}^3/\text{gm} \tag{5.9}$$

The constant K is a property of the coils being used. Since the coils are never exactly balanced to zero without a sample, and since their balance changes with magnetic field and temperature, it is necessary to take readings with the sample in (f_i, sometimes called "full") and with the sample out (f_o, sometimes called "empty") of the coils. Consequently

$$\chi = Rc(f_i - f_0) K/m \quad cm^3/gm$$
 (5.10)

The constant K is determined by measurement of a known paramagnet, in this case Ferric Ammonium Alum, whose susceptibility is given by 52

$$\chi_{\text{FAA}} = 9.02 \times 10^{-3} / \text{T cm}^3 / \text{gm}$$
 (5.11)

The constant K can be determined to at least 1% accuracy. If we assume that the practical limit of measurement with a typical set of coils is 10 fine units with c=10 and R=0.1, then in terms of susceptibility of a 0.1gm sample this practical limit (see Table I for K) is

$$\chi_{\min} = 2 \times 10^{-7} \text{ cm}^3/\text{gm} \text{ or about } 10^{-7} \text{ e.m.u./cm}^3$$

C. The Parametric Apparatus

We have discussed the theoretical behavior of susceptibility as a function of the parameters H, T, and θ . We now wish to describe the design, construction, and use of the apparatus necessary to vary these parameters.

र -
.: :5
٠.
_
्र :
:
;
;
i
:

1. Susceptibility vs. temperature.

All experiments were done in conventional Helium four cryostats^{52,53} between 4.8 and 1.2 Kelvins. The temperature was determined from vapor pressure measurements using the T 58 temperature table.

Measurements of susceptibility vs. temperature are generally done with the hope of attaining accurate values for chi. It is essential that each data point shall consist of a balance taken with and without the sample in the coil because the empty value of the coils is a function of temperature, applied field, and time. The zero field measurements are made with quartz sample holders eliminating the need for background corrections (see part C). The zero field data is taken with coil \$2, which has a small inside diameter and enough turns of wire to make it very sensitive. The susceptibility vs. T measurements done in applied field are, naturally, made in the superconducting solenoid apparatus (see section 3) where one is usually interested in the transition temperature or field rather than absolute susceptibility.

2. Susceptibility vs. orientation.

In order to vary the orientation of a crystal while measuring the susceptibility one needs apparatus capable of rotating a crystal inside the susceptibility coils while immersed in liquid helium. The crystal rotation device (Fig. 10) shall be referred to as the <u>rotator</u> and the small axle on which the crystal is mounted shall be referred to as the <u>rotor</u>. The rotator essentially consists of two perpendicular threaded

Figure 10. The crystal rotation device

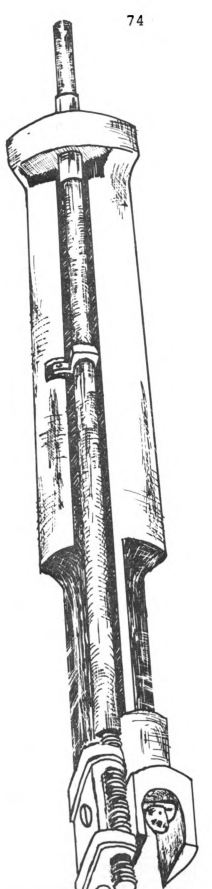


Figure 10

shafts, a vertical shaft that is passed through an O-ring vacuum seal and a horizontal shaft (the rotor) to which the crystal is attached. The vertical shaft has a simple screw thread that mates a thread cut around the circumference of the horizontal rotor with a tap set perpendicular to the rotor axis. When the vertical shaft is turned by hand at room temperature, a corresponding rotation is produced in the rotor. The turns ratio for the rotator in coil #5 is 29:1, the original rotator for coil #6 was 19:1, the present rotator is 29:1. The rotors are made of nylon with fiberglass-epoxy bearings to allow for thermal contraction. The body of the rotator is made of a low susceptibility material (see part C) to reduce the background. The vertical shaft is indexed at the dewar head, the 29:1 ratio allows one to easily change the orientation of the crystal by less than one degree.

Measurement of susceptibility vs. angle for various temperatures is an excellent method of determining the principal magnetic axes of the crystal and the type of ordering it undergoes. 54

Many of these experiments in zero field can be understood from equation 4.29 for the uniaxial antiferromagnet

$$\chi(\theta) = \chi^{"}\cos^2\theta + \chi^{!}\sin^2\theta$$

where the easy or hard axes correspond to extrema in the susceptibility. Using equations 4.10 and 4.23 we see that the parallel axis susceptibility is a maximum in the paramagnetic state and a minimum in the antiferromagnetic state. Two independent rotations allow one to determine the easy direction with an accuracy that depends on the amount of anisotropy and the actual magnitude of the susceptibility.

Table I. Physical parameters of the susceptibility coils.

Coil Number	2	5	6	
Function	χ vs. T	. Τ χ vs. θ χ vs	χ vs. H 2.73	
Sensitivity, x 10 ⁸	1.85	2.20		
Type Secondary	double	triple		
Primary Turns	2093	3285	1100	
Gauge	#30	#34	#36	
Length	7"	14"	4"	
I.D.	5/8"	15/16"	5/8"	
R,300Kelvins	35	220	100	
Secondary Turns	10,946	34,208	8,255	
Gauge	#36	#36	#38	
Length	3"	8"	2"	
O.D.	l"	2"	29/32"	
R,300Kelvins	1100	4400	1100	
Rotator Ratio	none	29:1	29:1	

Since most of the rotator is actually in the susceptibility coils and since it has some susceptibility, measurements of chi are not extremely accurate. The best χ vs. θ data is taken with coil #5 (Fig. 11) which is very long and has uniform sensitivity over an approximately one centimeter length. This is necessary because the rotors produce some up and down motion of the sample.

3. Susceptibility in applied magnetic fields.

The magnetic fields for our experiments are generated by a superconducting solenoid wound on a coil form of Synthane type G-11 fiberglass epoxy. The solenoid itself has an i.d. of 2.61 cm, and o.d. of 5.02 cm and a length of 10.0 cm. The wire is 0.0178 cm diameter Niobium - Zirconium with copper coating and nylon insulation. The solenoid is wound with two pieces of wire with a total length of 1700 m giving 14,712 turns. The field at the center of the solenoid is given by 56

$$H = [4\pi I \lambda b/(10a_w)] \ln \left(\frac{a_2 + \sqrt{a_2^2 + b^2}}{a_1 + \sqrt{a_1^2 + b^2}}\right)$$
 (5.12)

where λ is the filling factor

$$\lambda = N(\pi/4) (d_w^2) / [L(a_2 - a_1)]$$
 (5.13)

and

 $d_w = 0.0178$ cm the diameter of the wire $a_w = 2.48 \times 10^{-4}$ cm the cross sectional area of the wire $a_1 = 1.31$ cm the inside radius of the solenoid $a_2 = 2.51$ cm the outside radius of the solenoid $a_3 = 5.00$ cm the half length of the solenoid

I is the current

Figure 11. Coil #5 with rotator

Figure 11

		٠.
		* <u>*</u>
		<u>:</u> :
		÷
		:
		:
		·.
		:
		;
		3
		;
		;

The result of this calculation is

H = 1720 Oersted/ampere

The magnetic field is measured with a Bismuth magnetoresistor ⁵⁷ that is calibrated in place (Fig. 12) against the spin flop critical field ⁵⁸ of copper chloride mounted on the rotor. This calibration gives

 $H_{mr} = 1680 \pm 10 \text{ Oersted/ampere}$

The homogeneity is estimated from an RCA Magnet Design Aid⁵⁹ as 0.3% on a 1 cm diameter sphere. The magnet is usually capable of reaching 12.0 amperes before quenching producing a field of 20.0 kiloOersted.

The spin flop transition can be quite narrow in angle, for instance in copper chloride the spin flop transition can only be observed with magnetic fields applied within one degree of the easy axis, so measurements of parallel and perpendicular susceptibility require very careful orientation. Consequently, the apparatus for measuring susceptibility in applied field includes a crystal rotator similar to that described in section 2 (Fig. 13).

The present rotators have only one axis of rotation, so one must mount the crystal with the easy axis in the plane perpendicular to the axis of rotation. Assuming that this is done properly, the crystal is rotated in some constant magnetic field H_O . If we examine the results of the theoretical calculation of chi vs. θ in applied field (chapter IV, part B2) we see that if H_O is slightly greater than H_{SF} the susceptibility will be strongly peaked around the easy axis with a precipitous dip at the easy axis (see Fig. 9). As one approaches H_{SF} from

above, the peak becomes nearer to the axis and the dip becomes sharper, providing an excellent guide to orient the crystal.

We have used this apparatus primarily for plotting the H-T phase diagrams described in chapter III. In general, the boundaries are easier to see at lower temperatures while spin flop boundaries, representing greater changes in the magnetization, are much easier to see than paramagnetic boundaries. Spin flop boundaries are usually found by orienting the crystal as described above and measuring susceptibility as a function of applied field at constant temperature. The very strong peak in the susceptibility (the theoretical results are shown in Fig.'s 6 and 7) occurs at the spin flop field. The paramagnetic boundaries, especially at temperatures near the Néel point, can only be observed by measuring the susceptibility as a function of temperature at fixed field, the transition occurring at the point of maximum dg/dT⁶⁰.

The apparatus has two characteristics that make absolute measurement of susceptibility impractical: the empty value of the coils is a strong function of field, and the noise induced by current instabilities and flux jumps greatly reduces the accuracy.

D. Low Susceptibility Materials

Accurate measurement of susceptibility is dependent upon the ability to measure the susceptibility of the sample of interest and only the sample of interest. Our attempts to subtract background due to extraneous materials such as rotators or sample holders degraded the results by an

Figure 12. Calibration of resistance vs. H for the magnetoresistor

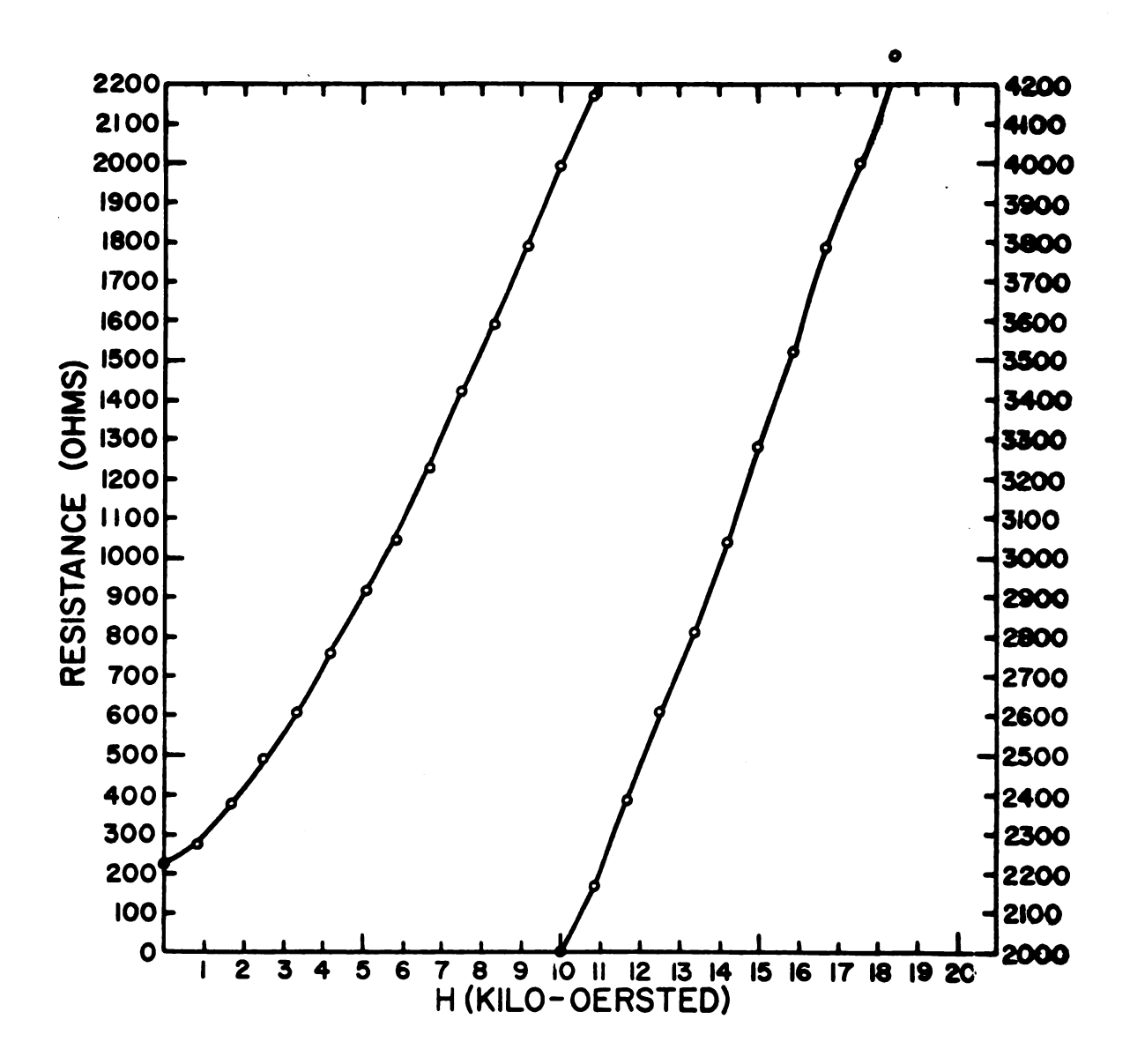


Figure 12

Figure 13. A cross section of the apparatus for measuring susceptibility in applied field

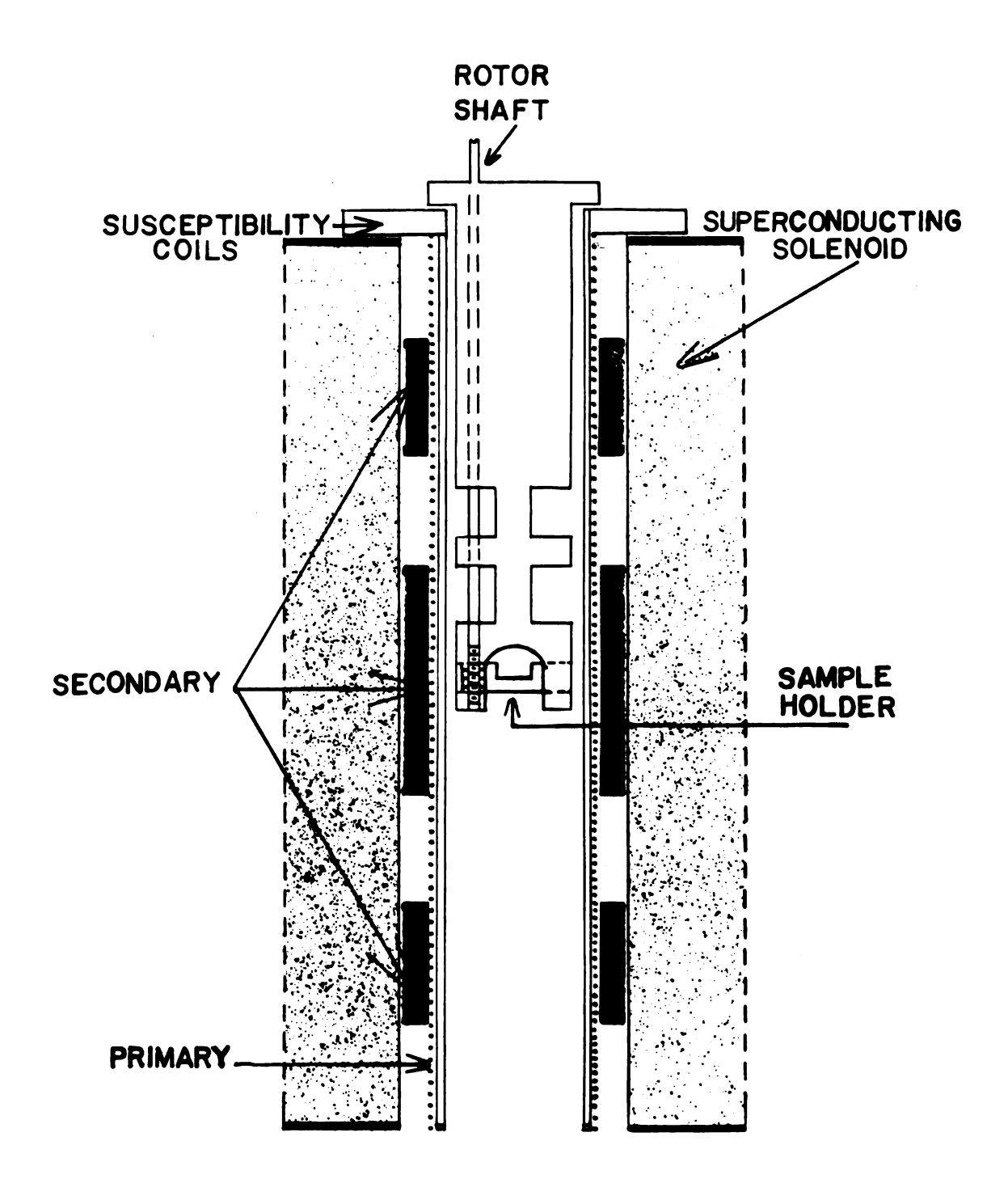


Figure 13

objectionable amount. Consequently, material in the coils must have very low susceptibility. In general, metals should be avoided because of eddy current effects and non-metals should be easily machinable (eliminating quartz from most applications). The following is a list of the approximate susceptibilities of various materials at four Kelvins, those available from Synthane Corporation⁵⁵ are denoted with an *. The materials are divided into four groups according to desirability.

SUSCEPTIBILITY OF MISCELLANEOUS MATERIALS AT FOUR KELVINS

I.
$$0 < \chi < 1 \times 10^{-6} \text{ cm}^3/\text{gm}$$

1. Quartz

2. XXXP-IR* paper phenolic

3. C-M* cotton melamin

4. EP-22* paper epoxy

5. Black nylon

II. $1 < y < 5 \times 10^{-6} \text{ cm}^3/\text{cm}$

1. White nylon

2. XP* paper phenolic

3. XXP* paper phenolic

4. C* cotton phenolic

5. L* cotton phenolic

6. Hardwood (Birch)

7. Pure epoxy

8. Epibond 100A

III. $5 < \chi < 10 \times 10^{-6} \text{ cm}^3/\text{cm}$

- 1. G-11* glass epoxy
- 2. Glastic
- 3. Pyrex

IV. $\chi > 10 \times 10^{-6} \text{ cm}^3/\text{gm}$

1. XX* paper phenolic

2. L-XB* cotton phenolic and graphite

3. G-3* glass epoxy

4. G-5* glass epoxy

5. N-l* nylon phenolic

6. Lavite

The best material by far is EP-22 epoxy and paper which has almost unmeasureable susceptibility and is an excellently machining material, second best is C-M. The superconducting solenoid and all susceptibility coils were wound on forms of G-11 glass epoxy which is an unusually strong material.

VI. EXPERIMENTAL RESULTS AND DISCUSSION

Susceptibility measurements have been made on Rb₂MnCl₄·2H₂O, Cs₂MnCl₄·2H₂O and CuCl₂·2H₂O. We have measured zero field susceptibility as a function of temperature and angle in Cs₂MnCl₄·2H₂O and Rb₂MnCl₄·2H₂O. We have also measured susceptibility in applied field for all three crystals and in the cases of Cs and Rb₂MnCl₄·2H₂O we have used this data to plot the H-T magnetic phase diagram. Our goal is to compare these results with the theory and to evaluate the molecular field constants. In addition, we have taken from the literature data on MnCl₂·4H₂O, a very thoroughly investigated material, and applied the molecular field theory to these results. For crystallographic details concerning these crystals, see Appendix B.

A. $Cs_2MnCl_4 \cdot 2H_2O$ and $Rb_2MnCl_4 \cdot 2H_2O$

 ${\rm Cs_2MnCl_4\cdot 2H_2O}$ and ${\rm Rb_2MnCl_4\cdot 2H_2O}$ are isostructural triclinic crystals with one chemical formula per unit cell. Nuclear magnetic resonance 61 and specific heat 62 measurements indicate that they order antiferromagnetically with ${\rm T_N}=1.84$ K for the cesium salt and ${\rm T_N}=2.24$ K for the rubidium salt. They are two sublattice antiferromagnets, which our susceptibility measurements indicate are essentially uniaxial. The manganese ion resides in the center of a distorted square of chlorines with oxygen atoms above and below. The easy direction was determined by measuring chi vs. θ , (Fig. 14) to be approximately 10° from the O-Mn-O direction, in agreement with earlier measurements by Spence et al. 61 The angle dependence of the zero field susceptibility is well represented by equation 4.29.

The temperature dependence of the zero field susceptibility is typical of antiferromagnetic ordering (Fig.'s 15,16). We can compare this data with the molecular field result shown in Figure 5. Note that the molecular field calculation for the paramagnetic susceptibility included the assumption that $T >> T_N$ and does not apply near the transition.

The paramagnetic susceptibility has been fit to the Curie-Weiss law (equation 4.7)

$$\chi = C/(T+F) \text{ cm}^3/\text{mole}$$
 (6.1)

where the theoretical value of C is

$$C = Ng^2 u_R^2 S(S+1)/(3k_R) = 4.39 \text{ cm}^3 K/\text{mole}$$
 (6.2)

The experimental results (Table II) show a large deviation from this value, indicating that the measurements were made sufficiently near T_N to be affected by both short range order and neglected terms in the expansion 42 .

The paramagnetic data can be used with equation 4.7 to obtain a value for the crystal field anisotropy

$$Q = 1/\chi_p^n - 1/\chi_p^\perp = (2S+3)gu_B^H_L/(10k_B^C)$$
 (6.3)

Solving for the anisotropy field

$$H_{I.} = 10k_{B}CQ/((2S+3)gu_{B})$$
 (6.4)

and using the experimental values of C and Q we find the anisotropy to be approximately 8 kOe (Table II) for both materials. The exchange field can be calculated from the experimental value of the perpendicular susceptibility at the transition temperature. We solve equation 4.24 for the exchange field (Table II)

Figure 14. Susceptibility vs. angle for Rb₂MnCl₄·2H₂O in the paramagnetic and antiferromagnetic states with zero applied field

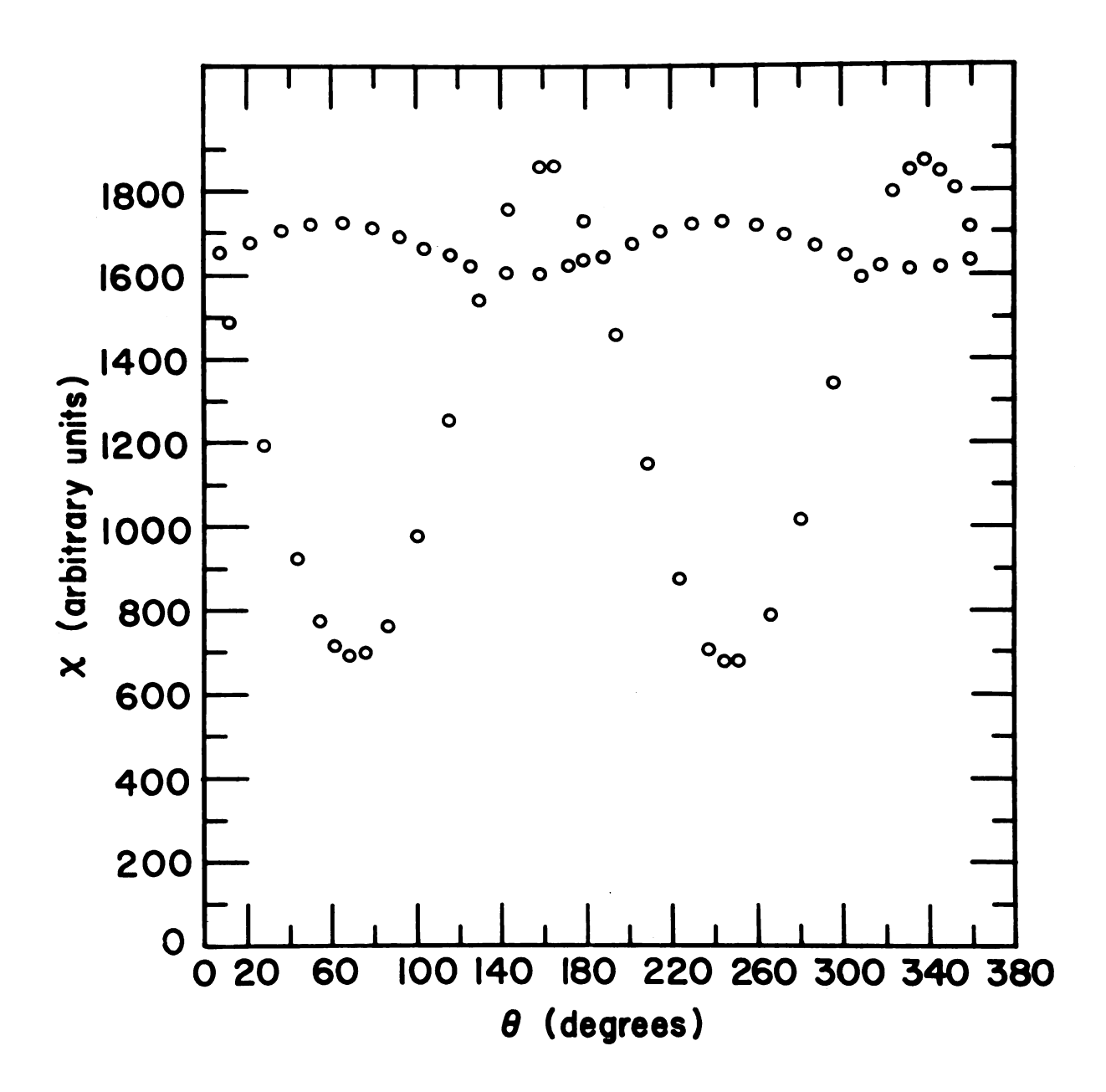


Figure 14

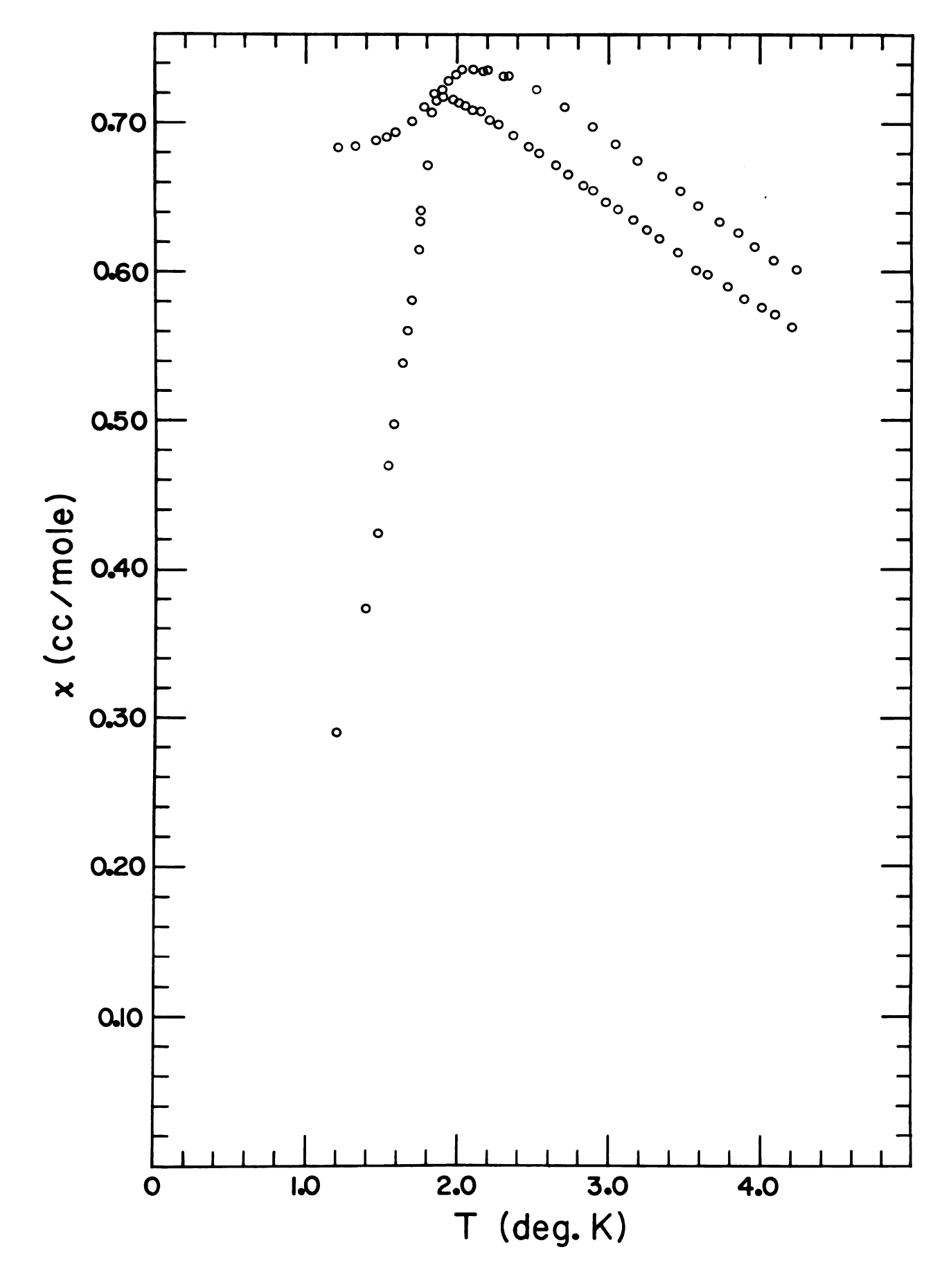
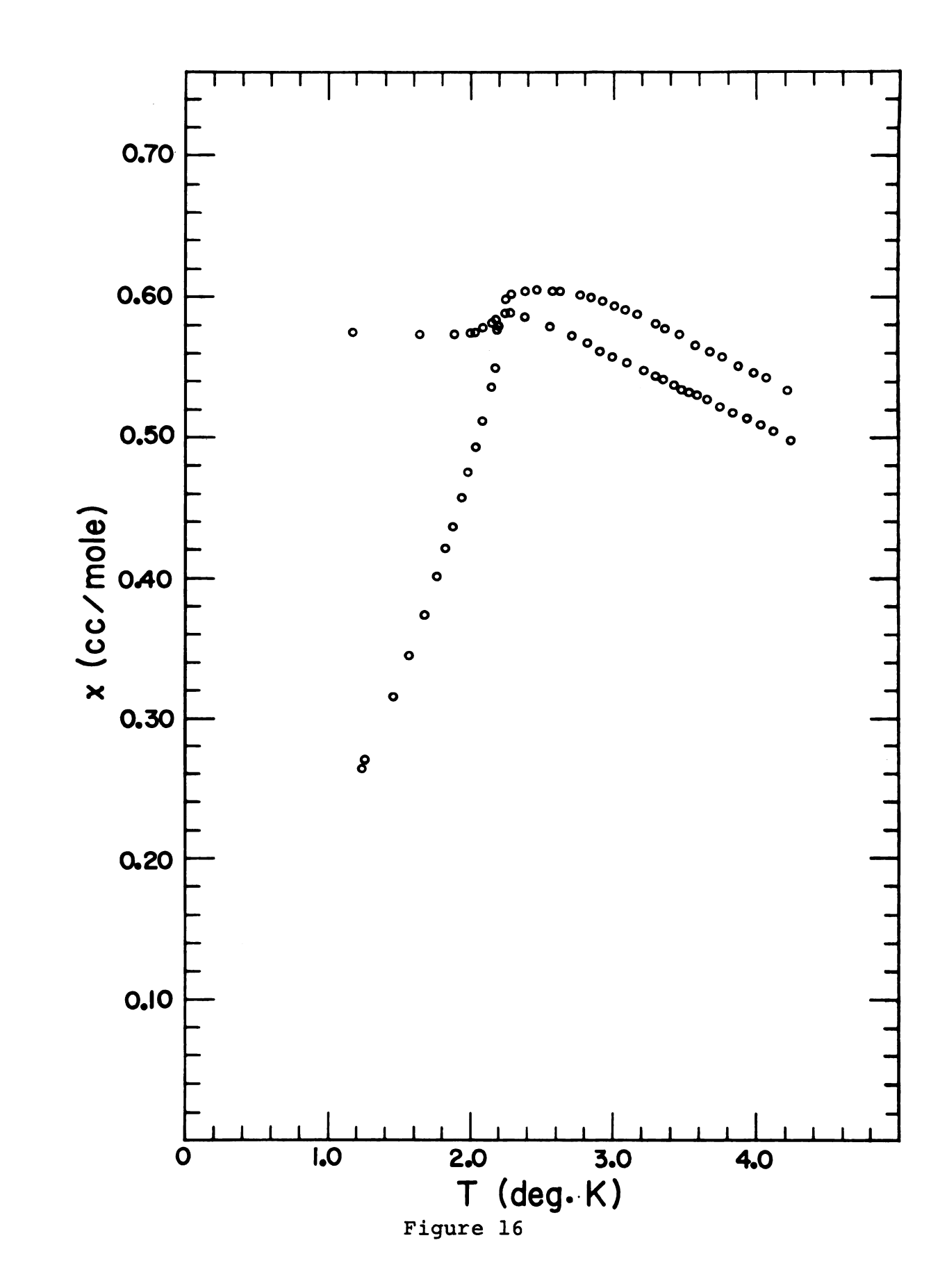


Figure 15

Figure 16. Zero field susceptibility vs. temperature for ${\rm Rb_2MnCl_4\cdot 2H_2O} \ \ {\rm in \ the \ parallel \ and \ perpendicular}$ orientations



$$H_{E} = N_{O}gu_{B}S/(2\chi^{1}(T_{N})) - H_{L}/2$$
 (6.5)

Since these materials have essentially spin only g values of 2.0, we have assumed that $H_{\rm K}$ and $H_{\rm D}$ are zero⁶³. Neglecting the anisotropic term in equation 6.5, Smith and Friedberg⁶³ have calculated $H_{\rm E}$ = 20 kOe from susceptibility data for ${\rm Cs_2MnCl_4 \cdot 2H_2O}$. Excellent agreement with our value $H_{\rm E}$ = 16.7 kOe can be obtained by subtracting $H_{\rm L}/2$ = 3.8 kOe from Friedberg's value.

We have measured the H-T magnetic phase diagrams for both materials (Fig.'s 17, 18) using the temperature dependence of the susceptibility in applied field. In this temperature range (1.2 - 4.2 K) we have found only paramagnetic boundaries. An example of the chi vs. T data in applied field for Cs₂MnCl₄·2H₂O is shown in Figure 14. A log-log plot of the phase boundaries (Fig.'s 20, 21) shows excellent agreement with the T^{1/2} dependence of the critical fields predicted in equations 3.43 and 3.44.

We have extrapolated the phase boundaries to zero temperature and used equations 3.21 and 3.28 (assuming $H_K=0$) to evaluate the molecular fields.

$$H_{E} = (H_{p}(0) + H_{p}(0))/4$$
 (6.6)

$$H_{L} = (H_{p}^{\perp}(0) - H_{p}^{n}(0))/2$$
 (6.7)

The exchange fields are in good agreement with the paramagnetic values but the anisotropy fields are almost a factor of two larger (Table II). From the phase boundary results we find the reduced anisotropy field

Figure 17. Magnetic phase diagram of Cs₂MnCl₄·2H₂O. The predicted spin flop boundary is represented by a dotted line

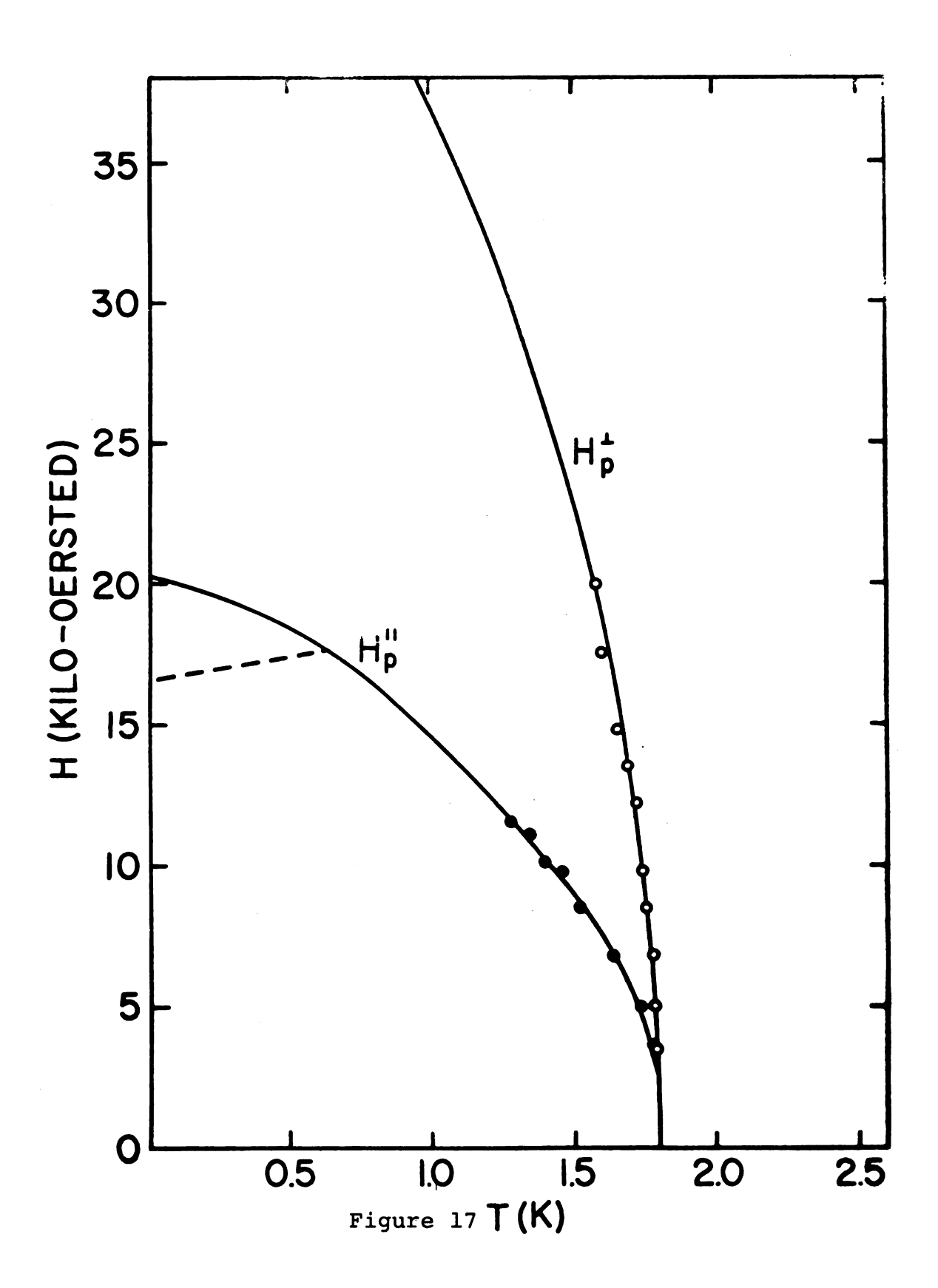


Figure 18. Magnetic phase diagram of Rb2MnCl4·2H2O. The predicted spin flop boundary is represented by a dotted line

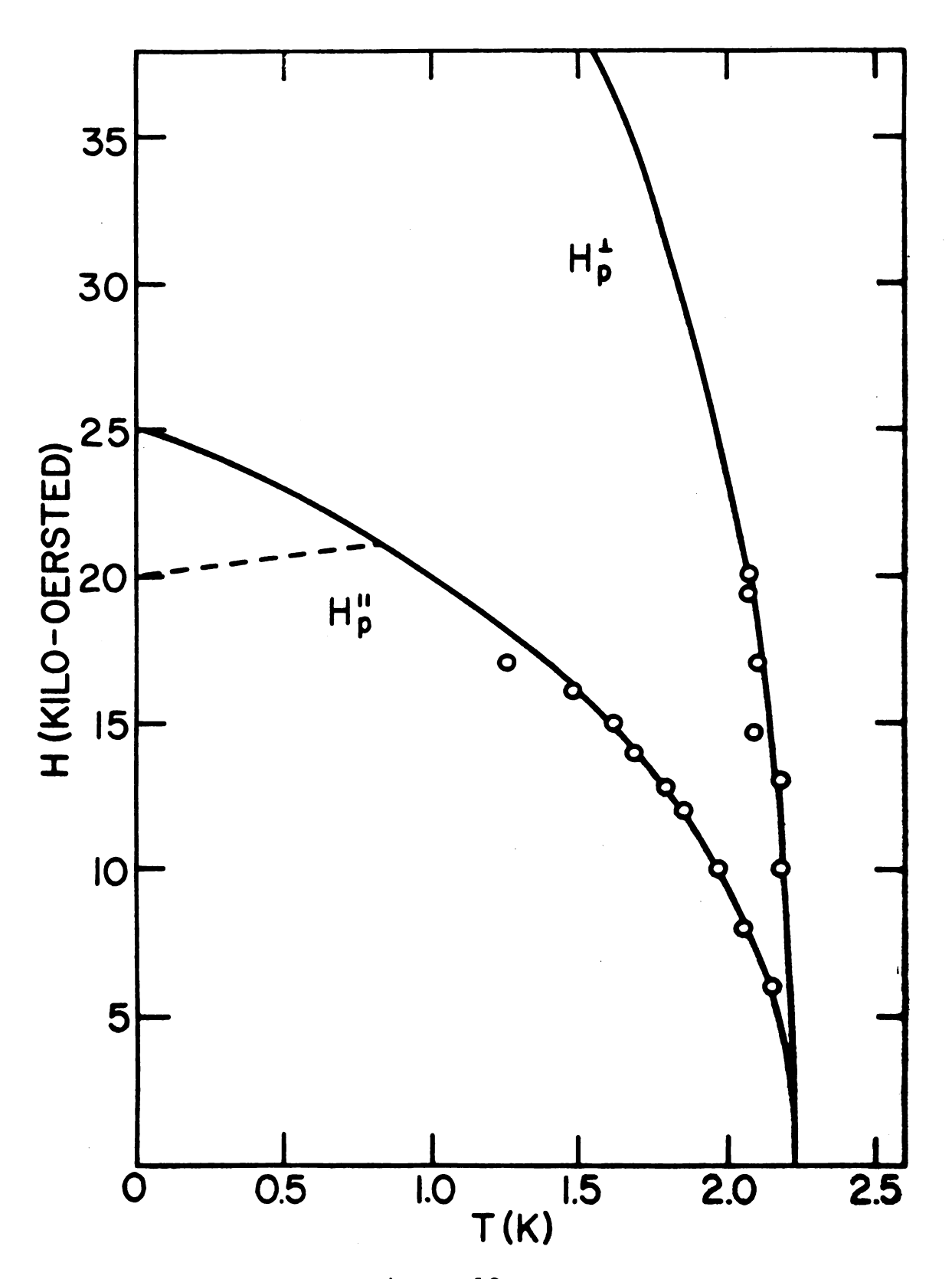


Figure 18

$$h_{T_1} = H_{T_1}/H_{E}$$

is approximately 0.8 for both materials. A calculation of the zero temperature spin flop field from equation 3.22

$$H_{th} = ((2H_E - H_L)H_L)^{\frac{1}{2}}$$
 (6.8)

qives

$$H_{th} = 16.7 \text{ kOe}$$
 $Cs_2MnCl_4 \cdot H_2O$

$$H_{th} = 20.0 \text{ kOe}$$
 $Rb_2MnCl_4 \cdot H_2O$

If we assume the temperature dependence of equation 3.52, we find the theoretical value of the triple point to be

$$H_{tp} = 17.4 \text{ kOe}$$
 $T_{tp} = 0.55 \text{ K}$ $Cs_2MnCl_4 \cdot H_2O$

$$H_{tp} = 21.0 \text{ kOe}$$
 $T_{tp} = 0.83 \text{ K}$ $Rb_2MnCl_4 \cdot H_2O$

The predicted spin flop boundaries are shown as dotted lines in Figures 17 and 18.

The anisotropy of these two salts has several unusual features:

- 1. The easy axis is approximately 10° from the local coordination axis formed by O-Mn-O.
- 2. The anisotropy appears to be much larger in the ordered state than in the paramagnetic state.
 Friedberg⁶³ has shown that the dipolar anisotropy is negligible in the paramagnetic state but this calculation has not been done in the ordered state.

Figure 19. Susceptibility vs. temperature in applied field for ${\rm Cs_2MnCl_4\cdot 2H_2O}, \ {\rm typical\ data\ used\ for\ obtaining}$ phase boundaries

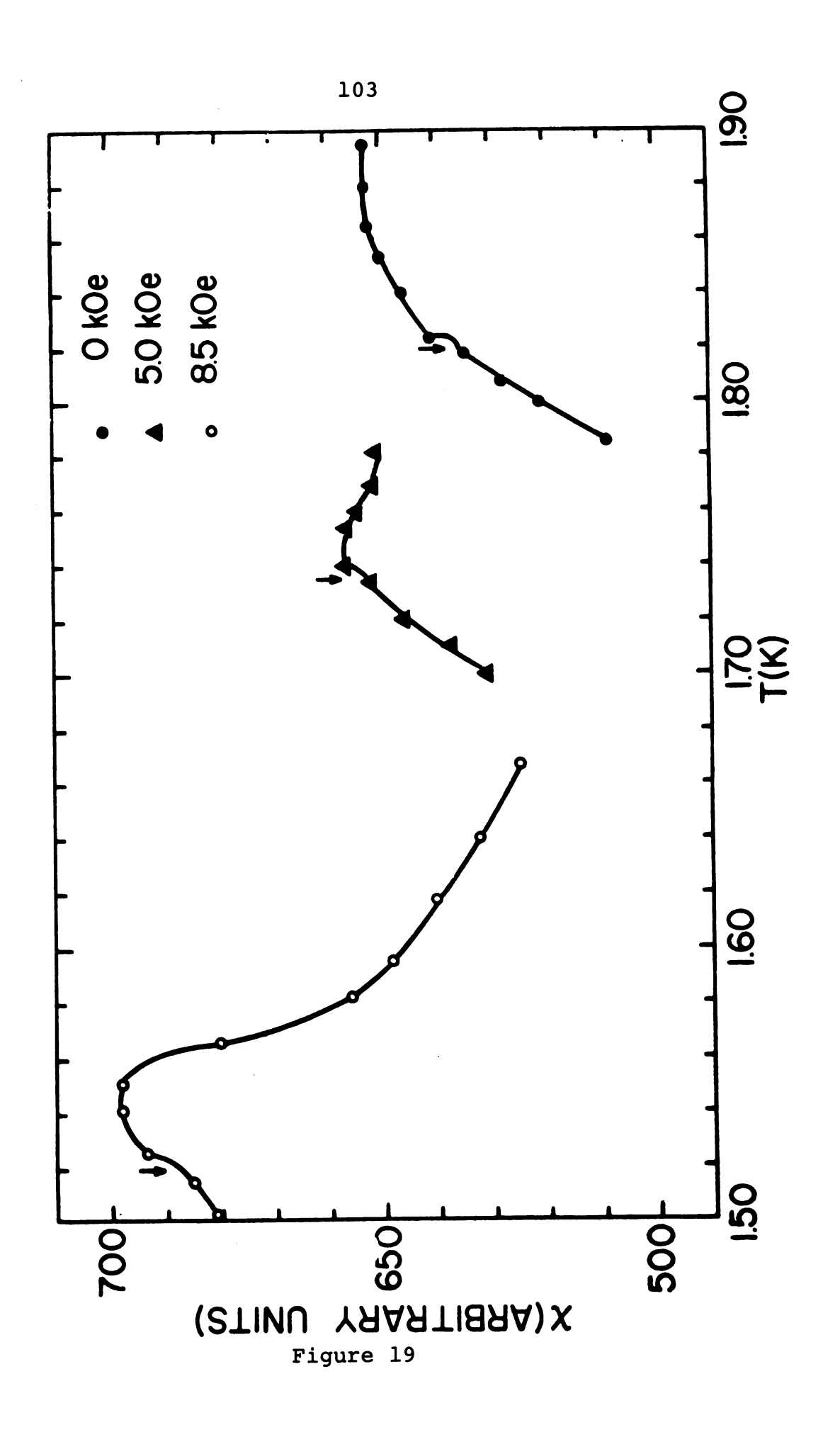


Figure 20. Extrapolation of the phase boundaries to T=0 for ${\rm Cs_2MnCl_4\cdot 2H_2O}$

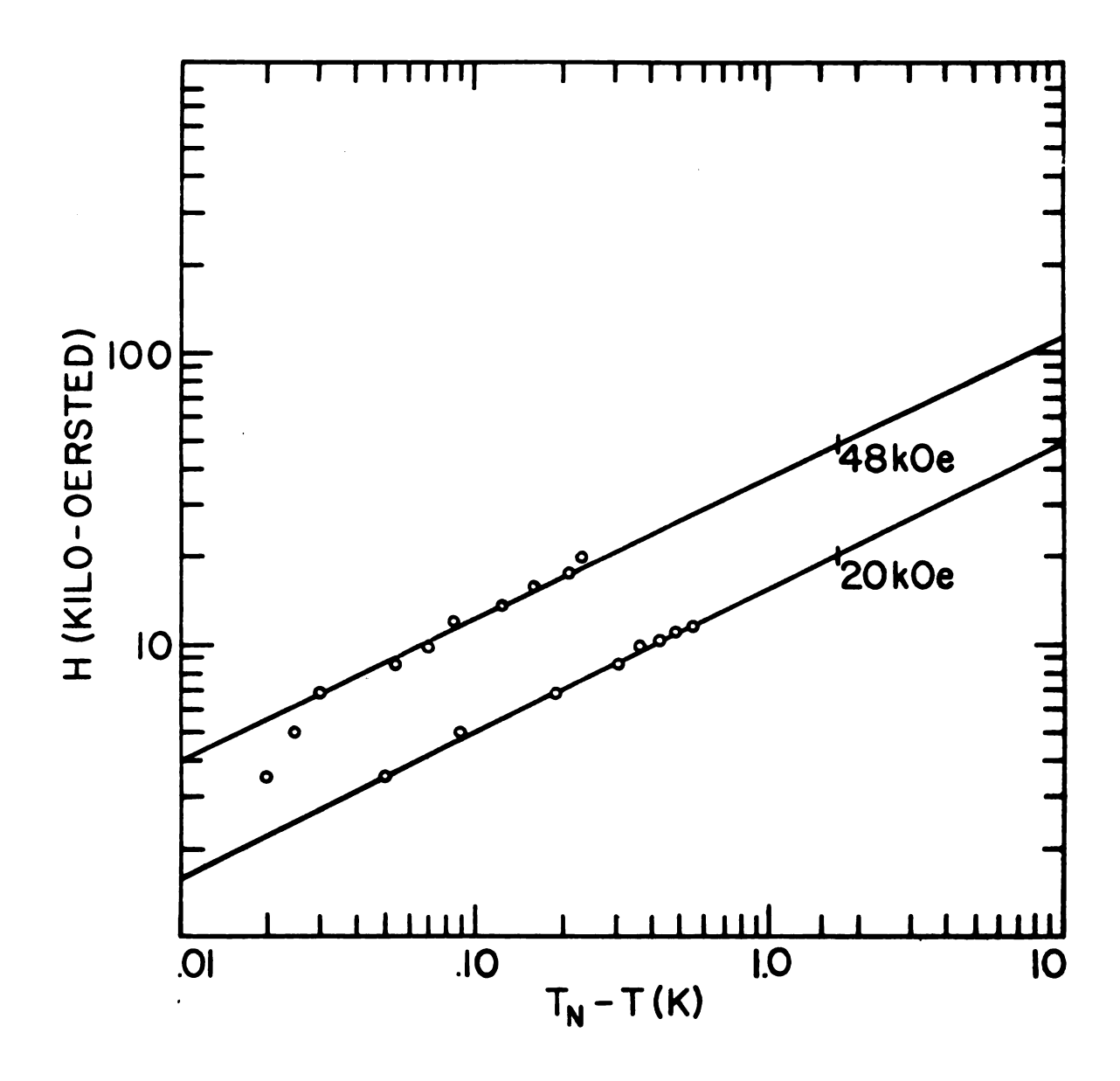
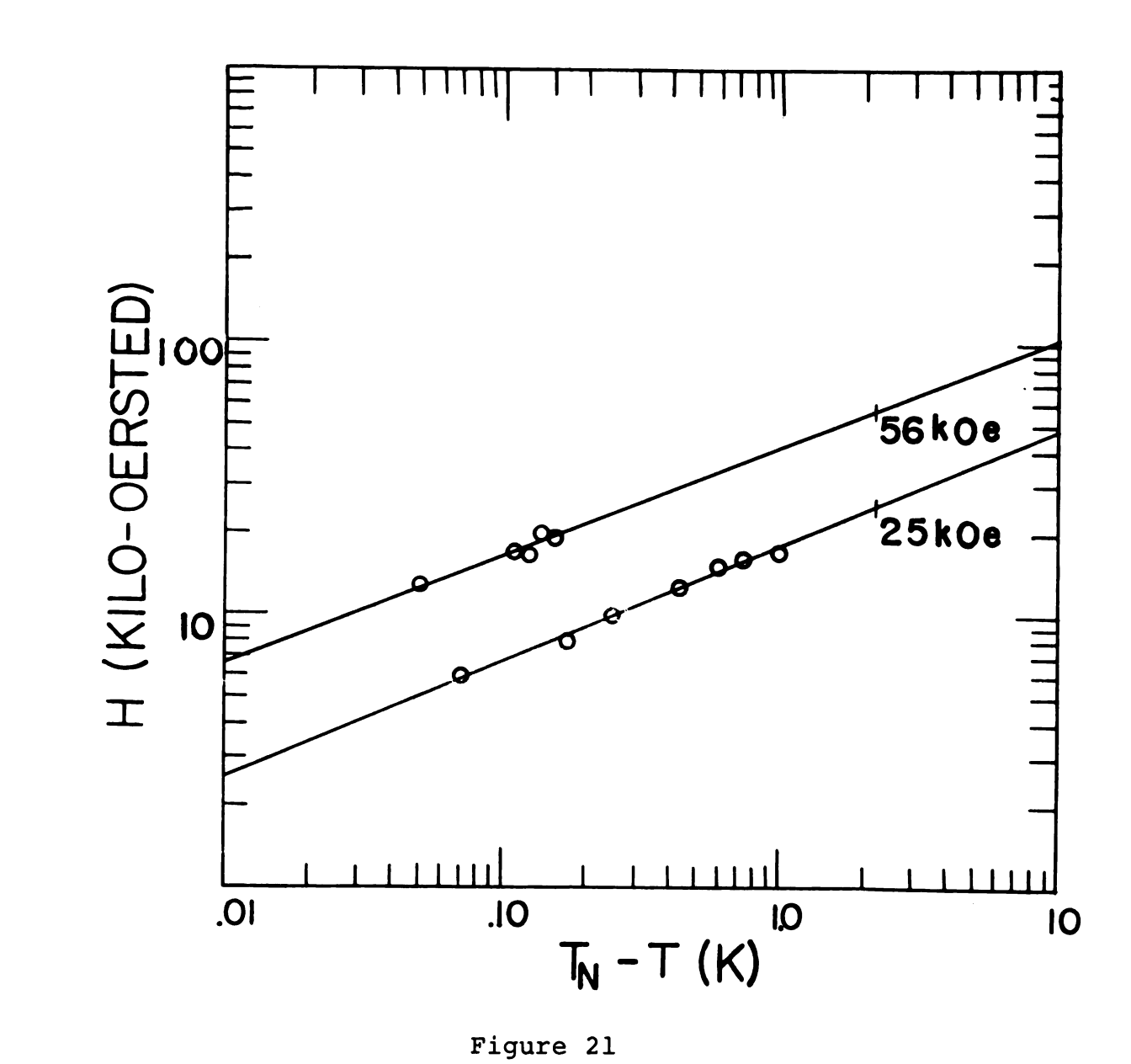


Figure 20

Figure 21. Extrapolation of the phase boundaries to T=0 for $Rb_2MnCl_4 \cdot 2H_2O$



3. The anisotropy is an order of magnitude greater 64 than any obtained by paramagnetic resonance of Mn⁺⁺ ions as impurities in diamagnetic lattices. Unfortunately, no diamagnetic host has been found with the same local coordination.

B.
$$CuCl_2 \cdot 2H_2O$$

Copper chloride has been studied extensively and is believed to be a four sublattice antiferromagnet 65 . We have chosen this crystal in order to study the behavior of the susceptibility in applied field particularly near the spin flop critical field. Copper chloride is a good choice to test our zero temperature theory because at 1 Kelvin $T/T_N \cong \frac{1}{4}$.

We have measured chi vs. T at constant field from the spin flop region at low temperatures to the antiferromagnetic region at high temperatures. The prominent peaks in the susceptibility (Fig. 22) occur at the spin flop-antiferromagnetic boundary and are in sharp contrast to the small effects seen in the paramagnetic transition of $Cs_2MnCl_4 \cdot H_2O$ (Fig. 19). We can extrapolate the transition to the limit of zero amplitude (Fig. 23) to estimate the triple point temperature as $T_{tp} = 4.31 \text{ K}$ in excellent agreement with the values $T_{tp} = 4.31 \text{ K}$ and $T_{tp} = 4.31 \text{ K}$

Copper chloride has orthorhombic symmetry and may have a D-M interaction, so we take great liberties in applying our uniaxial theory to it. We have measured the zero field susceptibility in the perpendicular direction and find

$$\chi^{\perp}(T_N) = 3.3 \times 10^{-2} \text{ cm}^3/\text{mole}$$

Table II. Experimental data and molecular field calculations for Cs₂MnCl₄·2H₂O and Rb₂MnCl₄·2H₂O.

Cs ₂ MnCl ₄ ·2H ₂ O	Rb ₂ MnCl ₄ ·2H ₂ O
1.84	2.24
0.68	0.58
0.16	0.16
5.2	5.7
5.1	5.8
4.0	6.5
4.9	7.8
20.0	25.0
48.0	56.0
16.7	20.0
17.0	20.3
7.7	8.5
14.0	15.5
16.7	20.0
17.5	22.5
0.53	0.77
	1.84 0.68 0.16 5.2 5.1 4.0 4.9 20.0 48.0 16.7 17.0 7.7 14.0

Figure 22. Susceptibility vs. temperature in applied field for $CuCl_2 \cdot 2H_2O$

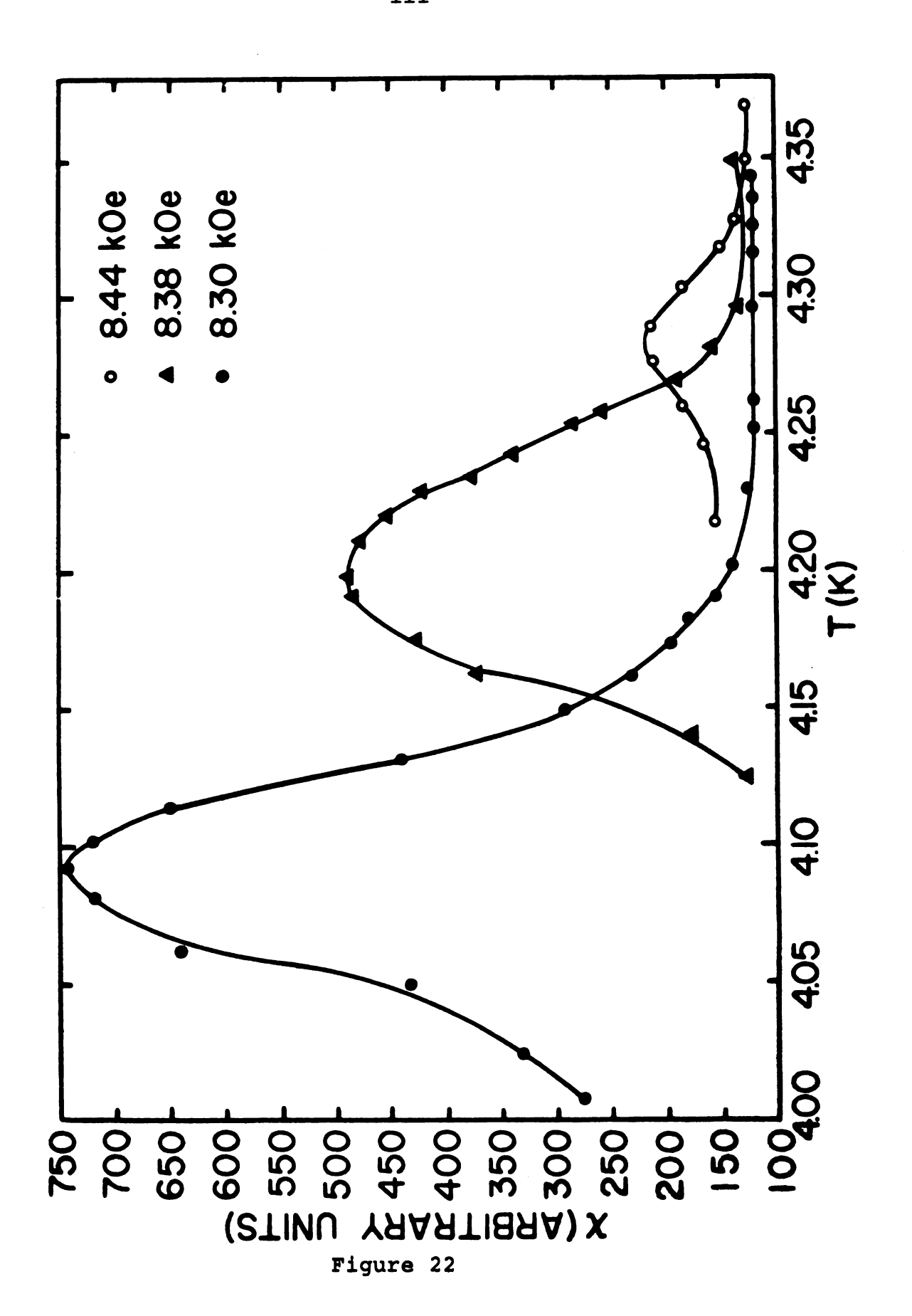


Figure 23. Extrapolation of the amplitude of the spin flop transition vs. temperature for CuCl₂·2H₂O

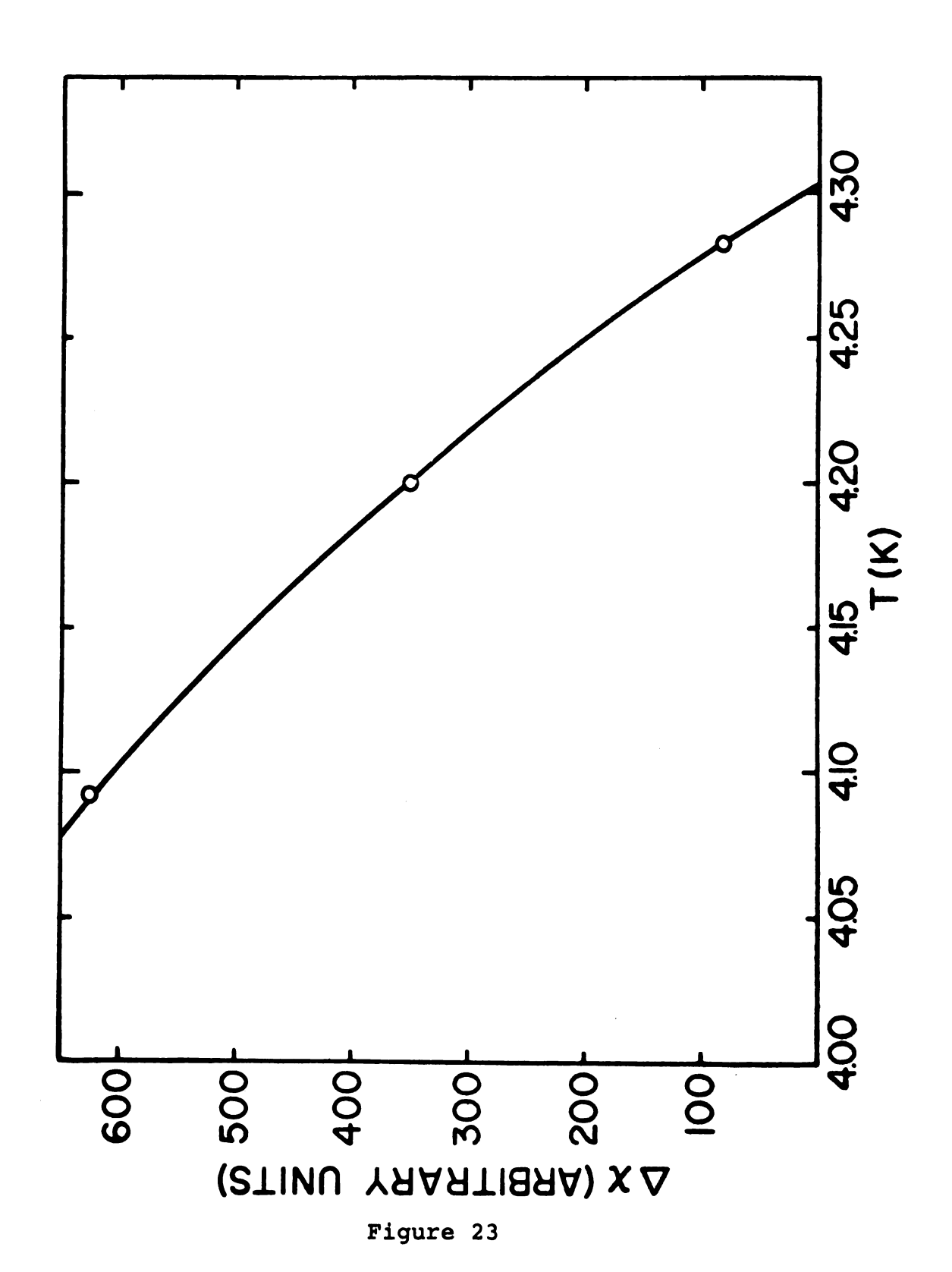
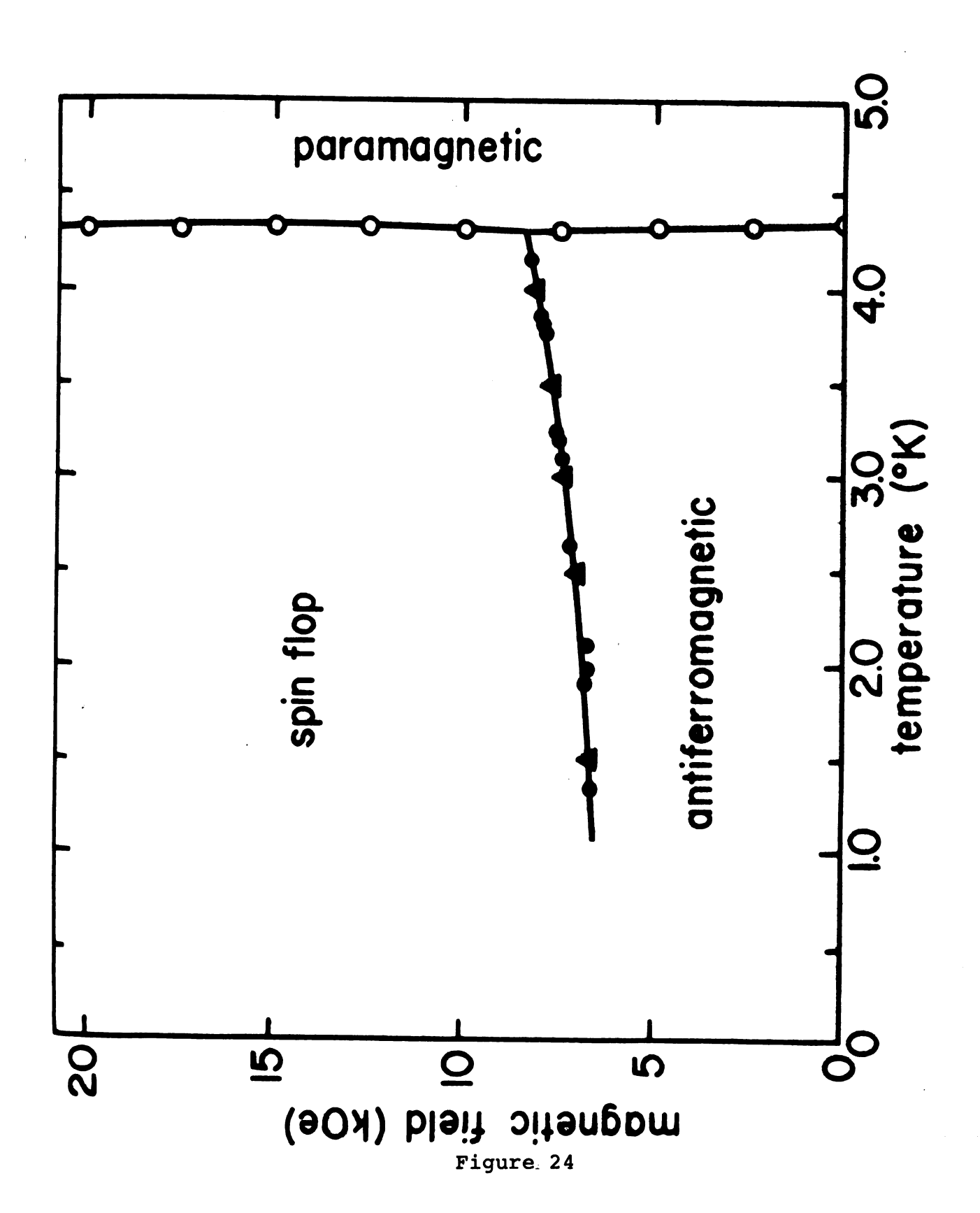


Figure 24. Magnetic phase diagram of CuCl₂·2H₂O (Ref. 58)



From Butterworth's phase diagram (Fig. 24) we estimate the zero temperature spin flop field as

$$H_{th} = H_{SF} = 6.0 \text{ kOe}$$

Solving for the exchange and anisotropic exchange fields using equations 3.22 and 4.43 ($H_T=0$ for spin $\frac{1}{2}$) we find

$$H_E = 85 \text{ kOe}$$
 $H_K = 0.21 \text{ kOe}$
 $CuCl_2 \cdot H_2O$

We have measured chi vs. θ for various fields and fit the data to the theoretical curves of chapter IV by normalizing the experimental parallel and perpendicular susceptibility at zero field to the theoretical zero field values. If the anisotropy is much less than the exchange, crystal field anisotropy or anisotropic exchange give the same angle dependence of the susceptibility so we apply the calculations of chapter IV by substituting h_K for h_L . The theoretical values were calculated assuming

$$h_{\kappa} = H_{\kappa}/H_{r} = 2 \times 10^{-3}$$

There is surprisingly good agreement between the theoretical and experimental behavior of the susceptibility in applied field (Fig. 25).

We have measured χ vs. H at constant temperature (Fig. 26) for this crystal and again the agreement with the theory of chapter IV is very good. Notice that the susceptibility remains very small above the spin flop transition in agreement with equation 4.40

$$\chi_{SF}^{"} = M_O/(2H_E + H_K)$$

Here H_E is very large.

Figure 25. Susceptibility vs. angle for various applied fields for CuCl₂·2H₂O; experimental and theoretical results normalized to the zero field parallel and perpendicular values

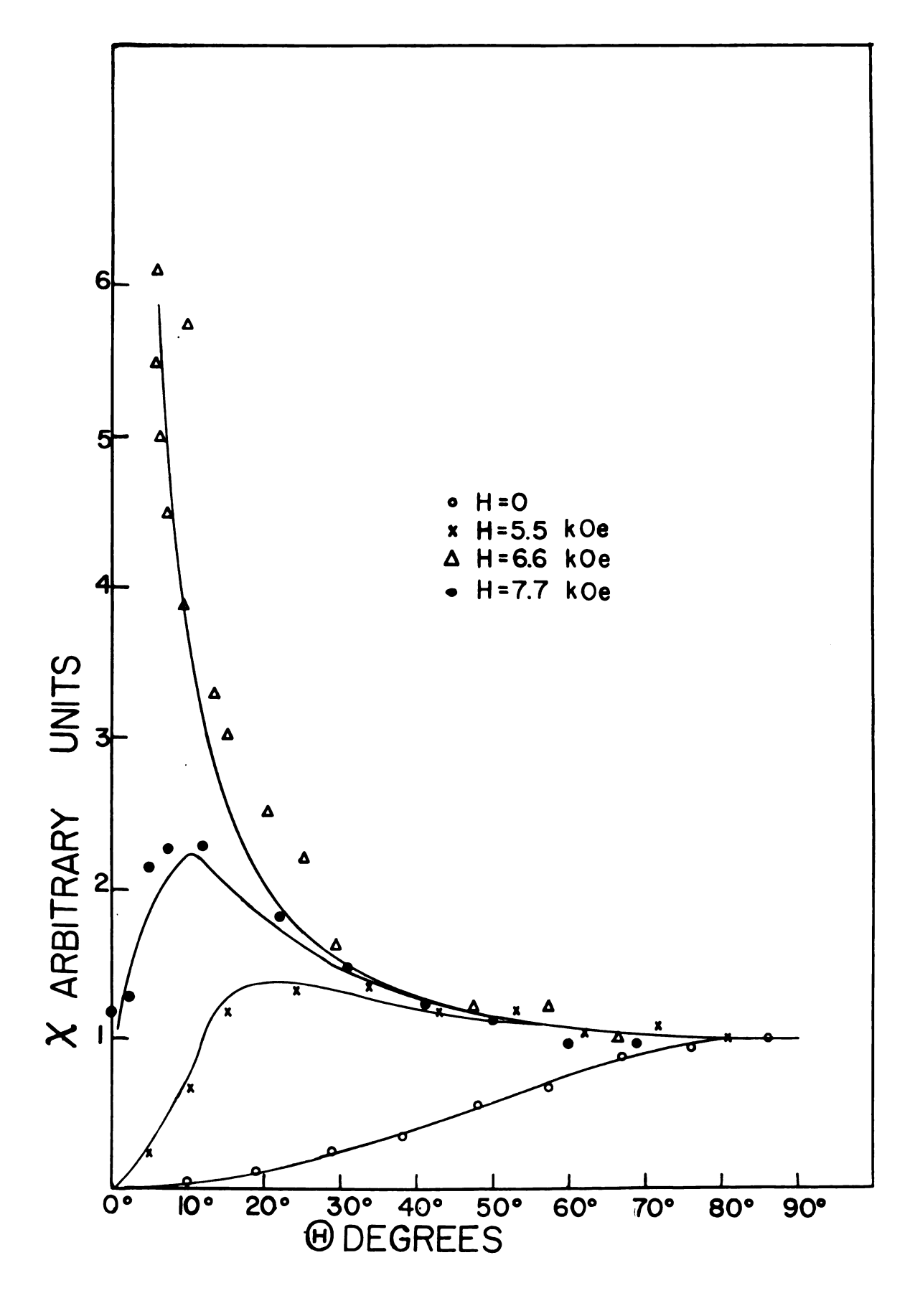


Figure 25

Figure 26. Susceptibility vs. applied field at constant temp-erature for CuCl₂·2H₂O

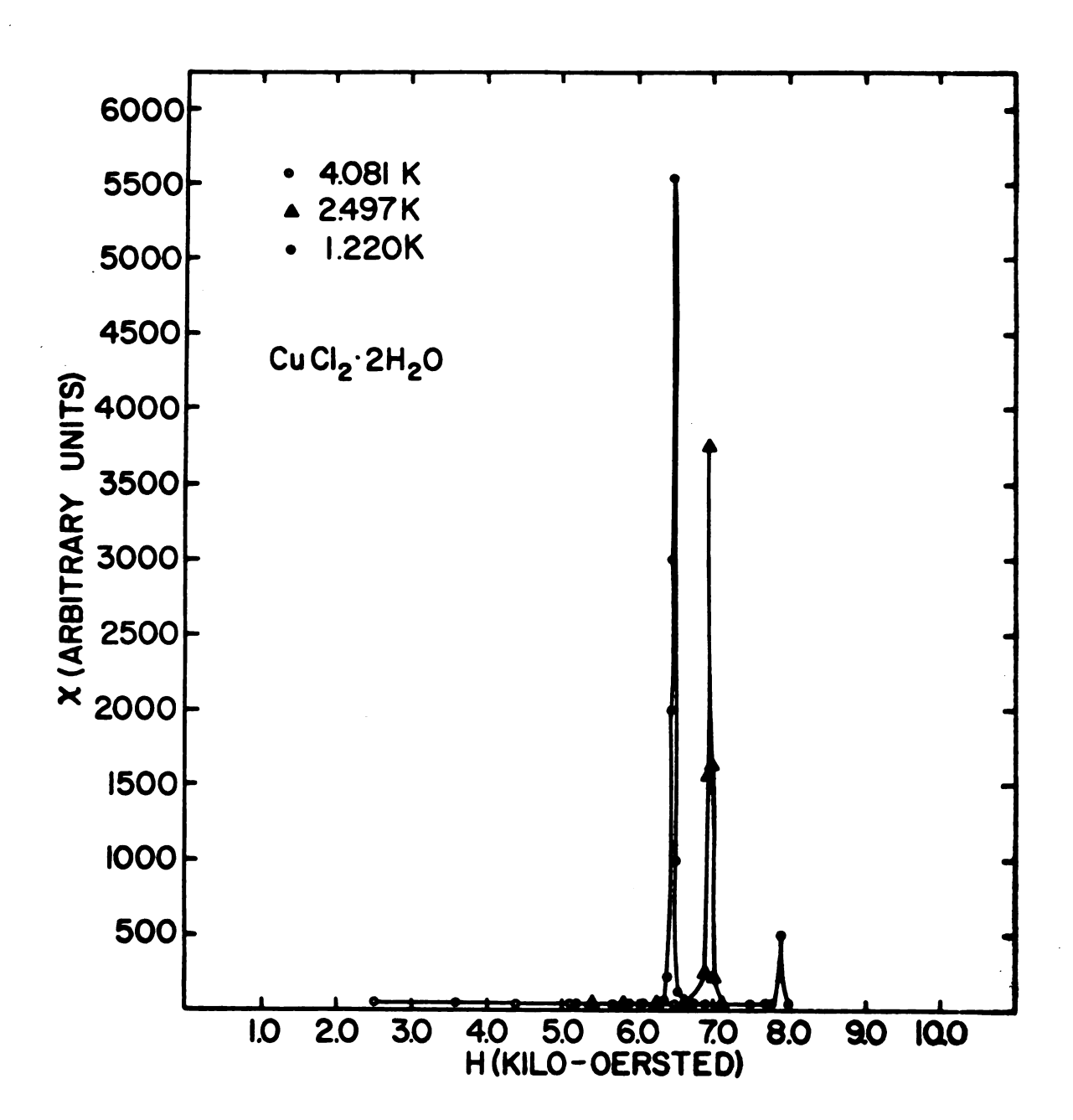


Figure 26

C. MnCl₂·4H₂O

Manganese chloride is a particularly good candidate to which to apply the molecular field theory. A great deal of data is available and the phase diagram is quite complete. The crystal symmetry is monoclinic with rather odd local coordination. Manganese chloride orders antiferromagnetically at $T_N = 1.62$ K. Rives has plotted the parallel phase diagram (Fig. 27) by measuring χ vs. H at constant temperature. An example of his data (Fig. 28) can be compared with the theoretical results of chapter IV (Fig.'s 6, 7). Gisjman et al. have used proton and electron spin resonance to determine the perpendicular paramagnetic boundary and Giauque et al. have measured the entire phase diagram employing isentropic and specific heat techniques. A summary of their results extrapolated to zero temperature is given in Table III.

Assuming that $H_{th} = H_{SF}$, equations 3.21, 3.22, and 3.28 can be solved for the molecular fields

$$H_{E} = \frac{1}{2} [H_{p}^{\perp}(0) - H_{SF}^{2}(0)/H_{p}^{\parallel}(0)]$$
 (6.9)

$$H_{L} = \frac{1}{2} [H_{p}^{(0)} - H_{p}^{(0)}]$$
 (6.10)

$$H_{K} = H_{SF}^{2}(0)/H_{p}^{"}(0) - \frac{1}{2}[H_{p}^{1}(0) - H_{p}^{"}(0)]$$
 (6.11)

The results of these calculations are given in Table III.

The zero field perpendicular susceptibility and the spin flop parallel susceptibility measured by Lasheen et al. 70 and Rives 66, respectively, are compared with the values calculated from equations 4.40 and 4.44 using the molecular fields

Figure 27. Magnetic phase diagram of MnCl₂·4H₂O (Refs. 66 and 67)

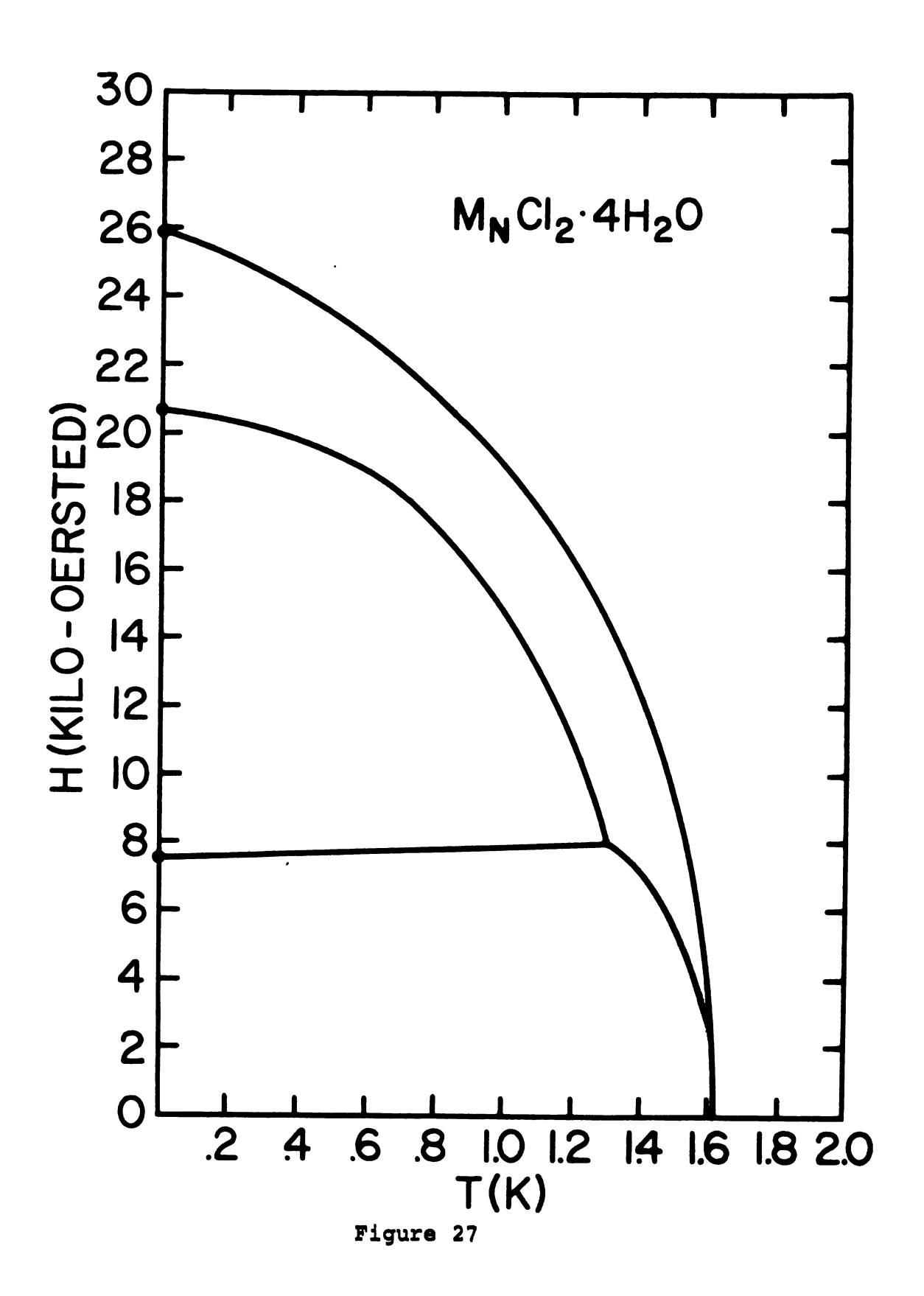


Figure 28. Susceptibility vs. applied field at constant temperature for MnCl₂·4H₂O (Ref. 66)

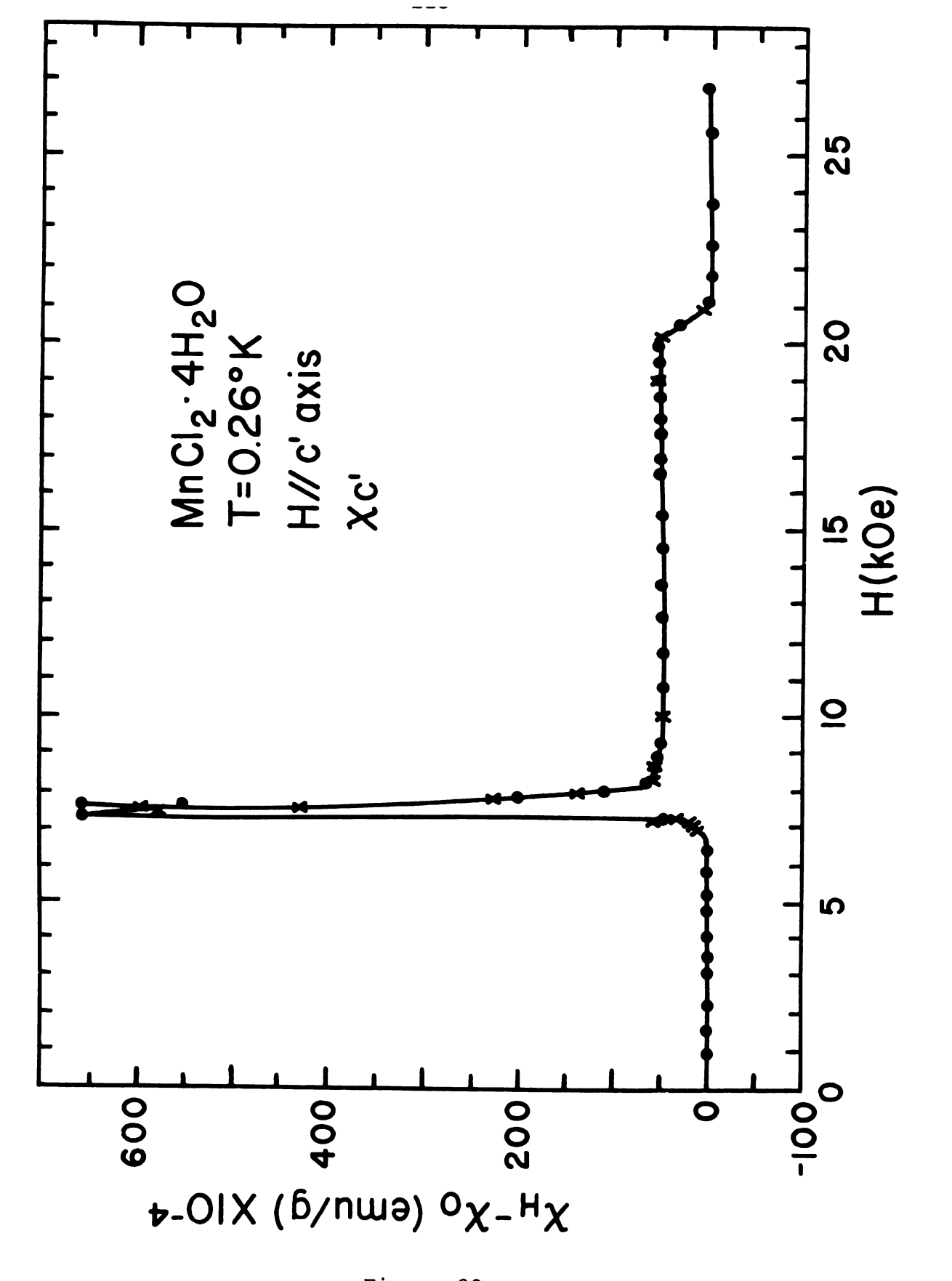


Figure 28

Table III. The zero temperature phase boundaries and molecular fields for MnCl₂·4H₂O

		Rives-Gisjman	Giauque et al.
H _{SF} (0) kOe	7.55	7.80
H"(0)	k0e	20.6	19.0
H _p (0)	k0e	25.5	25.9
$^{ m H}{_{ m E}}$	k0e	11.6	11.5
$^{ m H}_{ m L}$	k0e	2.50	3.45
H _K	k0e	-0.24	-0.26

determined from the Rives-Gisjman phase diagram.

	EXPERIMENTAL	THEORETICAL
XAF	1.09 cm ³ /mole	1.09 cm ³ /mole
X "	1.2 cm ³ /mole	$1.35 \text{ cm}^3/\text{mole}$

One should note that $H_{\overline{K}}$ could well be zero to within experimental accuracy.

D. Conclusions

The molecular field theory developed in chapter III and IV has been applied to $\text{Cs}_2\text{MnCl}_4\cdot 2\text{H}_2\text{O}$, $\text{Rb}_2\text{MnCl}_4\cdot 2\text{H}_2\text{O}$, $\text{CuCl}_2\cdot 2\text{H}_2\text{O}$ and $\text{MnCl}_2\cdot 4\text{H}_2\text{O}$. The data used for the first three was taken in apparatus described in chapter V. The analysis of $\text{MnCl}_2\cdot 4\text{H}_2\text{O}$ was based on data taken from the literature.

The results are very encouraging but not conclusive. Molecular field theory gave consistent results for MnCl₂·4H₂O within the accuracy of the data. In the case of CuCl₂·2H₂O we correctly described the behavior of the susceptibility in applied field. The theory gave different results for the anisotropy of Cs₂MnCl₄·2H₂O and Rb₂MnCl₄·2H₂O from data taken in the paramagnetic or ordered state. It is possible this difficulty can be resolved by a dipolar anisotropy calculation in the ordered state.

It is of particular interest to compare the theoretical and experimental values for the ordering temperature. Using the experimentally determined values for $H_{\rm E}$ in the molecular field equation (4.8)

$$T_N = gu_B^H_E(S+1)/3k_B$$

and Rushbrooke and Wood's equation for the two sublattice cubic antiferromagnet 32 with z nearest neighbors (assumed to be 6) derived by high temperature expansion

$$T_N = (J/2k_B) (5/96) (z-1) (11S(S+1)-1) (1+2/(3zS(S+1))$$

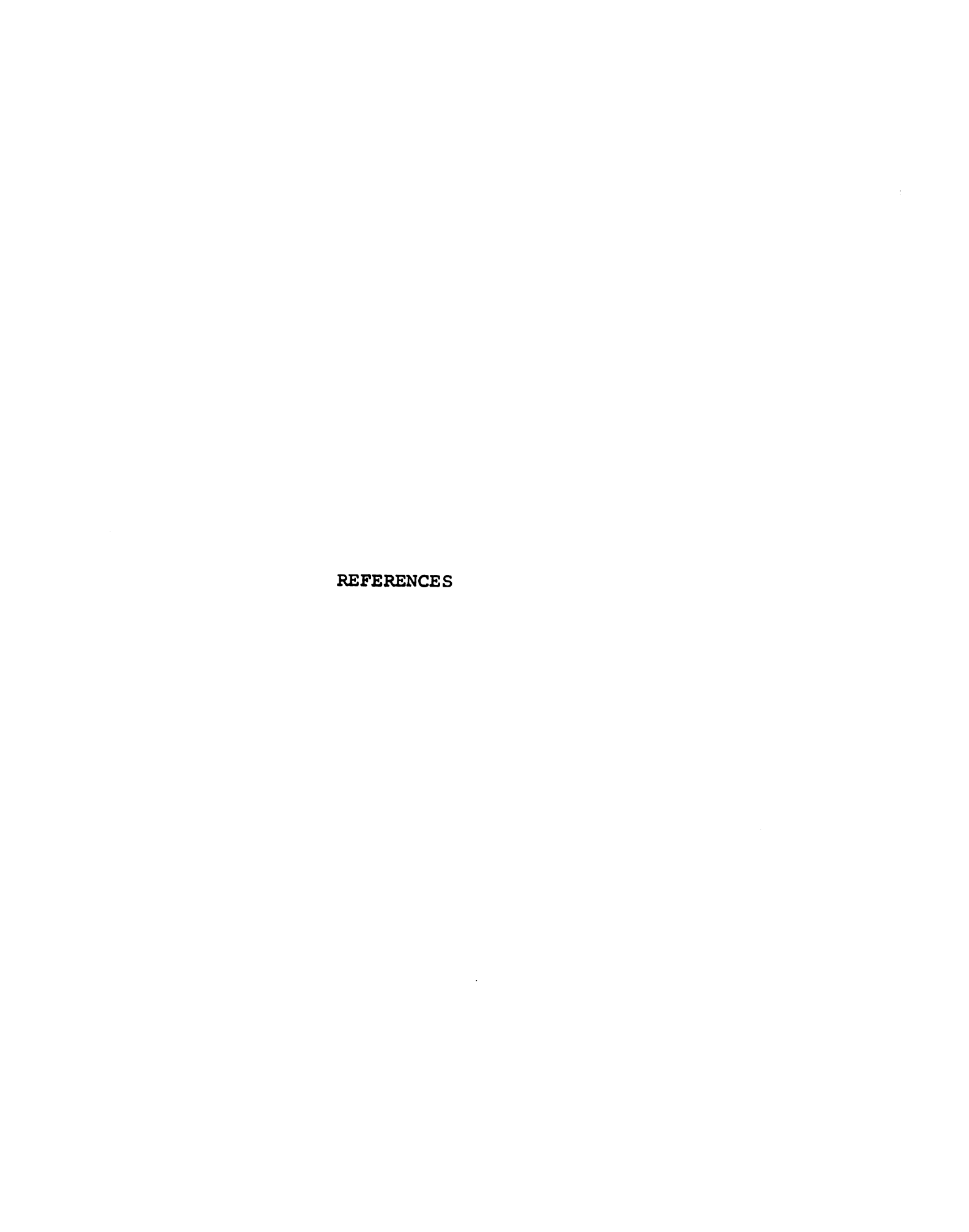
we calculate the transition temperatures for isotropic antiferromagnets. Using Lines 20 calculations of $T_N(L')/T_N(0)$ employing molecular field and Green function theory we obtain transition temperatures for the anisotropic antiferromagnets

	T _N (MFT) K	T _N (HTE-GF) K	T _N (Exp.) K
MnCl ₂ ·4H ₂ O	1.85	1.60	1.62
Cs2MnCl4 · 2H2O	2.85	2.53	1.84
Rb ₂ MnCl ₄ ·2H ₂ O	3.45	3.05	2.24
CuCl ₂ ·2H ₂ O	5.70	4.10	4.33

These transition temperatures are calculated using exchange and anisotropy constants determined by molecular field interpretation of experimental susceptibility and phase diagram data. The discrepancies for the cesium and rubidium suggest two things: applying a simple cubic theory to a triclinic lattice may be overly optimistic (z=4 greatly improves the results) and the difference in the anisotropy above and below the transition implies that our understanding of these crystals is very incomplete.

We have used molecular field theory expressions for the phase diagram and susceptibility of the antiferromagnet to determine the exchange and anisotropy of four magnetic salts.

We have tested the consistency of the molecular field by using these results to accurately predict the behavior of the susceptibility in applied for CuCl₂·2H₂O and MnCl₂·4H₂O. Similarly, we have predicted the existence of a spin flop transition in Cs₂MnCl₄·2H₂O and Rb₂MnCl₄·2H₂O. An experimental test of this prediction cannot be made with our present apparatus. The transition temperatures were calculated and, as expected, the molecular field theory overestimated T_N by 30%-50%. A combination of high temperature expansion and Green function theory was also used and the results of T_N for CuCl₂·2H₂O and MnCl₂·4H₂O were very good. In conclusion, molecular field theory has given a reasonable description of the behavior of the susceptibility of the antiferromagnet as a function of temperature, magnitude and orientation of applied field.



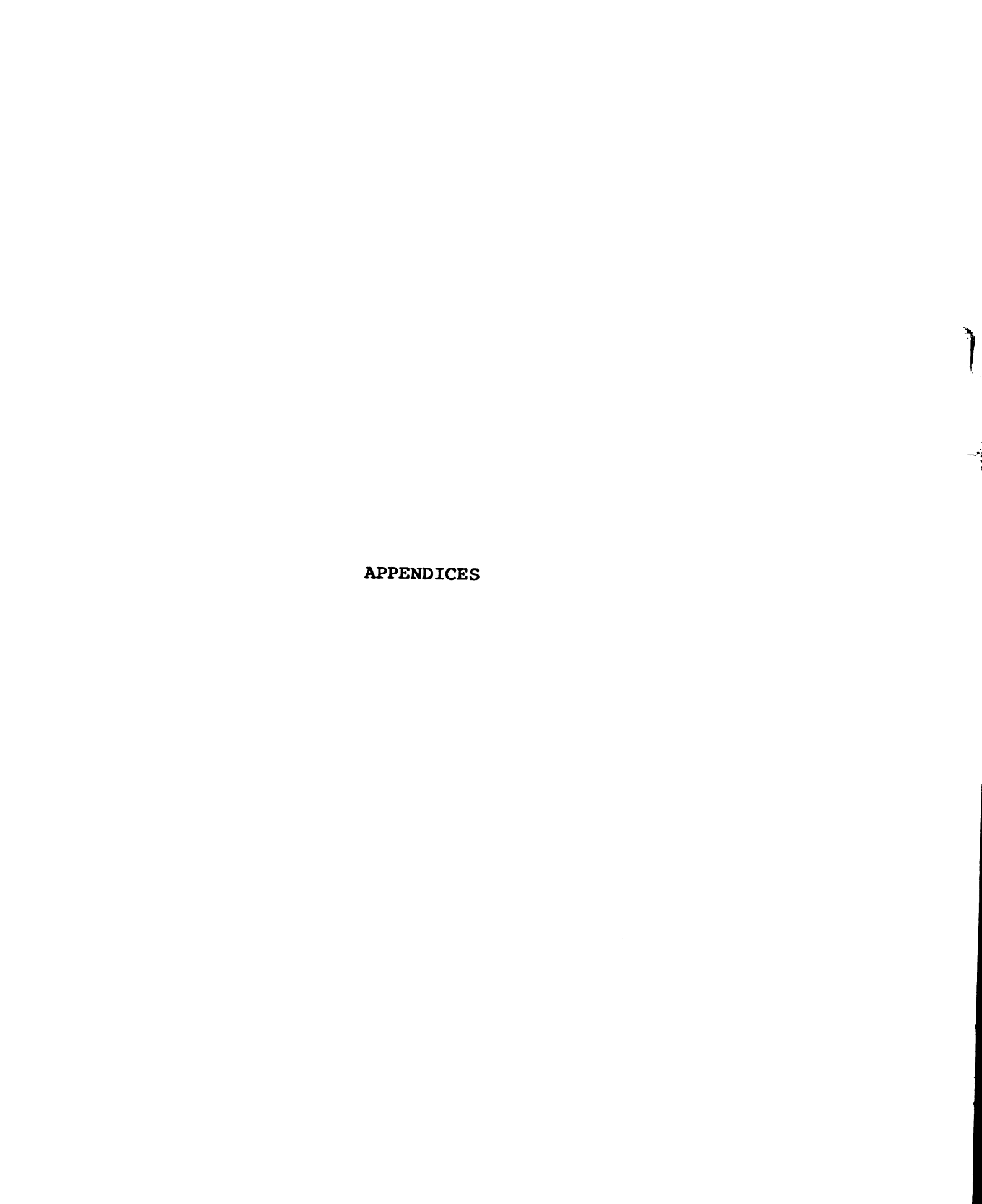
REFERENCES

- 1. W. Heisenberg, Z. Phys. 38, 411 (1926).
- 2. G. H. Wannier, Elements of Solid State Theory (Cambridge University Press, New York, 1959).
- 3. R. M. White, Quantum Theory of Magnetism, (McGraw-Hill, New York, 1970) p. 49.
- 4. D. C. Mattis, The Theory of Magnetism, (Harper and Row, New York, 1965) p. 46.
- 5. P. A. M. Dirac, Proc. Roy. Soc. Al23, 714 (1929).
- 6. T. Nagamiya, R. Kubo, and K Yosida, Phil. Mag. Suppl. $\underline{4}$, 1 (1955).
- 7. P. W. Anderson, Phys. Rev. 79, 350 (1950).
- 8. P. W. Anderson, "Exchange in Insulators" in <u>Magnetism</u> edited by G. T. Rado and H. Suhl (Academic Press, New York, 1963) Vol. I, pp. 25-83.
- 9. H. Kramers, Physica 1, 182 (1934).
- 10. J. H. van Vleck, Phys. Rev. 78, 1178 (1937).
- 11. C. J. Ballhausen, <u>Introduction to Ligand Field Theory</u>, (McGraw-Hill, New York, 1962).
- 12. J. Kanamori, "Anisotropy and magnetostriction of ferromagnetic and antiferromagnetic materials" in Magnetism edited by G. T. Rado and H. Suhl (Academic Press, New York, 1963) Vol. I, p. 146.
- 13. M. Tinkham, Group Theory and Quantum Mechanics, (McGraw-Hill, New York, 1964).
- 14. T. Moriya, Phys. Rev. 120, 91 (1960).
- 15. W. H. Zacharaisen, Theory of X-ray Diffraction in Crystals, (Wiley, New York, 1944).
- 16. E. F. Bertaut, "Spin Configuration of Ionic Structures Theory and Practice" in Magnetism edited by G. T. Rado and H. Suhl (Academic Press, New York, 1963) Vol. III, p. 160.
- 17. L. Onsager, Phys. Rev. 65, 117 (1944).
- 18. J. S. Smart, Effective Field Theories of Magnetism, (W. B. Saunders, Philadelphia, 1966) p. 6.
- 19. M. Freiser, Phys. Rev. <u>123</u>, 2003 (1961).
- 20. M. E. Lines, Phys. Rev. 156, 534 (1967).

- 21. D. N. Zubarev, Soviet Phys. Uspk. 3, 320 (1960).
- 22. L. P. Kadanoff and G. Baym, Quantum Statistical Mechanics, (Benjamin, New York, 1962).
- 23. A. A. Abrikosov, L. P. Gorkov and I. E. Dzyaloshinski, Methods of Quantum Field Theory in Statistical Physics, (Prentice-Hall, Englewood Cliffs, 1963).
- 24. M. E. Lines, Phys. Rev. 135, Al336 (1964).
- 25. R. D. Spence and J. Devlin, unpublished.
- 26. P. Heller and G. Benedek, Phys. Rev. Lett. 14, 71 (1965).
- 27. H. Callen, Phys. Rev. 130, 890 (1963).
- 28. R. Tahir-Kheli and M. S. Jarret, Phys. Rev. 180, 544 (1969).
- 29. F. Bloch, Z. Phys. 74, 295 (1932).
- 30. D. H. Lyons and T. A. Kaplan, Phys. Rev. 120, 1580 (1960).
- 31. J. M. Luttinger and L. Tisza, Phys. Rev. 70, 954 (1951).
- 32. G. S. Rushbrooke and P. J. Wood, Mol. Phys. 1, 257 (1958).
- 33. A. H. Morrish, The Physical Principles of Magnetism, (Wiley, New York, 1965).
- 34. H. Rohrer and H. Thomas, J. Appl. Phys. 40, 1025 (1969).
- 35. J. Feder and E. Pytte, Phys. Rev. 168, 604 (1968).
- 36. F. B. Anderson and H. B. Callen, Phys. Rev. 136, A1068 (1964).
- 37. G. Cinader, Phys. Rev. 155, 453 (1966).
- 38. M. S. Seehra and T. G. Castner, Phys. Rev. Bl, 2289 (1970).
- 39. K. P. Belov, A. M. Kadomtseva, and R. Z. Bevitin, JETP <u>51</u>, 1306 (1966).
- 40. K. W. Blazey et al, Phys. Rev. Lett. 24, 105 (1970).
- 41. Y. Shapira and S. Foner, Phys. Rev. Bl, 3083 (1970).
- 42. K. Yosida, Prog. Th. Phys. 6, 691 (1951).
- 43. R. M. Bozworth, H. J. Williams and E. E. Walsh, Phys. Rev. 103, 572 (1956).
- 44. S. A. Friedberg, Physica 18, 714 (1952).
- 45. F. R. McKim and W. P. Wolf, J. Sci. Inst. 34, 64 (1957).

- 46. T. Moriya, "Weak Ferromagnetism" in Magnetism edited by G. T. Rado and H. Suhl (Academic Press, New York, 1963) Vol. I, p. 103.
- 47. C. W. Fairall, D. D. Swinehart and J. A. Cowen, J. Appl. Phys. 41, 2509 (1970).
- 48. C. Kittel, <u>Introduction to Solid State Physics</u>, (Wiley, New York, 1966) p. 428.
- 49. S. Foner, Rev. Sci. Inst. 30, 548 (1959).
- 50. W. R. Abel, A. C. Anderson and J. C. Wheatley, Rev. Sci. Inst. <u>35</u>, 444 (1964).
- 51. Cryotronics, Inc., High Bridge, New Jersey.
- 52. A. C. Rose-Innes, Low Temperature Techniques, (English Universities Press, London, 1964).
- 53. G. K. White, Experimental Techniques in Low-Temperature Physics, (Oxford Press, London, 1968).
- 54. C. W. Fairall and J. A. Cowen, Bull. Am. Phys. Soc. <u>14</u>, 79 (1969).
- 55. Synthane Corporation, Oaks, Pennsylvania.
- 56. D. Flood, unpublished.
- 57. American Aerospace Control Co., Type MRA-11.
- 58. G. J. Butterworth and V. S. Zidell, J. Appl. Phys. <u>40</u>, 1033 (1969).
- 59. P. A. Thompson, R. C. A. Magnet Design Aid, RCA (1966).
- 60. M. E. Fisher, Phil. Mag. 7, 1731 (1962).
- 61. R. D. Spence, J. A. Casey and V. Nagarajan, Phys. Rev. <u>181</u>, 488 (1969).
- 62. H. Forstat, N. D. Love and J. N. McElearny, Phys. Lett. <u>25A</u>, 253 (1967) and Bull. Am. Phys. Soc. <u>12</u>, 285 (1967).
- 63. T. Smith and S. A. Friedberg, Phys. Rev. <u>177</u>, 1012 (1969).
- 64. C. Kittel, Phys. Rev. 82, 565 (1951).
- 65. J. van den Handel, H. M. Gisjman and N. J. Poulis, Physica 18, 862 (1952).
- 66. J. E. Rives, Phys. Rev. 162, 491 (1967).
- 67. H. M. Gisjman, N. J. Poulis, J. van den Handel, Physica 25, 954 (1959).

- 68. R. A. Reichert and W. F. Giauque, J. Chem. Phys. <u>50</u>, 4205 (1969) and 52, 2901 (1970).
- 69. K. W. Blazey and H. Rohrer, Phys. Rev. 173, 574 (1968).
- 70. M. A. Lasheen, J. van den Broek and C. J. Gorter, Physica 24, 1061 (1958).
- 71. S. J. Jensen, Acta Chem. Scand. <u>18</u>, 2085 (1964).
- 72. A. Zalkin, J. D. Forrester, and D. H. Templeton, Inorg, Chem. 3, 529 (1964).
- 73. S. W. Peterson and H. A. Levy, J. Chem. Phys. 26, 220 (1957).



APPENDIX A

NEWTON'S METHOD

Newton's method is a numerical process for finding the zeroes of sets of functions. If we consider the equations

$$f(x) = 0 (A1)$$

Newton's method consists of evaluating f(x) and f'(x) at an arbitrary point x_0 and approximating the solution to Al by finding the intersection with the x axis of a striaght line constructed tangent to the curve f(x) at x_0 . The line intersects the x axis at a point given by

$$x' = x_0 - f(x_0) / f'(x_0)$$
 (A2)

Newton's method is usually used in an iterative process where each successive x' is employed in equation A2 as an x_0 .

If we have N equations in N unknowns

$$f_n(x^0, x^2, \dots x^N) = 0 (A3)$$

and we define

$$f_n^i = df_n/dx^i \tag{A4}$$

The approximation to a simultaneous root of N equations is

$$x^{i} = x_0^i - x^i \tag{A5}$$

where x is the solution to the set of N linear equations

$$\sum_{i} x^{i} f_{n}^{i}(x_{0}) = f_{n}(x_{0}) \tag{A6}$$

The parameter xⁱ of equation A5 can be represented by

$$x^{i} = \begin{bmatrix} f_{i} & f_{1}^{2} \dots f_{1}^{i-1} & f_{i} & f_{1}^{i+1} & f_{1}^{N} \\ f_{2}^{1} & f_{2} & f_{2}^{2} \\ \vdots & \vdots & \vdots \\ f_{N}^{1} \dots & f_{N}^{N} \end{bmatrix}$$

$$det(F)$$

where F is the matrix formed by the coefficients of $f_n^i(x_o)$.

Newton's method is very rapidly convergent but one can have difficulty inducing convergence to a particular solution of interest.

APPENDIX B

CRYSTALLOGRAPHY

1. Cs_2MnCl_4 $2H_2O$ and Rb_2MnCl_4 $2H_2O$

These crystals are grown by evaporation from aqueous solutions of XCl and $MnCl_2$ $4H_2O$. They are whitish pink in color and fairly stable in air. The structure is triclinic, $P\bar{l}$ with one chemical formula per unit cell⁷¹. The lattice parameters are

	Cs ₂ MnCl ₄ 2H ₂ O	Rb ₂ MnCl ₄ 2H ₂ O
a Å	5.74	5.66
b "	6.66	6.48
C "	7.27	7.01
deg.	67.0	66.7
**	87.8	87.7
n	84.3	84.8

2. MnCl₂ 4H₂O

Manganese chloride tetrahydrate is grown by evaporation of aqueous solutions of manganous chloride and HCl. The crystals are reddish pink in color and fairly stable in air. The structure is monoclinic, P2/m with four chemical formulae per unit cell⁷². The lattice parameters are

	MnCl ₂ 4H ₂ O
a Å	11.19
b "	9.51
c "	6.19
deg.	99.74

3. CuCl₂ 2H₂O

Copper chloride dyhydrate is grown by evaporation of aqueous solutions of ${\rm CuCl}_2$. The crystals are blue-green in color and fairly stable in air. The c axis defines an excellent cleavage plane. The structure is orthorhombic, $V_h^7({\rm Pbmn})$ with two chemical formulae per unit cell⁷³.

	CuCl ₂ 2H ₂ O
a Å	7.38
b "	8.04
c "	3.72

APPENDIX C

COMPUTER PROGRAMS

```
RUN(S)
LGO.
0000000000000000000000
             PROGRAM ANIS(INPUT.OUTPUT.TAPE61=OUTPUT)
              THIS PROGRAM CALCULATES THE EQUILIBRIUM ANGLES FOR A TWO SPIN
C
              SYSTEM WITH GENERAL ANISOTROPY. IT ALSO CALCULATES THE
С
             MAGNETIZATION, ENERGY, AND STABILITY OF EACH STATE WITH AN
C
C
              APPLIED FIELD.
C
C
C
C
             DEFINE FUNCTIONS
C
              AF STATE
             EBAF (A+B+H+HK+HL+HD) = (2+HK+HL+COS(2+A)) +SIN(2+B) -2+HD+COS(2+B)
            1+2*H*SIN(A) *COS(B)
             EAAF (A.B.H.HC.+HL.+HD) = ((HK+HL+COS(2+B))+SIN(A)+ H+SIN(B))+COS(A)
             EBAFB(A.B.H.+HK.+HL.+HD)=2+((2+HK+HL+COS(2+A))+COS(2+B)+2+HD+SIN(2+B)
            1-H*SIN(A)*SIN(B))
             EAAFB(A+B+H+HK+HL+HD)=COS(A)+(H+COS(B)-2+HL+SIN(2+B)+SIN(A))
             EBAFA (A+B+H+HK+HL+HD) = 2+ (H+COS(A)+COS(B)-HL+SIN(2+B)+SIN(2+A))
             EAAFA(A,B,H,HK,HL,HD)=COS(A)# (HK+HL*COS(2*B))*COS(A)-SIN(A)*((
            1HK+HL*COS(2*B))*SIN(A)+H*SIN(B))
             SAF(A+B+H+HK+HL+HD) = ((2 + HK + HL+COS(2+A))+COS(2+B) + 2+HD+SIN
            1(2+B) - H+SIN(A)+SIN(B))+((HK +HL+COS(2+B))+COS(2+A)-H+SIN(A)
           2*SIN(B)) - (HL*SIN(2*A)*SIN(2*B) - H*COS(A)*COS(B))**2
             UAF (A+B+H+HK+HL+HD) =-COS(2*B)-HL*(COS(2*B)*COS(A)*COS(A)+SIN(B)*
            1SIN(B))-HK*(COS(A)*COS(A)-SIN(B)*SIN(B))-HD*SIN(2*B)
           2+2*H*SIN(A) *SIN(B)
             SF STATE
             ESF(B_0H_0HK_0HL_0HD) = (2 + HK - HL)*SIN(2*B) - 2*HD*COS(2*B) - 2*HD*COS(2*
            1H*COS(B)
             USF(B+H+HK+HL+HD) = -1+SIN(B)+((2+HK-HL)+SIN(B)-2+H-2+HD+COS(B))
             SSF(B_0H_0HK_0HL_0HD) = -((2 + HK - HL) + COS(2+B) + 2+HD+SIN(2+B) + H+
            1SIN(B)) * (HK +HL*COS(2*B)-H*SIN(B))
             ESFB(B+H+HK+HL+HD) = 2*(2 + HK - HL)*COS(2*B) + 4*HD*SIN(2*B)
           1+ 2*H*SIN(B)
             PERPENDICULAR STATE
             EP(B_0H_0HK_0HL_0HD) = (2 + HK + HL)*SIN(2*B) - 2*HD*COS(2*B) - 2*H*
            1COS(B)
             SP(B_0H_0HK_0HL_0HD) = (2 + HK + HL)*COS(2*B) + 2*HD*SIN(2*B) + H*SIN
            1(B)
```

```
UP(B+H+HK+HL+HD) =1-(2+HK+HL)+(COS(B))++2-HD+SIN(2+B) -2+H+SIN(B)
C
      PARAMAGNETIC STATE
      UPMRL(B+H+HK+HL+HD) = 1 + HK - HL -2*H
      UPMDR(B+H+HK+HL+HD) = 1 + HK + HL -2+H
C
С
      L = 0
      CHIP = 1/(2+HK+HL)
      CHIAF = 0
      SMZAF = 0
      SMYP = 0
      PI = 3.1415926536
      HK=0.1
      HL = 0.1
      HD=0.1
      SHD
             = HD
      SHK
             = HK
      SHL
             = HL
      A=0.0
      B=HD/(2+HK+HL)
      C = B
      H=-0.005
      DO 100 J = 1.500
      H=H+0.005
      K = 0
   10 A=A-(EAAF(A.B.H.HK.HL.HD)*EBAFB(A.B.H.HK.HL.HD)-EBAF(A.B.H.HK.HL.
     1HD) #EAAFB(A.B.H.HK.HL.HD))/(EAAFA(A.B.H.HK.HL.HD)#EBAFB(A.B.H.HK.
     2HL+HD)-EAAFB(A+B+H+HK+HL+HD) *EBAFA(A+B+H+HK+HL+HD))
      B=B-(EBAF(A+B+H+HK+HL+HD)#EAAFA(A+B+H+HK+HL+HD)-EAAF(A+B+H+HK+HL+
     THD) *EBAFA(A+B+H+HK+HL+HD))/(EAAFA(A+B+H+HK+HL+HD) *EBAFB(A+B+H+HK+
     2HL+HD)-EAAFB(A+B+H+HK+HL+HD) *EBAFA(A+B+H+HK+HL+HD))
      K = K+1
      EAAFX= ABS(EAAF(A+B+H+HK+HL+HD))
      EBAFX = ABS(EBAF(A \cdot B \cdot H \cdot HK \cdot HL \cdot HD))
      S = EAAFX+EBAFX
      IF(K.GT.50)GO TO 35
      IF(S.GE.0.000001)G0 TO 10
   35 SEAF = S
      SSAF
                = SAF (A+B+H+HK+HL+HD)
      SUAF =UAF (A+B+H+HK+HL+HD)
      X=SMZAF
      SMZAF = -SIN(A) *SIN(B)
      CHIAF = (SMZAF-X)/0.005
      KSKAF
                 = K
              = A+180.0/PI
      SA
      SBAF
                = B*180.0/PI
      K = 0
      B=C
   50 B = B-ESF(B+H+HK+HL+HD)/ESFB(B+H+HK+HL+HD)
      K = K + 1
      ESFX = ESF(B+H+HK+HL+HD)
```

```
S = ABS(ESFX)
      IF(K.GT.50)G0 TO 60
      IF(S.GE.0.00001)GU TO 50
                 = ESF(B+H+HK+HL+HD)
   60 SESF
      SSSF
                  = SSF(B+H+HK+HL+HD)
                  = USF(B+H+HK+HL+HD)
      SUSF
      SMZSF = SIN(B)
                  = B*180.0/PI
      SBSF
      KSKSF
                   = K
      C=B
      K =0
   70 B = B-EP(B+H+HK+HL+HD)/(2*SP(B+H+HK+HL+HD))
      K = K+1
      EPX = EP(B \cdot H \cdot HK \cdot HL \cdot HD)
       S = ABS(EPX)
      IF (K.GT.50)GO TO 80
      IF(S.GE.0.00001)G0 TO 70
   80 SEP
                = EP(B+H+HK+HL+HD)
      SSP
                = SP(B \cdot H \cdot HK \cdot HL \cdot HD)
      SUP
                = UP(B+H+HK+HL+HD)
      Y=SMYP
      SMYP = SIN(B)
CHIP=(SMYP-Y)/0.005
      SBP = B*180.0/PI
      SUPMRL
                   = UPMRL(B+H+HK+HL+HD)
      SUPMOR
                    = UPMDR(8+H+HK+HL+HD)
      KSKP
                  = K
С
С
С
      WRITE OPERATIONS
      L = L-1
      IF(L.LE.0)200+300
  200 WRITE(61+210)
  210 FORMAT(1H1 + HK
                            HL
                                 HD
                                            EAF
                                                   BAF
                                                                  K ESF BSF
                                                           MYP
     1EP
           BP
                    SAF
                            SSF
                                   SP
                                           MZAF
                                                  MZSF
                                                                    CHIAF
     2HIP *)
      L = 60
  300 WRITE(61+310)(SHK+SHL+SHD+SH+SEAF+SBAF+SA+KSKAF+SESF+SRSF+SEP+SBP+
     1SSAF + SSSF + SSP + SMZAF + SMZSF + SMYP + CHIAF + CHIP)
  310 FORMAT(X)F4.2,2F5.2+F6.3+F4.1+2F7.2+I3+F4.1+F7.2+F4.1+F7.2+6F7.4+
     12F9.4)
  100 CONTINUE
  120 CONTINUE
  130 CONTINUE
      END
0000000000000000000000
```

```
FAIRALL, T30 , CM44100, P2.
                                   FAIRALL
MAP (OFF)
RUN(S)
LGO.
0000000000000000000000
      NO LIST
      PROGRAM HSC(INPUT+OUTPUT+TAPE61=OUTPUT)
      USF(C+H+HK+HL+HD)=-1+SIN(C)*((2+HK-HL)*SIN(C)-2*H-2*HD*COS(C))
      ESF(C \cdot H \cdot HK \cdot HL \cdot HD) = (2 + HK - HL) *SIN(2*C) - 2*HD*COS(2*C) - 2*
     1H+COS(C)
      ESFH(C+H+HK+HL+HD) = -2*COS(C)
      ESFC(C_9H_9HK_9HL_9HD) = 2#(2 + HK - HL)#COS(2#C) + 4#HD#SIN(2#C)
     1+ 2*H*SIN(C)
      SSFC(C+H+HK+HL+HD) = -2+HL+SIN(2+C)-H+COS(C)
      SSFH(C+H+HK+HL+HD) = -SIN(C)
      SSF(C+H+HK+HL+HD) = HK+HL+COS(2+C)-H+SIN(C)
      SAF(A+B+H+K+HL+HD) = ((2 + HK + HL+COS(2+A))+COS(2+B) + 2+HD+SIN
     1(2#B) - H*SIN(A)*SIN(B))*((HK +HL*COS(2*B))*COS(2*A)-H*SIN(A)
     2*SIN(B) - (HL*SIN(2*A)*SIN(2*B) - H*COS(A)*COS(B))**2
      L=0
      PI=3.1415926536
      HK = 0
      HD = 0.01
      HL=0.5
      SHL=HL
      SHD=HD
      H = ((2+HK-HL)*(HK+HL))**0.5
      H=H+0.001
      C = ((HK+HL)/(2+HK-HL))**0.5
      HK=-0.01
      DO 110 J=1+150
      HK=HK+0.01
      SHK=HK
      K=0
   10 C=C-(ESF(C+H+HK+HL+HD)+SSFH(C+H+HK+HL+HD)-ESFH(C+H+HK+HL+HD)+
     1SSF(C+H+HK+HL+HD))/(ESFC(C+H+HK+HL+HD)+SSFH(C+H+HK+HL+HD)-ESFH(
     2C+H+HK+HL+HD) *SSFC(C+H+HK+HL+HD))
      H=H-(ESFC(C+H+HK+HL+HD)+SSF(C+H+HK+HL+HD)-SSFC(C+H+HK+HL+HD)+
     1ESF(C+++HK+HL+HD))/(ESFC(C+++HK+HL+HD)+SSFH(C+H+HK+HL+HD)-ESFH(
     2C+H+HK+HL+HD) *SSFC(C+H+HK+HL+HD))
      K=K+1
      S = ABS(ESF(C + H + HK + HL + HD)) + ABS(SSF(C + H + HK + HL + HD))
      IF (K.GT.50)GO TO 35
      IF(S.GE.0.000001)GO TO 10
   35 SESF = ESF(C+H+HK+HL+HD)
      SSSF = SSF(C+H+HK+HL+HD)
      SUSF = USF(C+H+HK+HL+HD)
      SCSF=C*180.0/PI
      KSF =K
      SH =H
      WRITE OPERATIONS
C
      L = L-1
      IF(L.LE.0)200,300
```

```
SPENCE + T40 + CM44100 + P2.
                                  FAIRALL
MAP (OFF)
RUN(S)
LGU.
NO LIST
      PROGRAM HSH(INPUT,OUTPUT,TAPE61=OUTPUT)
      EBAF (A+B+H+HK+HL+HD) = (2+HK+HL+COS(2+A)) +SIN(2+B)-2+HD+COS(2+B)
     1+2*H*SIN(A) *COS(B)
      \Sigma A4F(A+B+H+HK+HL+HD)=((HK+HL+COS(2+B))+SIN(A)+ H+SIN(B))+COS(A)
     EBAFB (A+B+H+HK+HL+HD) =2+((2+HK+HL+CUS(2+A))+COS(2+B)+2+HD+SIN(2+B)
     1-H*SIN(A)*SIN(B))
     EAAFB(A+B+H+HK+HL+HD)=COS(A)+(H+COS(B)-2+HL+SIN(2+B)+SIN(A))
     FBAFA:A+B+H+HK+HL+HD)=2*(H*U0>(A)*COS(B)=HL*SIN(2*B)*SIN(2*A))
     EAAFA(A+B+H+HK+HL+HD)=COS(A) + (HK+HL+COS(2+B))+COS(A)-SIN(A)+((
     1HK+HL*COS(2*B))*SIN(A)+H*SIN(B))
     UAF(A+B+H+HK+HL+HD)=-COS(2+B)-HL+(COS(2+B)+COS(A)+COS(A)+SIN(B)+
     1SIN(B))-HK*(COS(A)*COS(A)-SIN(B)*SIN(B))-HD*SIN(2*B)
     2+2*H*SIN(A)*SIN(B)
     EBAFH(A+B)=2*SIN(A)*COS(B)
     EAAFH(A+B)=SIN(B)+COS(A)
     $1AF(A+B+H+HK+HL+HD)=(2+HK+HL+COS(2+A))+COS(2+B)+2+HD+SIN(2+B)
     1-H*SIN(A) *SIN(B)
     $1AFB(A,B,H,HK,HL,HD) =-2#(2+HK+HL#COS(2#A))#$IN(2#B)+4#HD#COS(
     12+B) -H+SIN.A) +CO5(B)
      SIAFH(A:B) =-SIN(A) +SIN(B)
      52AF(A+B+H+HK+HL+HD) = (HK+HL+CUS(2+B))+COS(2+A)-H+SIN(A)+SIN(B)
      52AFA(A+B+H+HK+HL+HD)=-2*(HK+HL*COS(2*B))*SIN(2*A)-H*COS(A)*SIN(B)
      52AFB(A+B+H+HK+HL+HD)=-2+HL+SIN(2+B)+COS(2+A)-H+SIN(A)+COS(B)
      SZAFH(A+B) =-SIN(A) *SIN(B)
      S3AF (A+B+H+HK+HL+HD)=HL+SIN(2+A)+SIN(2+B)-H+COS(A)+COS(B)
      $3AFA(4+B+H+HK+HL+HD)=24HL#COS(24A)#$IN(24B)+H#$IN(A)#COS(B)
      53AFB(A+B+H+HK+HL+HD)=2+HL+SIN(2+A)+COS(2+B)+H+COS(A)+SIN(B)
     S3AFH(A+B) = -COS(A) + COS(B)
     SAF (A+B+H+HK+HL+HD)=SIAF (A+B+H+HK+HL+HD) *S2AF (A+B+H+HK+HL+HD)=
     1 S3AF (A+B>H+HK+HL+HD) **2
     SAFA (A+B+H+HK+HL+HD) = $1AFA (A+B+H+HK+HL+HD) +$2AF (A+B+H+HK+HL+HD)
     1 +S1AF(A+B+H+HK+HL+HD)+S2AFA(A+B+H+HK+HL+HD)=2*S3AF(A+B+H+HK+HL+
     2 HD) #S3AFA(A+B+H+HK+HL+HD)
     SAFB (A.B.H.HK.HL.HD) = S1AFB (A.B.H.HK.HL.HD) + S2AF (A.B.H.HK.HL.HD)
     1+S1AF(A+B+H+HK+HL+HD)*S2AFB(A+B+H+HK+HL+HD)=2*S3AF(A+B+H+HK+HL+HD)
     2*S3AFU(A+B+H+HK+HL+HD)
     SAFH(A+B+H+HK+HL+HD)=SIAFH(A+B)+S2AF(A+B+H+HK+HL+HD)
     : +S1AF (A+B+H+HK+HL+HD) #S2AFH(A+B)
                                                 -2*S3AF (A+B+H+HK+HL+HD)
     2 *S3AFH(A+B)
     DELTA (A+B+H+HK+HL+HD) = EAAFA (A+B+H+HK+HL+HD) * (EBAFB (A+B+H+HK+HL+HD)
     1*SAFH(A+B+H+HK+HL+HD)=SAFB(A+B+H+HK+HL+HD)*EBAFH(A+B))=EBAFA(A+
     2B+H+HK+HL+HD) + (EAAFB (A+B+H+HK+HL+HD) +SAFH (A+B+H+HK+HL+HD) -SAFB (
     3A+B+H+HK+HL+HD) *EAAFH(A+B)) *SAFA(A+B+H+HK+HL+HD) *(EAAFB(A+B+H+HK+
    4HL+HD) *EBAFH(A+B) -EBAFB(A+B+H+HK+HL+HD) *EAAFH(A+B))
     L=0
     PI = 3.1415926536
     HK=0.1
```

```
HL=0.3
      SHK=HK
      SHL =HL
      H = ((2+HK+HL)*(HK+HL))**0.5
      \Delta = 0
      B=0
      C=0
      HD = -0.005
      DO 100 J=1.10
      H=H+0.01
      HD=HD+0.005
      SHD = HD
      K=0
   10 CONTINUE
      A=A-(EAAF(A.B.H.HK.HL.HD) +(EBAFB(A.B.H.HK.HL.HD)+SAFH(A.B.H.HK.HL.
     1HD)-SAFB(A+B+H+HK+HL+HD)+EBAFH(A+B))-EBAF(A+B+H+HK+HL+HD)+(EAAFB(
     2A.B.H.HK.HL.HD) +SAFH(A.B.H.HK.HL.HD) -SAFH(A.E.H.HK.HL.HD) +EAAFH(
     3A.B))+SAF(A.B.H.HK.HL.HD)+(EAAFB(A.B.H.HK.HL.HD)+EBAFH(A.B)-
     4 EBAFB(A+B+H+HK+HL+HD)*EAAFH(A+B)))/DELTA(A+B+H+HK+HL+HD)
      1HD) -SAF(A+B+H+HK+HL+HD)+EBAFH(A+B))-EBAFA(A+B+H+HK+HL+HD)+(
     2EAAF (A+B+H+HK+HL+HD) +SAFH (A+B+H+HK+HL+HD) -SAF (A+B+H+HK+HL+HD) +
     3EAAFH(A+B))+SAFA(A+B+H+HK+HL+HD)+(EAAF(A+B+H+HK+HL+HD)+EBAFH(A+B)
     4-EBAF (A+B+H+HK+HL+HD) *EAAFH(A+B)))/DELTA(A+B+H+HK+HL+HD)
      H=H-(EAAFA(A+B+H+HK+HL+HD)+(EBAFB(A+B+H+HK+HL+HD)+SAF(A+B+H+HK+HL+
     1HD)-SAFU(A+B+H+HK+HL+HD)+EBAF(A+B+H+HK+HL+HD))-EBAFA(A+B+H+HK+HL+
     2HD) * (EAAFB (A+B+H+HK+HL+HD) *SAF (A+B+H+HK+HL+HD) =SAFB (A+B+H+HK+HL+HD)
     3) *EAAF (A+B+H+HK+HL+HD)) +SAFA (A+B+H+HK+HL+HD) * (EAAFB (A+B+H+HK+HL+
     4HD) *EBAF (A·B·H·HK·HL·HD) -EBAFB (A·B·H·HK·HL·HD) *EAAF (A·B·H·HK·HL·
     5HD)))/DELTA(A+B+H+HK+HL+HD)
     K=K+1
      S=ABS (EAAF (A+B+H+HK+HL+HD))+ABS (EBAF (A+B+H+HK+HL+HD))+ABS (SAF (A+
     1B.H.HK.HL.HD))
      IF (K.GT.50) GO TO 35
      IF(S.GE.0.0000001)GO TO 10
   35 SS ≈S
      KSK =K
      SH =H
      A=ASIN(SIN(A))
      SA=A+180.0/PI
      SB=B+180.0/PI
      SC=C+180.0/PI
C
      WRITE OPERATIONS
      L = L-1
      IF(L.LE.0)200.300
  200 WRITE(61.210)
  210 FORMAT(1H1 *
                   HK
                           HL
                                HD
                                       н
                                               S
                                                                 8
                                                                        C
           K#)
      L=60
  300 WRITE(61+310)(SHK+SHL+SHD+SH+SS+SA+SB+SC+K)
  310 FORMAT(X+F5.3+2F6.3+F8.4+F8.6+3F8.3+13)
  100 CONTINUE
      END
```

```
RUN(S)
LGO.
000000000000000000000
      PROGRAM HTH (INPUT + OUTPUT + TAPE 61 = OUTPUT)
      AF STATE
C
      EAF(B+H+HK+HL+HD) = ((2+HK+HL)-H+H+(HK+HL)/(HK+HL+COS(2+B))++2)+
     1SIN(2*B)-2*HD*COS(2*B)
      UAF(B+H+HK+HL+HD) =-(1+HK+HL)+(2+HK+HL)+SIN(B)+SIN(B)-H+H+SIN(B)
     1*SIN(B)/(HK+HL*COS(2*B))-HD*SIN(2*B)
      EAFH(B+H+HK+HL+HD) = -2+H+(HK+HL)+SIN(2+B)/(HK+HL+COS(2+B))++2
      UAFH(B+H+HK+HL+HD) = -2+H+SIN(B)+SIN(B)/(HK+HL+COS(2+B))
      EAFB(B+H+HK+HL+HD)=-4*SIN(2*B)*SIN(2*B)*H*H*HL*(HK+HL)/(HK+HL*COS
     1(2+B))++3+2+((2+HK+HL)-H+H+(HK+HL)/(HK+HL+COS(2+B))++2)+COS(2+B)
     2+4*HD*SIN(2*B)
      DH(B \bullet C \bullet H \bullet HK \bullet HL \bullet HD) = -2*H*SIN(B)*SIN(B)/(HK \bullet HL *COS(2*B)) + 2*SIN(C)
C
       SF STATE
      USF(C+H+HK+HL+HD)=-1+SIN(C)+((2+HK-HL)+SIN(C)-2+H-2+HD+COS(C))
      ESF(C+H+HK+HL+HD) = (2 + HK - HL)+SIN(2+C) - 2+HD+COS(2+C) - 2+
     1H#COS(C)
      ESFH(C+H+HK+HL+HD) = -2*COS(C)
      ESFC(C_{\theta}H_{\theta}HK_{\theta}HL_{\theta}HD) = 2*(2 + HK - HL)*COS(2*C) + 4*HD*SIN(2*C)
     1+ 2*H*SIN(C)
      USFH(C+H+HK+HL+HD) = -2*SIN(C)
      1 =0
      PI=3.1415926536
      HK = 0
      HL = 0.001
      SHD=HD
      SHK=HK
      H=((2+HK-HL)+(HK+HL))+0.5
      B=0.0
      C = 0.0
      B=90.0*PI/180.0
      HL=0.0
      DO 100 J=1.10
      HL=HL+0.001
      H=H+0.005
      SHL=HL
      K=0
   10 D= UAF(B+H+HK+HL+HD)-USF(C+H+HK+HL+HD)
      DELTA = EAFB(B+H+HK+HL+HD)+(ESFC(C+H+HK+HL+HD)+DH(B+C+H+HK+HL+HD)
     1+ESF(C+H+HK+HL+HD)+ESFH(C+H+HK+HL+HD))-EAF(B+H+HK+HL+HD)+ESFC(C+H+
     2HK+HL+HD) *EAFH(B+H+HK+HL+HD)
      B=B-(EAF(B+H+HK+HL+HD)+(ESFC(C+H+HK+HL+HD)+DH(B+C+H+HK+HL+HD)+
     3H+HK+HL+HD) **2-D*ESFC(C+H+HK+HL+HD)))/DELTA
      C=C-(EAFB(B+H+HK+HL+HD)+(ESF(C+H+HK+HL+HD)+DH(B+C+H+HK+HL+HD)-
     1D*ESFH(C+H+HK+HL+HD))*EAF(B+H+HK+HL+HD)*(EAF(B+H+HK+HL+HD)*ESFH(C
     2.H.+HK.+HL.+HD) -ESF(C.+H.+HK.+HL.+HD) +EAFH(B.+H.+HK.+HL.+HD)))/DELTA
      H=H-(EAFB(B+H+HK+HL+HD)+(ESFC(C+H+HK+HL+HD)+D+ESF(C+H+HK+HL+HD)++2
     1)-EAF(B+H+HK+HL+HD)++2+ESFC(C+H+HK+HL+HD))/DELTA
      D= UAF (B+H+HK+HL+HD) -USF (C+H+HK+HL+HD)
```

```
S=ABS(EAF(B+H+HK+HL+HD))+ABS(ESF(C+H+HK+HL+HD))+ABS(D)
      K=K+1
      IF (K.GT.50)GO TO 35
      IF(S.GE.0.0000001)G0 10 10
   35 SS=S
      A=-91.0*PI/180.0
      X=-H*SIN(B)/(HK+HL*COS(2*B))
      IF (ABS(X).GT.1.0)GO TO 20
      A=ASIN(X)
   20 CONTINUE
     KSK =K
      SH =H
      SA=A*180.0/PI
      SB=B*180.0/PI
      SC=C*180.0/PI
С
     WRITE OPERATIONS
     L = L-1
     IF(L.LE.0)200+300
  200 WRITE(61+210)
                           HL
                                HD
  210 FORMAT(1H1 + HK
                                      н
                                           S
                                                       A
                                                               В
                                                                       C
          K*)
    1
     L=60
  300 WRITE (61+310) (SHK+SHL+SHD+SH+SS+SA+SB+SC+K)
  310 FORMAT(X+F5.3+2F6.3+F8.4+F8.6+3F8.3+I3)
  100 CONTINUE
     END
000000000000000000000
```

